Optical Loading of a Bose–Einstein Condensate

Vom Fachbereich Physik der Universität Hannover

zur Erlangung des Grades
Doktor der Naturwissenschaften
-Dr. rer. nat.-

genehmigte Dissertation

von

Dipl. Phys. Filip Floegel
geboren am 15.07.1973 in Hamburg

2003

Referentin: Prof. Dr. M. Lewenstein

Korreferent: Prof. Dr. J. Arlt

Tag der Promotion: 19.05.2003

Abstract

During the last years, the fruitful combination of laser–cooling and evaporative cooling has allowed the experimental achievement of the Bose–Einstein condensation (BEC) in weakly interacting trapped alkali gases. Among the results related to BEC, one of the most important experimental achievements has been the realization of an *Atom Laser*. As a coherent source of matter waves, the atom laser should lead to new applications in atom optics. However, without a continuous refilling of the BEC, the atom laser output lasts only as long as some atoms in the BEC are kept. Additionally, the controlled continuous loading of a BEC could be employed to repair the losses induced by either background collisions or two- and three-body losses.

It is the purpose of this thesis to analyze the continuous loading of a BEC by means of spontaneous emission. We shall discuss the difficulties to achieve this aim, in particular the photon reabsorption problem, and propose the corresponding solutions in different physical scenarios.

In the first scenario we analyse the optical loading of a BEC in the so-called Boson Accumulation Regime for a three-dimensional case, in which more than one trap level of the excited-state trap is considered. By solving the corresponding quantum many-body master equation, we demonstrate that contrary to intuition, for this general situation the photon reabsorptions can help, due to quantum interferences, to increase the condensate fraction.

In another case we consider atoms with an accessible three-level Λ scheme, in which one of the atomic transitions has a very much shorter life-time than the other one. We found that in such scenario the photon reabsorptions (in the slowest transition) can be considered negligible. If in addition inelastic processes can be neglected, we find that optical pumping can be used to continuously load and refill Bose-Einstein condensates. i.e. it provides a possible route towards a continuous atom laser.

In the final part we discuss the optical loading of a Bose-Einstein condensate in the Thomas-Fermi regime, where the mean-field effects become dominant. By means of the master equation formalism, Gross-Pitaevskii and Bogoliubov equations, we discuss the modification of the condensate temperature during the loading. We identify the threshold temperature, T_{th}, above (below) which the loading process leads to cooling (heating), respectively. The consequences of our analysis for the continuous loading of an atom laser are discussed.

Keywords: Bose-Einstein Condensation, Laser Cooling, Cold Gases

Zusammenfassung

Während der letzten Jahre haben die Kombination von Laserkühlung und Verdampfungskühlung zur experimentellen Demonstration der Bose–Einstein Kondensation (BEC) geführt. Unter all den wichtigen Resultaten um BEC ist die Entwicklung des *Atomlasers* eine der Beeindruckensten, denn als eine Quelle von kohärenten Materiewellen kann er zu völlig neuen Experimenten und Anwendungen in der Atom-Optik führen. Jedoch ohne das kontinuierliche Nachladen des BECs mit Atomen arbeitet der Atomlaser maximal so lange, bis das BEC von Atomen entvölkert ist. Zusätzlich ist das kontrollierte kontinuierliche Laden des BECs interessant, um die Verluste aufgrund von Hintergrundgas- und/oder nicht-elastischen Dreikörperstößen auszugleichen.

Das Ziel der hier vorliegenden Doktorarbeit ist es, das kontinuierliche Laden des BECs mittels spontaner Emission zu untersuchen. Dazu werden die beim optischen Laden auftretenden Schwierigkeiten, insbesondere die Photonenreabsorptionen, diskutiert und entsprechende Lösungen für verschiedene Szenarien aufgezeigt.

In einem der Szenarien wird das optische Laden eines BECs im sogenannten Bosonischen Akkumulation Regime (BAR) für den dreidimensionalen Fall untersucht, bei dem die angeregten Atome mehr als nur einen externen Fallenzustand besetzen. Durch das Lösen der entsprechenden Mehrteilchen-Quanten-Mastergleichung wird hier gezeigt, dass im allgemeinen Fall entgegen der Intuition die Photonenreabsorption aufgrund von Quanteninterferenzen helfen kann, die Fraktion des BECs zu erhöhen.

In einem weiteren Fall werden Atome betrachtet, die durch ein Dreiniveausystem in Λ-Konfiguration beschrieben werden können, bei dem auf einem der Zerfallskanäle die Atome viel schneller zerfallen als auf dem anderen. Es wird gezeigt, dass in solch einem Szenario die Photonenreabsorption auf dem langsameren Zerfallskanal keine Rolle spielen. Unter der Voraussetzung, dass nicht-elastische Prozesse vernachlässigbar sind, wird demonstriert, dass optisches Laden in diesem Regime eine Methode darstellt, um ein BEC kontinuierlich nachlzuladen.

Zum Schluß wird das optische Laden des BECs im Thomas-Fermi Regime untersucht, bei dem die Effekte der molekularen Felder dominant werden. Mit Hilfe der entwickelten Mastergleichung und unter Verwendung der Gross-Pitaevskii-Gleichung und den Bogoliubov-Gleichungen, wird die Variation der Temperatur des BECs während des Ladens betrachtet. Es stellt sich heraus, dass bei einer Temperatur des BECs unterhalb (überhalb) einer Schwellentemperatur T_{th} das BEC während des Ladens aufgeheizt (gekühlt) wird. Die daraus resultierenden Konsequenzen für das kontinuierliche Laden eines Atomlasers werden diskutiert.

Schlagwörter: Bose-Einstein Kondensation, Laserkühlung, kalte Gase

Contents

Chapter 1

Introduction

During the last years, the fruitful combination of laser–cooling [1] and evaporative cooling [2, 3, 4] has allowed the experimental achievement of the Bose–Einstein condensation (BEC) in weakly interacting trapped alkali gases. Such remarkable achievement has stimulated an enormous interest from various communities as disparate as Quantum Optics, Condensed Matter Physics, Nonlinear Physics, and more [5]. The importance of this research field was recently recognized with the Nobel Prize Award 2001 to E. Cornell, C. Wieman and W. Ketterle, which add up to the Nobel Prize Award 1997 to W. Phillips, C. Cohen-Tannoudji and S. Chu, who have received the award for their developments in laser cooling and trapping of neutral atoms.

Among the results related to BEC, one of the most important experimental achievements has been the realization of an *Atom Laser*. As a coherent source of matter waves, the atom laser should lead to new applications in atom optics and its impact in the field could be comparable to the one of optical lasers in light optics. Since its first realization [6, 7], several groups have build atom lasers using (quasi-) continuous outcoupling from the BEC, either by using rf fields [8, 9], or by employing Raman pulses [10]. However, the continuous outcoupling represents just a half way towards a cw atom laser. The continuous loading of the condensate still remains to be incorporated in experiments, even though first experiments [11, 12] have been done towards a continuously loading of a BEC. Without a continuous refilling of

the BEC, the atom laser output lasts only as long as some atoms in the BEC are kept. Like in the development of light lasers the availability of cw atom lasers would open the way to "high power" and precision applications.

Additionally, the controlled continuous loading of a BEC could be employed to repair the losses induced by either background collisions or two- and three-body losses. If this losses could be repaired, the lifetime of the BEC experiments could be enlarged, in principle indefinitely, opening a way towards a new generation of BEC experiments.

It is the purpose of this thesis to analyze the continuous loading of a BEC by means of spontaneous emission. We shall discuss the difficulties to achieve this aim, in particular the photon reabsorption problem, and propose the corresponding solutions in different physical scenarios.

The structure of this Thesis is as follows:

- **Chapter 2: Physics of cold atoms**
  In this chapter we comment on several important concepts related with the physics of cold atoms and BEC. Additionally, we discuss the current international context.

- **Chapter 3: Optical loading in the Boson–accumulation regime**
  In this chapter, we generalize the previous simplified analysis of Ref. [13], to a three-dimensional case in which more than one trap level of the excited-state trap is considered. By solving the corresponding quantum many-body master equation, we demonstrate that also for this general situation the photon reabsorption can help due to quantum interferences to increase the condensate fraction.

- **Chapter 4: Optical loading in the Branching-ratio expansion**
  In this chapter we consider the case of atoms with an accessible three-level Λ scheme, in which one of the atomic transitions has a very much shorter life-time than the other one. We found that in such scenario the photon reabsorption (in the slowest transition) can be considered negligible. If in addition inelastic processes can be neglected, we find that optical pumping can be used to continuously load and refill Bose-

Einstein condensates. i.e. provides a possible route towards a continuous atom laser.

- **Chapter 5: Optical loading in the Thomas-Fermi regime**
  In the last part we discuss the optical loading of a Bose-Einstein condensate in the Thomas-Fermi regime, where contrary to the case of Chapter 4, the mean-field effects become dominant. By means of a master equation formalism, Gross-Pitaevskii and Bogoliubov equations, we discuss the modification of the condensate temperature during the loading. We identify the regime of parameters for which the temperature is effectively lowered during the loading process. The consequences of our analysis for the continuous loading of an atom laser are discussed.

Chapter 2

Physics of cold atoms

In this chapter we comment on several important concepts related with the physics of cold atoms and BEC. Additionally, we discuss the current international context.

2.1 Cold and slow Atoms

2.1.1 Concept of matter-waves

In 1923 de Broglie [14], guided by the analogy of Fermat principle in optics and the least-action principle in mechanics, was led to suggest that the dual wave-particle nature of radiation should have its counterpart in a dual particle-wave nature of matter. Thus particles should have wave properties under certain circumstances, and de Broglie suggested an expression associated with the particle. This is given by

$$\lambda_{dB} = \frac{h}{p}, \tag{2.1}$$

where h is Planck's constant, and p is the momentum of the particle. This expression is known as the *de Broglie* wavelength of the particle. Such a wave resemble the familiar concept of plane waves in optics. However a single-momentum wave is not localized in space, and in order to retrieve the intuitive particle idea it is introduced the very important concept of wave-

packet, which can be achieved by superposing waves of different frequencies, so that they interfere destructively with each other almost completely outside of a given spatial region. Of course the narrower the momentum bandwidth of the wave-packet (dp) the closer to the wave concept, and the larger the spatial dimensions of the wave-packet dx. This crucial observation is formally expressed by one of the most basic principles of Quantum Physics, i.e. the *Heisenberg uncertainty relation* which states that $dpdx \geq \hbar$ (where $\hbar = h/2\pi$).

2.1.2 Cold atoms

At this point we introduce the concept of Cold Atoms, which turns to be crucial in the rest of the thesis. It is well known from Statistical Mechanics [15] that a dilute gas in thermal equilibrium presents in absence of external force a Maxwell-Boltzmann momentum distribution function of the form:

$$f_0(\vec{p}) \sim e^{-(\vec{p}-\vec{p}_0)/2mK_BT}, \tag{2.2}$$

where $\vec{p}_0$ is some central momentum, m is the mass of the particles, K_B is the Boltzmann constant and T is the temperature of the sample. Therefore, the temperature can be defined in terms of the width of the energetic distribution. In this sense the narrower the energetic distribution the colder the atomic sample. Therefore a cooling technique is defined as a method which converts an initially broader distribution into a narrower one. Of course, a thermal distribution is not possible for a single atom or ion, but it is common in the literature the use of the term cold atom when dealing with an atom with a narrow energetic distribution of probability. The significance of a cold atom can be easily understood from Sec. 2.1.1. A cold free atom means an atom with a well defined momentum, i.e the momentum distribution of Eq. 2.2 is very peaked around the central value $\vec{p}_0$. Therefore the colder the atom the narrower its momentum bandwidth, and the more apparent the wave nature of the atom. To obtain an intuitive idea of what a cold atom means, let us present some estimates. An atom at normal temperature has a momentum bandwidth so large that can be considered as a particle, with

dimensions typically of the order of the Bohr radius, i.e.
Angstrom ($10^{-10}m$). An atom cooled with the most powerful cooling techniques (see. Sec.2.2.2) has a spatial distribution of the order of microns ($10^{-6}m$), i.e. 10000 times the Bohr radius. If one tries to compare this case with a person spread on a ten kilometer region one can develop a good idea of the huge dimensions (for atomic scale) of the cold atomic wave function. Let us remark that matter-wave behavior has also been observed in electrons [16], and neutrons [17]. What makes more interesting the case of atoms is the rich internal structure accessible by laser light. This allows the coherent manipulation of cold atomic samples, which is in the basis of laser cooling techniques and the majority of atom optics phenomena (Atom Optics).

2.1.3 Slow atoms

To finalize this section, let us remark the difference between a cold atom and a slow one. As defined previously a cold atomic sample has a peaked velocity distribution around some central value v_0. A slow atom can be classically defined as having a small velocity, and quantum-mechanically as having a low velocity average. Note that the velocity average can be large or small independently of the fact whether the velocity distribution is broad or narrow. Therefore cold and slow atom concepts are clearly different. However, the cooling and trapping techniques which have been developed (see next sections) allow not only to cool but also to slow down atomic samples. Both features are important for the experimental manipulation of the atoms, as discussed in the next sections.

2.2 Laser Cooling and Trapping

In this section we will briefly review different laser cooling techniques. In subsections 2.2.1 and 2.2.2 we discuss the case of free atoms. Subsection 2.2.3 is devoted to the issue of trapping of neutral atoms. Finally, in subsection 2.2.4 we analyze the laser cooling and evaporative cooling for trapped atoms.

2.2.1 Doppler cooling

Let us assume an atom with an accessible (electronic) two-level system, formed by the ground state $|g\rangle$ and an excited state $|e\rangle$, which are separated by a transition frequency ω_{eg}. Let us consider that this atom is affected by two counter-propagating lasers of frequency ω_l and wave vectors $\pm\vec{k}_l$ respectively. If the atom moves with some velocity $\vec{v}$, due to the Doppler effect the atom observes the photon with wave vector $\vec{k}_l$ as having a frequency $\omega\prime_l = \omega_l - \vec{k}_l\vec{v}$. As a consequence of that, if the laser is red-detuned with respect to the transition frequency ($\Delta = \omega_l - \omega_{eg} < 0$), the photons counter-propagating against the motion of the atom are absorbed with larger probability than those propagating in the direction of motion, and the radiation pressure damps the atom velocity. Of course after absorption the atom decays into the ground state by a spontaneous emission of a photon, experiencing a recoil in a random direction due to momentum conservation. However, in average, the effect of these random recoils is canceled. As a result, the momentum distribution of the atoms is compressed around $v = 0$, i.e. following the discussion of the previous sections, the atomic sample is both cooled and slowed. This cooling method is known as Doppler cooling, and was proposed by Hänsch and Schawlow [18], and first demonstrated by Chu *et al.* [19]. As a result of this effect, the atoms experience a viscous force, $\vec{F}_D \simeq -\vec{v}$, which has motivated the proper name of optical molasses for this effect. The competition between cooling and heating introduced by the randomness of the spontaneous emission results in a minimal temperature achievable with this method (see [20]), $K_B T = \hbar\Gamma/2$, where K_B is the Boltzmann constant, and Γ the line width of the optical transition $|e\rangle \rightarrow |g\rangle$.

Doppler cooling works only if the laser is not too strong. If the corresponding Rabi frequency becomes larger than the line-width of the transition, the atom experiences a periodic laser field. In that case, cooling has been observed for blue detuned lasers, and receives the name of Sysiphus cooling. This method allows for lower temperatures than Doppler cooling, down to few recoil temperatures ($T_{rec} = \hbar^2 k_l^2/2mK_B$). For a more detailed discussion on Sysiphus and polarization gradient cooling, see e.g. Ref. [20].

2.2.2 Subrecoil laser cooling

In order to reduce further the temperature of an atomic sample, it is necessary to overcome the heating introduced by the recoil of the spontaneously emitted photons. The subrecoil methods consist therefore in the suppression of the spontaneous emission under certain conditions, and are based in the concept of a dark state. A state is called dark, if it cannot absorb the cooling laser. Therefore, if an atom decays into a dark state, it will not leave this state anymore. This effect is known as population trapping. There are different subrecoil methods based in this effect, as e.g. Velocity Selective Coherent Population Trapping (VSCPT), cooling using the effect of Electromagnetically Induced Transparency [21], and Raman cooling [22].

2.2.2.1 VSCPT

As a first example of such techniques let us analyze the so-called Velocity Selective Coherent Population Trapping, known in the literature by its acronym VSCPT[23, 24]. Let us consider a three level λ configuration in which two degenerate ground sub levels $|g_{\pm}\rangle$ are coupled to an excited level $|e\rangle_0$ by two counter-propagating σ_+ and σ_- polarized laser beams with the same frequency ω_l. Let us firstly consider the atom at rest. For this case it was shown in the context of non-absorption resonances [25, 26] that there is a coherent superposition of $|g_+\rangle$ and $|g_-\rangle$ which is not coupled to $|e\rangle$ by the laser, and is therefore a dark state. Such situation occurs due to the destructive interference between the amplitudes of the counter-propagating lasers. Therefore an atom put in such a superposition of states, remains trapped there. Let us now introduce the atomic motion considering only the one-dimensional case. Now the internal atomic states are dressed by the external (center of mass) motion. It can be easily shown that the families of states of the form:

$$\zeta(p) = \{|e, p\rangle, |g_-, p - \hbar k_l\rangle, |g_-, p + \hbar k_l\rangle\} \tag{2.3}$$

remain closed respect to absorption and stimulated emission. Although this closed family resembles the case of an atom at rest, there is actually a key

difference. The crucial point is that now, and due to the kinetic energy, the ground levels do not have the same energy, and therefore any mixture of them is not an stationary state. This fact prevents the formation of a true trapping state. Only for the case of the family $\zeta(0)$ the same case of the atom in rest is recovered, i.e. a trapping state is formed. The spontaneous emission provides the way to jump (randomly) from one family of states to another. Therefore the atoms describe a random path in the momentum space until reaching the family $\zeta(0)$ where they have a probability to remain trapped. The larger the interaction time between the atoms and the lasers the larger the amount of atoms in the trapped state, and hence there is no fundamental limit for this cooling mechanism. In particular the atoms can be cooled into a momentum distribution with a width smaller than the recoil momentum.

2.2.2.2 Raman Cooling

Let us now consider a three-level system composed by two ground states $|a\rangle$,$|b\rangle$ separated by a frequency ω_{ab} and an excited state $|e\rangle$, irradiated by two counter-propagating lasers of frequencies ω_1 and ω_2, in such a way that $\omega_{12} = \omega_1 - \omega_2$ is quasi-resonant with ω_{ab}. The lasers are sufficiently far of resonance respect to $|e\rangle$ to consider $\{|a\rangle\ ,|b\rangle\}$ as a two-level system coupled by a two-photon Raman process with an effective Rabi frequency Ω_{eff} [27]. When ω_{12} is red-detuned an atom with velocity $+v$ is kicked towards v = 0 as in usual Doppler cooling (but now with momentum $2\hbar k_l$ in each step). Reversing the laser directions the atoms moving with $-v$ are pushed now to v = 0. Using sequences of Raman pulses of different frequency width, detuning and propagation direction, the process can be designed to excite all atoms except those with velocities closed to $v = 0$, then forming a dark state in the velocity (momentum) space. The cooling cycle is closed by using a third laser which excites the transition $|b\rangle \rightarrow |e\rangle$, where the atom can be optically pump into $|a\rangle$ via spontaneous emission. This last process produces a random component of the velocity, so that some atoms acquire velocities sufficiently close to v = 0. This method is called Raman Cooling [22]. It

allows temperatures well below the recoil limit (of the order of tenths of this value).

2.2.3 Trapping of neutral atoms

Contrary to charged particles which can be relatively easily confined, the trapping of neutral atoms demands the employ of certainly more sophisticated techniques. In the following we briefly summarize the main standard trapping techniques for neutral atoms:

- Magnetic trap [28]: Magnetic trapping is based on the Zeeman effect experienced by an atom in a spatially inhomogeneous magnetic field. The atom energy acquires then a spatial dependence of the form:

$$E(\vec{r}) = \mu_B g_F m_F B(\vec{r}) \tag{2.4}$$

  where F is the total angular momentum of the particular atomic level considered, m_F is the magnetic quantum number, μ_B is the Bohr magneton, and g_F is the gyromagnetic moment. The atomic level is called weak-field (strong-field) seeking if $g_F m_F > 0$ ($g_F m_F > 0$), since in that case the atoms are driven towards low (high) magnetic fields. Therefore, since it is not possible to create a local maximum with a static magnetic field, only weak-field seeking states can be trapped by an inhomogeneous magnetic field $\vec{B}(\vec{r})$ with a local minimum. An example for an weak-field seeker is provided by the $|F = 2, m_F = 2\rangle$ in Rubidium.

- Dipole trap [29]: The principle of the dipole trap is based on the interaction of an electric field $\vec{E}(\vec{r}, t)$ with a two level ($|g\rangle$,$|e\rangle$) atom

$$H_{int} = -\vec{d}\vec{E}(\vec{r}, t), \tag{2.5}$$

  where $\vec{d}$ is the dipole moment associated to the corresponding transition. If the field is spatially inhomogeneous the interaction and the associated energy level AC-Stark shifts of the atom vary in space. The

oscillating electric field is provided by a laser either red ($\Delta < 0$) or blue detuned ($\Delta > 0$) with respect to the atomic transition, where $\Delta = \omega_{laser} - \omega_{eg}$, and ω_{eg} is the transition frequency. The laser detuning must be sufficiently large to avoid the losses related to photon scattering. In a semi-classical approximation the confining potential is given by

$$V_{tr}(\vec{r}) = \frac{\hbar\Omega_R(\vec{r})^2}{4\Delta}, \tag{2.6}$$

where $\Omega_R(\vec{r})$ is the Rabi frequency (Ω_R^2 is proportional to the laser intensity). When the laser is red (blue) detuned, the atoms are attracted to the intensity maximum (minimum) of the laser field. This allows for the creation of optical traps, as well as for the achievement of e.g. optical mirrors, optical wave guides, and optical lattices. An optical trap has certain clear advantages when compared to a magnetic trap. In particular, an optical trap is not limited to weak-field seekers. Additionally, the atomic density in a optical trap can be much larger than in a magnetic one because the trap frequency can be made much larger. Another interesting point is that by displacing the focus of the laser one can move the trap center, allowing for the so-called optical tweezers [11].

- Magneto Optical Trap (MOT) [30]: The MOT is a hybrid model, using both optical and magnetic fields. Let us consider an atom with a zero-spin ground level and a spin-one excited level (and then with three Zeeman sublevels $m_F = 1, -1, 0$). If a weak inhomogeneous magnetic field $B(z) = bz$ is applied, the Zeeman sublevels are split by an amount $\Delta E(z) = \mu_B g_F m_F bz$ (see also 2.4). The atom is affected by two counter-propagating laser beams with opposite circular polarization, σ^- in direction $-z$ and σ^+ in direction $+z$. If the laser is red-detuned with respect to the optical transition at $B = 0$, the atom at $z > 0$ absorbs more σ^- than σ^+ photons, and consequently feels an average force toward $z = 0$. For $z < 0$ the Zeeman effect is the opposite, being the atom directed again to the origin. Therefore, the atom is trapped around $z = 0$. The scheme is easily extended to three

dimension by using 6 laser beams, two counter-propagating in each direction, and a spherical quadrupole magnetic field which provides a linear magnetic field around the origin.

2.2.4 Cooling in a trap

By employing the previously discussed laser cooling and trapping techniques, it is possible to obtain an ensemble of trapped atoms at temperatures ranging between few μK to several mK. The latter depends on the particular laser pre-cooling employed, and on the atomic species used. In this subsection, we review those cooling techniques specifically designed to cool in a trap. The ultimate goal of these techniques is the accomplishment of a macroscopic population of the ground-state of the trapped system, i.e. to produce a Bose-Einstein condensate (see next section). We shall first present several laser cooling mechanisms for trapped atoms, and finalize with a discussion of collisional cooling methods.

2.2.4.1 Laser cooling

Let us consider a three-level λ-system composed by a ground-state level $|a\rangle$, a metastable state $|b\rangle$, and a third fast-decaying auxiliary state $|e\rangle$. Two lasers are assumed to excite coherently the Raman transition $|a\rangle \rightarrow |b\rangle$ (with some associated effective Rabi frequency Ω), while a repumping laser off-resonance with the transition $|b\rangle \rightarrow |e\rangle$ pumps optically the atom (via spontaneous emission) into $|a\rangle$. For a sufficiently large detuning of the repumping laser, the three-level scheme can be reduced to an effective two-level system with an effective spontaneous emission rate γ, which can be controlled by varying the intensity or the detuning of the repumping laser [31]. The atom is assumed to be confined in a harmonic (isotropic) potential of frequency ω. We denote the states of the harmonic oscillator as $|n\rangle$). We assume $\gamma < \omega$, i.e. the so-called Strong-Confinement Limit, also called Festina-Lente limit [32]. The latter turns out to be a crucial point in the many-atom case in order to avoid the reabsorption problem (see the last part of this chapter). In the Lamb-Dicke limit (LDL), i.e. when the dimensions of the trap are very small compared

with the laser wavelength λ, it is possible to use standard Sideband Cooling techniques (first employed for cooling of single trapped ions) to pump an atom into the ground state of the harmonic trap. In this cooling method the laser is assumed red-detuned, with detuning $\delta = -\omega$.The absorption of a laser photon induces the transition $|g, n\rangle \rightarrow |e, n-1\rangle$. In the LDL, $\eta^2 = E_R/\hbar\omega_{tr} \ll 1$, where E_R is the recoil energy, and hence, the recoil of the spontaneously emitted photon is not large enough to induce a jump between different states of the harmonic trap. As a consequence, only the transition $|e, n-1\rangle \rightarrow |g, n-1\rangle$ is possible. Hence, the global effect of a complete absorption-spontaneous emission cycle is a transition $|g, n\rangle \rightarrow |g, n-1\rangle$. This process is repeated until the particle reaches the ground state of the trap, where it can no longer be excited by the laser, i.e. $|g, 0\rangle$ is a dark state. As we discuss at the end of this chapter, in the many-body case the latter statement is only true if we operate in the regime $\gamma < \omega$.

Beyond the LDL, $E_R \geq \hbar\omega$, and hence in the spontaneous process, the atom undergoes transitions |e, $|g, n-1\rangle \rightarrow |g, n-1 \pm n'\rangle$ where n' ranges from 0 to $\mathcal{O}(\eta^2)$. This process introduces a heating of the atomic distribution which prevents the confinement of the atom into the ground state of the trap. Morigi *et al.*[33] designed a method to laser cool single trap atoms beyond the LDL towards the ground state of the trap. In a first step the atoms are confined in the levels $n \leq \eta^2$. This is achieved by using pulses with detunings $\delta = -\hat{\eta}^2\omega$, where $\hat{\eta}^2$ is the closest integer to η^2. The absorption of a laser photon produces a transition $|g, n\rangle \rightarrow |g, n - \mathcal{O}(\eta^2)\rangle$, and the spontaneous emission $|g, n-\mathcal{O}(\eta^2)\rangle \rightarrow |g, n-\mathcal{O}(\eta^2)\pm n'\rangle$, where n' ranges from 0 to $\mathcal{O}(\eta^2)$. As a result, in average some energy is lost in each cycle. Obviously, the states with $n < \eta^2$ remain dark, and therefore the atoms are finally confined in these states. Due to this, these pulses are called confinement pulses. Using pulses of selected frequencies one can empty the trap levels ($|g, 1\rangle$,$|g, 2\rangle$,$\cdots$) without affecting the population of $|g, 0\rangle$. Then, in each cooling cycle there is some probability to pump into $|g, 0\rangle$. There is also some probability of heating, and therefore one must repeat the confinement step, and so on. As a result of the cooling process, the atom can be confined in the ground state of the trap, as in the usual Sideband Cooling. Since the present cooling mechanism is

based on sequences of different pulses, the method has been called *Dynamical Cooling* [33]. This method was later on extended to three-dimensional traps by Santos and Lewenstein [34].

An alternative cooling mechanism has been recently proposed by Morigi *et al.* [21]. This method is based in the so-called Electromagnetically Induced Transparency (EIT), which as coherent population trapping relies on the quantum interference between the absorption probabilities in a three-level Λ system. The latter is formed by two ground states ($|a\rangle$,$|b\rangle$) and an excited state $|e\rangle$ with a line width γ. The ground states, which do not need to be degenerated, are coupled with the excited state through two different laser beams. EIT occurs if the detunings $\Delta_a = \omega_{ea} - \omega_l^a$ and $\Delta_b = \omega_{eb} - \omega_l^b$ of the two lasers (Ω_a,ω_l^a, Ω_b,ω_l^b) from the excited state $|e\rangle$ are equal. In the later case the system evolves into a coherent superposition of $|a\rangle$ and $|b\rangle$, like in VSCPT. In order to use this effect for cooling, the transition $|b\rangle \rightarrow |e\rangle$ is excited by an intense laser ($\Omega_b \sim \gamma$) with a detuning Δ_b above resonance, whereas the other transition $|a\rangle \rightarrow |e\rangle$ ("cooling transition") is affected by a weak laser with detuning Δ_a, also above the resonance. Due to that setup, the Fano-like absorption spectrum of the cooling transition $|a\rangle \rightarrow |e\rangle$ has the advantage to be asymmetric around the dark resonance, with a broad resonance at $\Delta_a = 0$, the dark resonance at $\Delta_a = \Delta_b$, and a narrow resonance at $\Delta_a = \Delta_b + \delta$, where δ is the AC-Stark shift, which is adjusted by controlling the intensity of the strong laser. For EIT cooling the lasers are set to the dark resonance condition $\Delta_a = \Delta_b$ which leads to a decoupling of the motional modes $|a, n\rangle$ and $|e, n\rangle$. When the intensity of the strong laser is chosen in such a way that the AC-Stark shift is $\delta = \omega$, the transition $|a, n\rangle \rightarrow |e, n-1\rangle$ match exactly to the maximum of the narrow resonance, whereas the transition $|a, n\rangle \rightarrow |e, n+1\rangle$ falls into the region of the spectrum of small excitation probability. That means that the transition $|a, n\rangle \rightarrow |e, n-1\rangle$ is enhanced, whereas the "bad" transitions are either forbidden $|a, n\rangle \rightarrow |e, n\rangle$ or less favorable $|a, n\rangle \rightarrow |e, n+1\rangle$. After several cooling cycles the atoms enter into the motional ground state.

The application of the Dynamical cooling technique to a many-body system was considered for the case of bosons by Santos and Lewenstein [35]. By

means of many-body quantum Master equation techniques, as those discussed in the next chapters of this Thesis, it was shown that the bosonic statistics can help significantly during the process of cooling. In particular, it was predicted that as long as the photon reabsorption can be neglected, purely optical cooling (without using the evaporative cooling techniques described in the next subsection) can lead to the accomplishment of Bose-Einstein condensation (see next section). The effects of interactions were also studied in the weak-interaction regime (when the mean-field energy is smaller than the energy separation between trap levels) by means of quantum Boltzmann Master equations (see next chapter). The atom-atom interactions were shown to provide an additional help towards the achievement of a purely optical condensation.

Recently, Idziaszek *et al.* [36] have analyzed the statistical effects in the laser cooling of trapped fermions. In particular, it has been shown that the coherent nature of the atom-laser interaction can allow for overcoming the inhibition of the spontaneous emission introduced by the Pauli exclusion principle [37]. In this way, it was reported that temperatures well below the Fermi temperature can be achieved. The collisional effects for the case of multicomponent Fermi gases where also recently considered by means of quantum Boltzmann Master equations [38, 39]. The laser cooling of fermions opens a fascinating alternative route towards the accomplishment of the Bardeen-Cooper-Schriffer (BCS) transition, i.e. the formation of Cooper pairs and the on-set of superfluidity (see e.g. [40]).

2.2.4.2 Evaporative cooling

Evaporative cooling of trapped atoms was developed in the decade of 1980's at MIT as a method for cooling atomic hydrogen [41] in order to achieve BEC after pre-cooling by cryogenic methods [42, 43]. This method constitutes nowadays the only method that (in combination with laser pre-cooling) has experimentally lead to Bose-Einstein condensation (see next section). Evaporative cooling is performed by continuously removing the high-energy tail of the thermal distribution from the trap. The evaporated atom carries away

more than the average energy per particle. This results in a reduction of the average energy per particle of the remaining atoms, and after rethermalization mediated by the atom-atom collisions, to a decrease of the temperature of the trapped gas. It is crucial that the thermalization time, provided by the inverse of the collisional rate γ_{col}, should be shorter than the rate of losses, either background losses or those induced by inelastic processes. If the latter is not the case, the thermalization is not successfully performed, and the evaporative cooling is frustrated. Therefore special care must be taken when designing the particular path for evaporative cooling [44], and a combination of laser and evaporative cooling must be employed. In principle, the potential barrier forming the trapping potential can be relaxed, leading to the evaporation of the hottest atoms. However, this leads to a deformation of the trapping potential, and in particular to a reduction of the gas density, inducing a decrease of the collisional rate, and therefore of the thermalization efficiency. In order to avoid this problem, the evaporation is actually performed in magnetic traps by means of radio frequency (rf) pulses, which flip the atomic magnetic moment (m_F), and therefore couples trapped with untrapped states [45]. Those atoms are therefore released from the trap. The rf-induced evaporation is energy selective because the resonance frequency is proportional to the magnetic fields. This technique, also known rf-knife, is also employed in the context of outcoupling of an atom laser, as discuss in Sec. 2.4. The theory of evaporative cooling has been throughly examined in Refs. [46, 47, 48, 49], see also Cohen-Tannoudji College de France Lectures 1997-1998.

2.3 Bose-Einstein Condensation

In this section we briefly review some important concepts related with the physics of BEC in harmonically trapped gases. We shall first discuss the non-interacting case. Later we shall introduce the effects of the interparticle interactions. For a more detailed discussion on BEC theory, see e.g. [50].

2.3.1 Bose Einstein Condensation for a ideal gas

Let us consider a system of non interacting bosons in thermal equilibrium, characterized by the chemical potential, μ, the total number of atoms in the trap, N, and the temperature, T. The occupation of the different energy levels is provided by the Bose-Einstein distribution

$$N_{\vec{n}} = \{\exp[\beta(E_{\vec{n}} - \mu)] - 1\}^{-1}, \tag{2.7}$$

where $\beta = K_B T$, and $\vec{n} \equiv \{n_x, n_y, n_z\}$ are the quantum numbers describing the harmonic oscillator levels. Without loosing of generality we assume in the following a spherical harmonic trap of frequency ω, such that the energy spectrum is given by $E_{\vec{n}} = \hbar\omega(n_x + n_y + n_z + 3/2)$. The total number of atoms is

$$N(T, \mu) = \sum_{\vec{n}} N_{\vec{n}} \tag{2.8}$$

and the total energy

$$E(T, \mu) = \sum_{\vec{n}} E_{\vec{n}} N_{\vec{n}}. \tag{2.9}$$

As in the case of a Bose gas in absence of trapping potential [15], we separate the contribution of the lowest eigenvalue from that of the rest of eigenstates.

$$N(T, \mu) - N_0 = \sum_{\vec{n}} \frac{1}{\exp[\beta E_{\vec{n}}] - 1}. \tag{2.10}$$

In order to obtain a close expression for the sum, we assume that the level spacing becomes progressively smaller when $N \to \infty$, in such a way that the energy spectrum can be considered as continuous, and the sum can be replaced by an integral. Knowing the density of states $\rho(\epsilon) = (1/2)(\hbar\omega)^{-3}\epsilon^2$ we can rewrite Eq. (2.10) as an integral over the energy:

$$N - N_0 = \int_0^\infty d\epsilon \frac{\rho(\epsilon)}{\exp[\beta\epsilon] - 1} = \zeta(3) \left(\frac{K_B T}{\hbar\omega}\right)^2, \tag{2.11}$$

where ζ is the Riemann Zeta function. The limit $N_0 \to 0$ defines the critical

temperature T_c for onset of the BEC

$$K_B T_c = \hbar\omega \left(\frac{N}{\zeta(3)} \right)^{1/3}. \tag{2.12}$$

Inserting the definition of T_c in Eq. (2.10) we obtain the expression for the fraction number of condensed atoms:

$$\frac{N_0}{N} = 1 - \left(\frac{T}{T_c} \right)^3. \tag{2.13}$$

In the same way one gets the equation for the energy per particle of the system:

$$\frac{E}{N K_B T_c} = \frac{3\zeta(4)}{\zeta(3)} \left(\frac{T}{T_c} \right)^4. \tag{2.14}$$

2.3.2 Weakly interacting Bose gas

Once the concept of BEC has been discussed for the case of an ideal gas, we shall consider in this section the effects of the interparticle interactions. The Hamiltonian in second quantization formalism that describes a system of bosons interacting by binary interactions is of the form:

$$\begin{aligned} \hat{H} &= \int d^3 r \hat{\psi}^\dagger(\vec{r}) \left(-\frac{\hbar^2 \triangle}{2m} + V(\vec{r}) \right) \hat{\psi}(\vec{r}) + \\ &+ \frac{1}{2} \int d^3 r \int d^3 r' V_{int}(\vec{r} - \vec{r}') \hat{\psi}^\dagger(\vec{r}) \hat{\psi}^\dagger(\vec{r}') \hat{\psi}(\vec{r}) \hat{\psi}(\vec{r}'), \end{aligned} \tag{2.15}$$

where $\hat{\psi}(\vec{r})$ is the annihilation operator of a boson at a position $\vec{r}$, which satisfies the usual bosonic commutation rules, $V(\vec{r})$ is the trap potential, and $V_{int}(\vec{r})$ is the interaction potential. We shall consider in the following that the interaction potential is of a van der Waals form (other interaction potentials, as dipole-dipole interaction has been recently discussed [51]).

At the very low temperatures at which the BEC is obtained, the interparticle scattering is characterized by the s-wave scattering length a_{sc}. The actual interaction potential can be then substituted by a pseudo potential

which describes the asymptotic behavior of the two-body scattering problem:

$$V_{int}(\vec{r}-\vec{r'}) = \frac{4\pi\hbar^2 a_{sc}}{m}\delta(\vec{r}-\vec{r'}), \tag{2.16}$$

where m is the mass of the particle. If $a_{sc} > 0$ the interaction potential is repulsive, whereas if $a_{sc} < 0$ it is attractive.

Our previous assumption concerning the binary character of the interactions rely on the diluteness of the gas. A gas is considered as dilute if

$$\langle n\rangle |a_{sc}|^3 \ll 1, \tag{2.17}$$

where $\langle n\rangle$ is the average density of the gas. In this regime two-body collisions are dominant in comparison with three-body ones. For typical densities $(10^{13} - 10^{15} cm^{-3})$ and typical values of a_{sc} $(1 - 100\text{nm})$, $\langle n\rangle |a_{sc}|^3 < 10^{-3}$. In the following we shall always considered this regime.

Substituting the pseudo-potential (2.16) into the Hamiltonian (2.15), we can write the Heisenberg equation for the $\hat{\psi}$ operator:

$$i\hbar\frac{\partial}{\partial t}\hat{\psi} = \left(-\frac{\hbar^2\triangle}{2m} + V(\vec{r}) + U_{gg}\hat{\psi}^\dagger\hat{\psi}\right)\hat{\psi}, \tag{2.18}$$

where $U_{gg} = 4\pi\hbar^2 a_{sc}/m$.

Equation (2.18) is the exact equation for the corresponding many-body system. The field operator can be written in the form $\hat{\psi}(\vec{r}) = \sum_n \psi_n(\vec{r})\hat{g}_n$, where $\hat{g}_n$ is the annihilation operator of an atom in the eigenstate $\psi_n(\vec{r})$. The mean occupation of each state is $N_n = \langle\psi|\hat{g}_n^\dagger\hat{g}_n|\psi\rangle$, where $|\psi\rangle$ is the state of the many body system. As previously discussed, the BEC consists in the macroscopic occupation of the ground state of the system, $N_0 \gg 1$. This fact allows for the approximate substitution of the operators $\psi_0\hat{g}_0$ and $\psi_0\hat{g}_0^\dagger$ by a c-number $\psi_0(\vec{r},t)$, which acts as the condensate wave function. This approximation is usually called Bogoliubov approximation. Then in the complete field operator the classical field of the condensate can be split from the rest: $\hat{\psi} = \psi_0(\vec{r},t) + \delta\hat{\psi}(\vec{r},t)$. At zero temperature one can neglect

$\delta\hat{\psi}$, and Eq. (2.18) transforms into the Gross-Pitaevskii Equation (GPE):

$$i\hbar\frac{\partial}{\partial t}\psi_0 = \left(-\frac{\hbar^2\triangle}{2m} + V(\vec{r}) + U_{gg}|\psi_0|^2\right)\psi_0. \tag{2.19}$$

also called nonlinear Schrödinger equation. In addition to the external trap $V(\vec{r})$, the particles feel the mean-field potential $U_{gg}|\psi_0|^2$ provided by the other condensate particles.

The ground-state solution is obtained from the time-independent GPE, which is obtained after substituting $\psi_0(\vec{r}) \rightarrow \psi_0(\vec{r})\exp[-i\mu t]$ in Eq. (2.19) :

$$H_{GP}\psi_0(\vec{r}) = \left(-\frac{\hbar^2\triangle}{2m} + V(\vec{r}) + U_{gg}|\psi_0(\vec{r})|^2 - \mu\right)\psi_0(\vec{r}). \tag{2.20}$$

The normalization of the condensate wave function $N = \int d^3r|\psi_0|^2$ provides the relation between chemical potential μ and number of atoms N in the condensate.

There are two main energy scales involved in the case of trapped BEC. On one side the interaction energy E_{int}, and on the other side the characteristic energy $E_{HO} = \hbar\omega$ of the harmonic oscillator. Depending on the relation between these scales, we can distinguish two interaction regimes: weak-condensation and Thomas-Fermi regime. The former is characterized by $E_{H0} \gg E_{int}$. In this regime the basis of harmonic oscillator states can be employed, and the effects of interactions can be included employing Boltzmann equations describing the collisional transitions between different energy levels [52]. On the contrary, the Thomas-Fermi regime is characterized by $E_{H0} \ll E_{int}$. In this regime the kinetic energy term in Eq. (2.20) can be neglected, and an analytical expression can be found for the density profile of the ground state:

$$n_{TF}(\vec{r}) = \psi_0^{TF}(\vec{r})^2 = \frac{\mu - V(\vec{r})}{U_{gg}}, \tag{2.21}$$

where the expression for the chemical potential μ is given by the normaliza-

tion of the density to the number of atoms:

$$\mu = \frac{\hbar\omega}{2}\left(\frac{15Na_{sc}}{x_0}\right)^{2/5}. \tag{2.22}$$

where $x_0 = \sqrt{\hbar/m\omega}$ is the oscillator length. The density profile has the form of an inverted parabola which vanishes at $\vec{R}$ (so-called Thomas-Fermi radius) defined by the condition $V(\vec{R}) = \mu$. In a spherical trap,

$$R = x_0\left(\frac{15Na_{sc}}{x_0}\right)^{1/5}. \tag{2.23}$$

2.3.3 Bogoliubov-de Gennes equations

For sufficiently low temperatures, one can consider the density of thermal particles much smaller than that of condensed ones. In that case we can linearize Eq. (2.18) in $\delta\hat{\psi}$ to obtain

$$i\hbar\dot{\delta\hat{\psi}} = \left(-\frac{\hbar^2\triangle}{2m} + V(\vec{r}) - \mu + 2U_{gg}|\psi_0|^2\right)\delta\hat{\psi} + U_{gg}(\psi_0^*)^2\delta\hat{\psi}^\dagger \tag{2.24}$$

$$-i\hbar\dot{\delta\hat{\psi}}^\dagger = \left(-\frac{\hbar^2\triangle}{2m} + V(\vec{r}) - \mu + 2U_{gg}|\psi_0|^2\right)\delta\hat{\psi}^\dagger + U_{gg}(\psi_0^*)^2\delta\hat{\psi}, \tag{2.25}$$

where the time dependence of the ground state has been explicitly separated $\delta\hat{\psi}(\vec{r},t) \rightarrow \exp[-i\mu t]\delta\hat{\psi}$. After applying the so-called Bogoliubov transformation

$$\delta\hat{\psi} = \sum_n u_n^*(\vec{r})\hat{g}_n\exp[-i\epsilon_n t] - v_n(\vec{r})\hat{g}_n^\dagger\exp[i\epsilon_n t] \tag{2.26}$$

to Eq. (2.25), we obtain a system of linear equations

$$\epsilon_n\begin{pmatrix} u_n \\ v_n \end{pmatrix} = \begin{pmatrix} H_{GP} + U_{gg}|\psi_0|^2 & U_{gg}\psi_0^2 \\ U_{gg}(\psi_0^*)^2 & -(H_{GP} + U_{gg}|\psi_0|^2)^* \end{pmatrix}\begin{pmatrix} u_n \\ v_n \end{pmatrix}, \tag{2.27}$$

where u_n,v_n are the eigenfunctions, and ϵ_n are the corresponding eigenvalues. The eigenfunctions u_n,v_n fulfill the orthonormalization relation

$$\int d^3r(u_n(\vec{r})u_k^*(\vec{r}) - v_n(\vec{r})v_k^*(\vec{r})) = \delta_{nk}. \tag{2.28}$$

In order to make sense of the diagonalization of the previous equations, the perturbation $\delta\hat{\psi}$ must be orthogonal to the condensate wave function. To this aim, we employ the projection operators [53]

$$\begin{aligned} Q &= 1 - |\psi_0\rangle\langle\psi_0| \\ Q^* &= 1 - |\psi_0^*\rangle\langle\psi_0^*|, \end{aligned}$$

to transform Eq. (2.27) into:

$$\epsilon_n \begin{pmatrix} u_n \\ v_n \end{pmatrix} = \mathcal{L} \begin{pmatrix} u_n \\ v_n \end{pmatrix}, \tag{2.29}$$

where

$$\mathcal{L} = \begin{pmatrix} H_{GP} + U_{gg}Q|\psi_0|^2Q & U_{gg}Q\psi_0^2Q^* \\ U_{gg}Q^*(\psi_0^*)^2Q & -(H_{GP} + U_{gg}Q|\psi_0|^2Q)^* \end{pmatrix}. \tag{2.30}$$

With this set of equations we ensure $\langle\psi_0|\delta\psi\rangle = 0$. After applying Eq. (2.26) to Eq. (2.18) we obtain

$$\hat{H} = \hat{H}_0 + \sum_{n\neq 0} \epsilon_n \hat{g}_n^\dagger \hat{g}_n, \tag{2.31}$$

where $\hat{H}_0 = E(N_0)\hat{g}_0^\dagger\hat{g}_0$ is the ground state energy, and $\hat{g}_n$ ($\hat{g}_n^\dagger$) is the annihilation (creation) operator of a quasiparticle with energy ϵ_n.

The mean thermal density can be easily obtained

$$n_{th}(\vec{r}) = \langle\delta\hat{\psi}^\dagger\delta\hat{\psi}\rangle = \sum_n \langle\hat{g}_n^\dagger\hat{g}_n\rangle(|u_n(\vec{r})|^2 + |v_n(\vec{r})|^2) + |v_n(\vec{r})|^2, \tag{2.32}$$

where $\langle\hat{g}_n^\dagger\hat{g}_n\rangle = [\exp[\epsilon_n/K_BT] - 1]^{-1}$. Note that even at zero temperature a finite number of thermal atoms remain, constituting the so-called quantum depletion of the condensate. The mean energy is obtained from the stationary form of Eq. (2.18)

$\langle E - \mu N\rangle =$

$$\sum_n \left\{ \langle \hat{g}_n^\dagger \hat{g}_n \rangle \epsilon_n - \int d^3r \epsilon_n |v_n|^2 + \frac{U_{gg}}{2}(2\langle \hat{g}_n^\dagger \hat{g}_n \rangle + 1) \int d^3r (u_n^* v_n - v_n^* u_n) \right\}$$
$$+ \langle \psi_0 | H_{GP} - \frac{U_{gg}}{2} |\psi_0|^2 |\psi_0 \rangle. \tag{2.33}$$

If the condensate wave function is real everything else (as Q,ψ_0^2,ϵ_n,u_n,and v_n) is also real.That simplifies the upper equation to:

$$\langle E \rangle = E_0(N_0) \tag{2.34}$$
$$- \int d^3r |v_n|^2 (\epsilon_n - \mu) + \sum_n \langle \hat{g}_n^\dagger \hat{g}_n \rangle (\epsilon_n + \mu \int d^3r (|u_n(\vec{r})|^2 + |v_n(\vec{r})|^2)),$$

where $E_0(N_0) = \langle \psi_0 | H_{GP} - \frac{U_{gg}}{2} |\psi_0|^2 |\psi_0 \rangle$.

2.3.4 What makes the Bose-Einstein Condensate interesting?

During the last years, and especially after its first experimental observation in 1995, the BEC has aroused a huge interest. It would be certainly difficult to summarize even briefly the large number of very important recent contributions, both theoretical and experimental, in this active field. We would like however to discuss as concise as possible why BEC has attracted such an attention. On one side, BEC offers an extraordinary opportunity to test condensed matter and low–temperature phenomena. In this respect, several striking results have been reported concerning superfluidity phenomena [54, 55], and generation and dynamics of vortices [56, 57]. On the other hand, the macroscopically occupied matter wave can be manipulated by atom optical elements, that can be combined to provide new tools for precision experiments [58]. Besides passive optical elements recently also active elements, that provide phase coherent gain have been demonstrated [59, 60]. Also a new field, called Non–Linear Atom Optics (NLAO), has rapidly developed during the last years. Several remarkable experiments have been recently reported in this area, as reflection of BEC from an optical mirror[61], four–wave mixing [62] of matter waves, dark–solitons [63, 64], bright–solitons [65, 66], and even condensate collapse [67]. The physics of BEC is therefore character-

ized by an intrinsic interdisciplinarity, being a common and fruitful research field for physicist belonging to disparate communities as Quantum Optics, Condensed Matter Physics, Nonlinear Physics, etc. This interdisciplinarity, and the large degree of control available for the experiments involved in this field, explain at least partially the interest on BEC. We should finally remark that the importance of this research field was recently recognized with the Nobel Price Award 2001 to E. Cornell, C. Wieman and W. Ketterle, which add up to the Nobel Price Award 1997 to W. Phillips, C. Cohen-Tannoudji and S. Chu, who receive the award for their developments in laser cooling and trapping of neutral atoms.

2.4 Atom Laser

During the last twenty years the improvement in cooling and trapping techniques has lead to the rapid growth of the so-called Atom Optics. Atom Optics explores the matter-wave phenomenology which appears in ultra cold atoms. Several remarkable effects have been reported in this area, as atom reflection, atom focusing, atom diffraction, etc. For a review, see e.g. [68]. The discovery of the laser constitutes without any doubts one of the most fundamental achievements in standard light optics, opening the way to a coherent control of atom-light interaction. Following with the analogy between atom and light optics, it was therefore natural to explore the possibilities to achieve an atom laser. In the following we shall define in more detail what can be understood under the concept of atom laser, and how it has been obtained experimentally. Finally, we shall address the issue of continuous loading of an atom laser, which constitutes an essential part of this Thesis.

2.4.1 What is an atom laser?

The term “Atom Laser” has been coined to describe a highly “monochromatic” coherent matter-wave source. When referred to matter waves, the concept of monochromaticity indicates a narrow momentum distribution, i.e. following our discussion in Sec. 1.2 an ultracold atomic sample. The concept

of coherence refers to the existence of a common phase between the atoms produced by an Atom Laser. Such a source of coherent monochromatic matter waves can be achieved by outcoupling atoms from a BEC. As previously discussed, the ultra cold atoms of a BEC share a common quantum state, and they are therefore natural candidates to accomplish a coherent matter-wave source.

Before continuing with the description of an atom laser, and how the atom lasers have been actually obtained experimentally, it is of interest to recall some important concepts related with the physics of optical lasers. The essential components of a laser are basically three: an active medium, a resonator, and an outcoupler. The active medium is composed by excited atoms, whose population has been inverted (more population in an excited electronic state than in the ground state) by means of an external pumping. The population inversion is a key concept to achieve the light amplification by stimulated emission [69], related with the concept of bosonic enhancement for the emission of photons in the laser mode. The resonator is composed by an optical cavity, which in its simpler version is formed by two oppositely-placed highly-reflecting mirrors. The resonator is employed to multiply the light amplification by passing multiple times through the active medium, and additionally acts as a Fabry-Pérot interferometer, selecting a specific wavelength. Finally, the laser light must be outcoupled, to this aim one of the mirrors possesses an imperfect reflectivity, and the laser light is outcoupled through it.

Let us return to the atom laser concept, comparing it with its light counterpart. As previously commented an atom laser can be achieved by outcoupling atoms from a trapped BEC. In a natural way, the trapping potential can be related with the resonator of a standard laser. The different energy levels within the trap play the role of the lasing modes, being the condensate the main mode of the atom laser. In the case of a light laser the pumped energy leads to an inverted population of the active medium, which finally leads to the production of the laser via stimulated emission. In the case of matter waves, the situation is certainly more complicated, since the atoms cannot be created by simply pumping energy to the system. It is necessary to possess

a reservoir of atoms, which must be pumped into the condensate mode. Of course this process is helped by the bosonic enhancement, and in this sense certainly resembles the physics of the active medium. The continuous pumping into a BEC constitutes nowadays an open question, and will be discussed extensively in the rest of this section, and in the following chapters of this Thesis. Finally, the condensate atoms must be outcoupled. The latter can be achieved in two different ways. If the atoms are confined in a magnetic trap, a properly designed radio frequency pulse can transfer part of the atoms into a state with different magnetic moment which is not trapped. These atoms are therefore extracted. This is the basis of the so-called rf-outcoupling [6]. This technique is exactly the same as that previously discussed in evaporative cooling, although in the present case the coldest atoms are outcoupled, and not the hottest ones as in evaporative cooling. The second technique consists in employing Raman pulses to transfer the corresponding recoil momentum to part of the condensate atoms [10]. The transferred energy is enough to outcouple the atoms. This technique presents the advantage of controlling the direction of the outcoupled atoms, whereas the rf-outcoupling usually relies in the gravitation field.

2.4.2 Continuous Loading of a BEC

Both rf- and Raman-outcoupling have been employed experimentally to achieve quasi-continuous outcoupling. However, the continuous outcoupling represents just a half way towards a cw atom laser. Without a continuous refilling of the BEC, the atom laser output lasts only as long as sufficient atoms in the BEC are kept. In addition, the continuous refilling of the condensate could be employed to repair a condensate against inelastic losses, and in this way it could allow to analyze the BEC physics at larger densities, at much longer time scales, and eventually without the necessity of a very high vacuum. Recently, an experiment using an optical tweezer has been performed in this sense at MIT [11]. Two different physical mechanisms could provide a continuous pumping into a condensate: collisional and optical loading. We shall discuss in this subsection both methods.

2.4.2.1 Collisional loading

The collisional loading of a BEC is based in the collision of two non-condensed atoms from a reservoir, which results in one of them being pumping into the condensate, whereas the other carries most of the energy and it is evaporated. as previously commented, the pumping of an atom into the condensate if favored by the bosonic enhancement, resembling the stimulated emission in the active medium of a laser. There are different possible routes to achieve the continuous or quasi-continuous collisional loading of a BEC. A first proposal

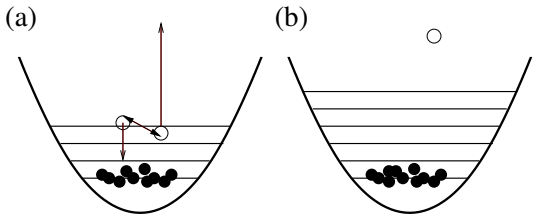

Figure 2.1: Collisional loading of a BEC: (a) two thermal atoms collide; (b) one atom is pumped into the condensate whereas the other is evaporated.

[70] considers the pumping of atoms into a long magnetic waveguide, where evaporative cooling is undergone in the radial direction. At the end of the waveguide the atoms are assumed to enter into the (3D) degenerated regime. This proposal, however, faces difficult technical problems. Due to the key role of evaporative cooling in the proposal, it is necessary a very large flux of cold and slow atoms into the guide. On one side the large flux should maintain a sufficient collisional rate, and on the other side the atoms must be slow enough since the guide is necessarily limited in space. A more recent proposal [71] discusses a similar approach. Although also relying on the effect of collisions and evaporative cooling, in this proposal a slow dense atomic beam is assumed, being the interest more focused in the role of collisions to achieve a continuous trapping of atoms. Under appropriate conditions the subsequent evaporative cooling in an non isotropic trap could lead to an increase of the phase-space density by a factor of $500 - 900$. Finally, a recent experimental work [11] has explored the refilling of a condensate by means of transporting a secondary BEC into the region where the main BEC is

placed. To this aim a BEC is kept in a a vacuum chamber, whereas another BEC is created in a secondary one. The newly produced BEC is transported by means of an optical tweezer into the region of the original BEC. The two BECs are merged, and the excess energy produced by the merging is rapidly evaporated.

2.4.2.2 Optical loading

The optical loading mechanism relies in the pumping of reservoir atoms in an (electronic) excited state into the BEC via spontaneous emission [72]. If the reservoir could be filled in a (quasi-) continuous way by laser cooling techniques, one would benefit from the large cooling efficiency of laser cooling compared to evaporative cooling, allowing for a considerable increase in atomic flux produced by an atom laser. For the latter, it is crucial that the spontaneously emitted photons cannot be reabsorbed, because otherwise a heating could be introduced in the system, and BEC can be neither achieved nor maintained [73] (see discussion below). This thesis is mainly devoted to the discussion of different issues related with the physics of the continuous optical loading of a condensate. Several aspects must be carefully considered in this sense, including the evolution of the condensate temperature during the loading, the condensate formation, the role of collisions in different interaction regimes, and the important problem of photon reabsorption. We shall consider the latter problem in detail in the next subsection. The other issues and other important points related with optical loading will be discussed in the next chapters of this Thesis.

2.4.3 Reabsorption problem

The subrecoil laser cooling techniques discussed in Sec. 1.3 were based in the key concept of dark state, i.e. a state which was dark with respect to the cooling laser. The dark character of a particular state is crucially determined by the coherent nature of the laser light. Therefore those photons spontaneously scattered by neighbor atoms can be absorbed by an atom in a dark state, and as a consequence the cooling mechanism becomes inefficient. This

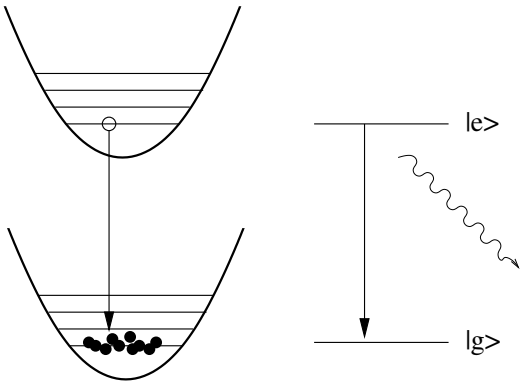

Figure 2.2: Optical loading of a BEC: a trapped atom in the electronic excited state $|e\rangle$ decays spontaneously into the (also trapped) ground-state $|e\rangle$. As a result a photon is emitted.

fact receives the name of reabsorption problem, and constitutes a serious limitation towards the all optical achievement of a BEC [73]. Similarly, photon reabsorption is an important problem which should be carefully addressed when considering models of optical loading.

The reabsorption can lead to "bad" processes, as illustrated in Fig. 2.3. An excited atom decays into the condensate, the emitted photon is reabsorbed by an already condensed atom, which after a second spontaneous emission ends in an excited external state of the $|g\rangle$-trap. All together this process leads clearly to heating. On the other hand reabsorption can lead

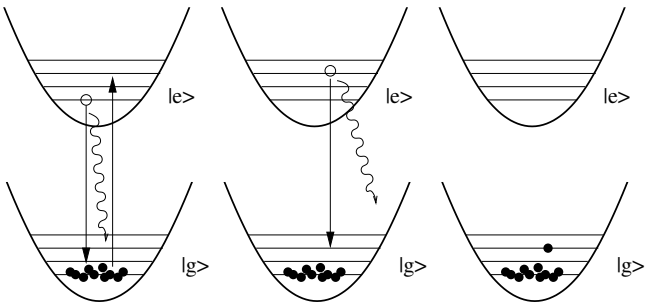

Figure 2.3: "Bad" reabsorptions. From left to right: an excited atom decays via spontaneous emission into the condensate; the photon is reabsorbed by an already condensed atom; after a final spontaneous emission this atom decays into an excited state of the ground-state trap.

also to "good" (cooling) processes, as shown in Fig. 2.4. An excited atom undergoes a transition into the condensate, and the emitted photon is not reabsorbed by a condensate atom but by an atom in an excited state of the ground-state trap. After a second spontaneous emission the second atom can finish in the condensate. That means that this process leads to two atoms more in the condensate by just one pumping process. Unfortunately, the

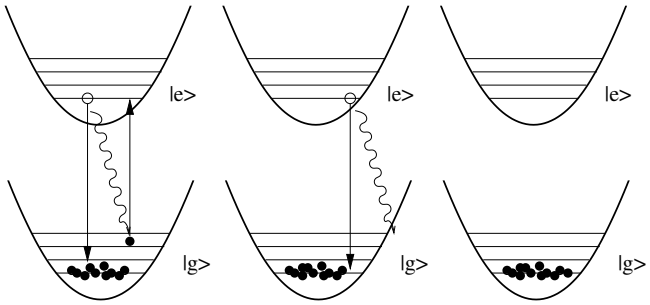

Figure 2.4: "Good" reabsorption. From left to right: an excited atom decays into the condensate; the photon is reabsorbed by an atom in an excited state of the ground-state trap; this atom decays into the condensate.

heating effects of the reabsorption are in general dominant, and the reabsorption problem becomes, as previously commented, a crucial problem in optical thick samples. The latter is easy to understand from purely geometrical considerations. Assuming an atomic cross section with the emitted photon $a_{cr} \sim \lambda^2$, with λ the photon wavelength, and a mean distance D between the atoms, the classically probability for the absorption of the photon is $p \sim \lambda^2/D^2$, i.e. the ratio of the cross section to the surface of a sphere of radius D around the emitting atom. D. Since D in a condensate is of the order of the thermal de-Broglie wave length, which is very small, the reabsorption probability becomes certainly large, leading (if not properly handled) to heating, and eventually to the destruction of the condensate.

2.4.3.1 Avoiding the reabsorption

Several possible dynamical and geometrical solutions for the reabsorption problem have been proposed during the last few years. The geometrical proposals are based on the reduction of the dimensionality of the traps [74,

73]. It is easy to understand that assuming that the reabsorption cross section for trapped atoms is the same as in free space, i.e. $\simeq \lambda^2$, the significance of reabsorptions increases with the dimensionality, in such a way that the reabsorptions should not cause any problem in one dimension, have to be carefully considered in two dimensions, and forbid condensation in three dimensions. Therefore, cigar- and disc-shape traps have been suggested. However even severe deformations of the trap do not allow more than modest reductions of the reabsorption heating [75]. Other suggestion consists in using a strongly confining trap with a frequency $\omega \simeq \omega_R$. In this case, it has been proved [76] that in two atom systems the relative role of reabsorption in such a trap can be significantly reduced. It is, however, not clear whether this result would hold for many atom systems.

Another promising remedy against reabsorption heating employs the dependence of the reabsorption probability for trapped atoms on the fluorescence rate γ, which can be adjusted at will in dark state cooling [75]. In particular, in the interesting regime, in which γ is much smaller than the trap frequency ω, i.e. in the so called *Festina Lente* limit [32], the reabsorption processes, in which the atoms change energy and undergo heating, are practically completely suppressed. This is easy to understand since in the Festina Lente regime, the atomic levels in the trap are well resolved, since their width is smaller than the level spacing. As a consequence subsequent reabsorptions cannot increase the energy of the trapped atoms. On the contrary if the width of the levels becomes larger than the spacing of the atomic levels, those processes increasing the energy of the atoms in the trap will be allowed, and heating could not be avoided. The conditions for the Festina Lente regime are more easily fulfilled in dipolar traps where the trap frequency can be made considerably larger than in a magnetic trap. However, the Festina Lente regime implies slow cooling (or loading) rates, and could therefore be of limited use in the case of e.g. loading of a BEC. In this Thesis we shall discuss two different alternative regimes where the negative effects of photon reabsorption can be avoided. In chapter 3 we show that due to quantum interferences the reabsorption could lead to cooling of the condensate in the so-called Bosonic–Accumulation regime [13]. In chapter 4, we

demonstrate that when an atom possesses an accessible three level Λ scheme, where one of the atomic transitions decays much faster than the other, the reabsorptions in the slow transition can be largely suppressed, without the time limitations of Festina Lente [77].

Chapter 3

Optical loading in the Boson–Accumulation Regime

3.1 Introduction

In this chapter we begin our analysis of the study of the loading of a BEC, which is formed in a trapped electronic ground–state $|g\rangle$, via spontaneous decay of atoms from an also trapped internal excited state $|e\rangle$. In particular, we shall consider in the present chapter the regime $N_0 \gg a, N - N_0$, where a is the effective number of levels other than the condensed one to which the excited atoms may decay, N is the total number of atoms in the $|g\rangle$ trap, and N_0 is the number of condensed ones. If this is the case the excited atom will decay into the condensate with high probability, due to bosonic enhancement. Such regime has been called the *Boson–Accumulation Regime* (BAR) [13]. Note, however, that even in the BAR, in the absence of reabsorption, simple arguments imply that the mean proportion of atoms in the condensate after the decay decreases [13]. If the reabsorptions are present, each subsequent decay would lead to an even larger decrease of the condensate proportion; thus for an optically thick sample (where many reabsorptions take place) the number of condensed atoms would be reduced dramatically. However, these arguments are not rigorously valid in general. In Ref. [13] it was reported that a fully quantum treatment shows that the reabsorption processes can,

under certain conditions, help to increase the proportion of atoms in the BEC. This counterintuitive result was explained by means of an interference effect between different paths (which include reabsorptions) that lead to the same final states. This effect offers an interesting mechanism of continuous refilling and loading of a condensate.

The treatment of Ref. [13] was based on an extremely simplified 1D model in which all the ground states were taken into account, but in which there was a single excited level. In addition, the calculations of Ref. [13] did not consider the different Frank-Condon factors for the different possible decays. In this chapter, we analyze the BAR regime in a much more general model. We consider a 3D trap, and the possibility of more than one excited trap level. In addition, the Frank-Condon factors for the different decays are explicitly included in the calculations. We demonstrate that even for this much more complicated situation, under some conditions the reabsorption still helps to load atoms into the condensate.

This chapter is organized as follows. In Sec. 3.2 we introduce the model under consideration. Sec. 3.3 is devoted to the discussion of the BAR expansion. In Sec. 3.4 we discuss our numerical results.

3.2 Model

Let us consider a set of bosonic atoms with two internal levels $|g\rangle$ and $|e\rangle$ confined in a dipole harmonic trap, which for simplicity is considered isotropic, with frequency ω. We denote as N_m the population of the m-th level of the $|g\rangle$ trap, where $m \equiv (m_x, m_y, m_z)$, and assume that the ground state trap verifies the BAR conditions. We analyze the situation in which a single atom in some state $|e, l\rangle$ ($l \equiv (l_x, l_y, l_z)$) decays via spontaneous emission into the $|g\rangle$ trap, producing a photon which can eventually be reabsorbed by another $|g\rangle$ atom (in particular by a condensed one), which in turn can later decay again, and so on. At some finite time, the scattered photon is no more reabsorbed and leaves the system. It is our aim to investigate how the atom distribution in the $|g\rangle$ trap changes during this process.

For simplicity we do not consider in this chapter the collisional mean–

field effects (for a discussion of these effects see chapter 5). For typical s–wave scattering lengths this implies that in principle our results could be obtained for few atoms only (since we consider relatively small traps); one should point out , however, that although our calculations are limited to small traps, the BAR effect should be present also for larger ones, and in the presence of collisions. Although the main purpose of this chapter is to discuss a fundamental quantum effect and to present the methodology needed to study it, we must also point out that recent experiments [78, 79] have shown that the s-wave scattering length can be modified by using Feshbach resonances. In particular, the regime of quasi–ideal gas can be experimentally achieved, in which the mean–field energy can be considered smaller than the trap energy. In such regime, the collisions introduce just a thermalization mechanism [80], and two and three–body collisional losses are almost absent [81]. For such modified scattering length our results are valid for much larger N.

Starting from the Hamiltonian which describes the bosons interacting with the quantized electromagnetic field, and using standard techniques, one can derive the master equation (ME) for the reduced density operator for the atomic degrees of freedom (see App. A), which assuming $\hbar = 1$ becomes

$$\dot{\rho} = -iH_{eff}\rho + i\rho H_{eff}^{\dagger} + J\rho, \tag{3.1}$$

where

$$H_{eff} = \sum_{l=0}^{\infty}(\omega_l^e+\omega_0-i\frac{\Gamma}{2})e_l^{\dagger}e_l+\sum_{k=0}^{\infty}\omega_k^g g_k^{\dagger}g_k-i\frac{\Gamma}{2}\sum_{l,l'}^{\infty}\sum_{m,m'}^{\infty}\alpha_{lmm'l'}g_{m'}^{\dagger}g_m e_l^{\dagger}e_{l'}, \tag{3.2}$$

is a non-Hermitian effective Hamiltonian, and

$$J\rho = \Gamma\sum_{l,l'}^{\infty}\sum_{m,m'}^{\infty}\alpha_{lmm'l'}^{r}g_{m'}^{\dagger}e_{l'}\rho e_l^{\dagger}g_m. \tag{3.3}$$

is the jump operator. Here, e_l (g_m) is the annihilation operator for atoms in the l–th (m–th) excited (ground) level, ω_l^e (ω_m^g) is the energy corresponding to such state, and Γ is the spontaneous emission rate from the excited level.

The complex coefficients $\alpha_{lmm'l'}$ (whose explicit form can be found in [13]) are related to the Frank-Condon factors for the different excited–ground transitions. We denote in the following $\eta_{lm} = \langle l| \exp[i\vec{k}\vec{r}]|m\rangle$ the Frank-Condon factor for the transition between the l–th excited level and the m-th ground level. The real part of the $\alpha_{lmm'l'}$ coefficient is

$$\alpha^r_{lmm'l'}(k_0) = \int d\Omega \mathcal{W}(\Omega)\eta_{lm}(k_0,\Omega)\eta_{l'm'}(k_0,\Omega)^* \tag{3.4}$$

and the imaginary part is

$$\alpha^i_{lmm'l'}(k_0) = -\frac{P}{\pi}\int_{-\infty}^{\infty} du \frac{u^3}{u-1}\alpha^r_{lmm'l'}(uk_0), \tag{3.5}$$

where P denotes the Cauchy Principal part of the integral, k_0 is the absolute value of the photon wavenumber associated with the $|g\rangle \leftrightarrow |e\rangle$ transition, and $\mathcal{W}(\Omega)$ is the dipole pattern of the spontaneous emission.

3.3 BAR expansion

We consider an initial situation in which N_m atoms occupy the m-th state of the ground–state trap, and a single excited atom is placed (with some probability given by a thermal distribution) in a state j of its corresponding trap. We denote the initial state as $|\psi_0\rangle$, and therefore the initial density matrix is defined as

$$\rho_N = |\psi_0\rangle\langle\psi_0| = |N_0, N_1, \cdots\rangle_g \otimes |j\rangle_e\langle j| \otimes_g \langle N_0, N_1, \cdots|. \tag{3.6}$$

After a photon is released without further reabsorptions, we obtain the formal solution ρ_{N+1} of the ME (3.1):

$$\rho_{\mathrm{N+1}} = \int_0^{\infty} dt \mathcal{J}[e^{-i\hat{H}_{eff}t}\rho_N e^{i\hat{H}_{eff}t}], \tag{3.7}$$

and calculate the probability to obtain a particular final state $|\psi_f\rangle = |N'_0, N'_1, \cdots\rangle_g \otimes |\Omega\rangle_e$ ($|\Omega\rangle$: vacuum) with N'_m atoms in the m-th $|g\rangle$ trap level

(and no atom in the excited state trap):

$$\langle\psi_f|\rho_{N+1}|\psi_f\rangle = \Gamma\int_0^\infty dt\int\frac{d\Omega}{4\pi}\left|\sum_{l,m=0}\eta^*_{lm}\langle\psi_f|g_m^\dagger e_l e^{-iH_{eff}t}|\psi_0\rangle\right|^2. \tag{3.8}$$

After expanding $\exp[-iH_{eff}t]$ into powers of the small parameter $N_0^{-1/2}$

$$\begin{aligned} e^{-iH_{eff}t} &= e^{-iH^{(0)}_{eff}t} \\ &\quad -i\int_0^t d\tau e^{-iH^{(0)}_{eff}(t-\tau)}H^{(1)}_{eff}e^{-i(H^{(0)}_{eff})^\dagger\tau} \\ &\quad -i\int_0^t d\tau e^{-iH^{(0)}_{eff}(t-\tau)}H^{(2)}_{eff}e^{-i(H^{(0)}_{eff})^\dagger\tau} \\ &\quad -i\int_0^t d\tau d\tau' e^{-iH^{(0)}_{eff}(t-\tau)}H^{(1)}_{eff}e^{-iH^{(0)}_{eff}(\tau-\tau')}H^{(1)}_{eff}e^{-i(H^{(0)}_{eff})^\dagger\tau'} \\ &\quad +O(N_0^{-3/2}) \end{aligned} \tag{3.9}$$

and neglecting terms of order $\mathcal{O}(N_0^{-3/2})$, such probability takes the form

$$\begin{aligned} &\langle\psi_f|\rho_{N+1}|\psi_f\rangle = \\ &\quad \frac{2}{N_0}\int_0^\infty dt\int\frac{d\Omega}{4\pi}\left|\sum_l\eta^*_{l0}|\langle\psi_f|g_0^\dagger e_l A_1|\psi_0\rangle + \sum_{l,m\neq0}\eta^*_{lm}\langle\psi_f|g_m^\dagger e_l A_0|\psi_0\rangle\right|^2 \end{aligned} \tag{3.10}$$

with $A_0(t) = \exp[-iH^{(0)}_{eff}t]$ and

$$A_1 = -i\int_0^t d\tau\exp[-iH^{(0)}_{eff}(t-\tau)]H^{(1)}_{eff}\exp[-iH^{(0)}_{eff}\tau] \tag{3.11}$$

being the terms of $\exp[-iH_{eff}t]$ of order 0 and 1 in $1/N_0^{1/2}$, where

$$H^{(0)}_{eff} = \omega_0^g g_0^\dagger g_0 - i\frac{\Gamma}{2}\sum_{l,l'}^\infty\alpha_{l00'l'}g_0^\dagger g_0 e_l^\dagger e_{l'}, \tag{3.12}$$

and

$$H^{(1)}_{eff} = -i\frac{\Gamma}{2}\sum_{l,l'}^\infty\sum_{m\neq0}^\infty\{\alpha_{lm0l'}g_0^\dagger g_m + \alpha_{l0ml'}g_m^\dagger g_0\}e_l^\dagger e_{l'}, \tag{3.13}$$

are respectively the terms of H_{eff} of zeroth and first order in $1/N_0^{1/2}$. Therefore, beginning from an initial relative number of condensate particles $n = N_0/N$, up to order $\mathcal{O}(1/N_0^2)$, the new relative number of condensed atoms after the last decay becomes

$$n' = \frac{N_0 + 1 + (P_{N_0+2} - P_{N_0})}{N+1}, \tag{3.14}$$

where P_{N_0+2} (P_{N_0}) is the probability to have after the process $N_0' = N_0 + 2$ (N_0). Let $|\psi_f^{(2,s)}\rangle$ be the final state with $N_0' = N_0 + 2$, $N_s' = N_s - 1$, and $N_{j\neq 0,2}' = N_j$. The probability to decay into such a state is given by:

$$P^s_{N_0+2} = \langle\psi_f^{(2,s)}|\rho_{N+1}|\psi_f^{(2,s)}\rangle = \frac{2}{N_0}\int_0^\infty dt \int \frac{\Omega}{4\pi}\left|\sum_{l,m\neq 0}\eta^*_{lm}\langle\psi_f^{(2,s)}|g_m^\dagger e_l A_0(t)|\psi_0\rangle\right|^2 . \tag{3.15}$$

The corresponding process is schematically represented in Fig. 3.1(a). Let us also define $|\psi_f^{(0,s)}\rangle$ as the final state with $N_0' = N_0$, $N_s' = N_s + 1$ and $N_{j\neq 0,2}' = N_j$.

The probability to decay into this state takes the form:

$$\begin{aligned} P^s_{N_0} = \langle\psi_f^{(0,s)}|\rho_{N+1}|\psi_f^{(0,s)}\rangle = & \\ \frac{2}{N_0}\int_0^\infty dt \int \frac{\Omega}{4\pi}\left|\sum_{l}\eta^*_{l0}\langle\psi_f^{(0,s)}|g_0^\dagger e_l A_1(t)|\psi_0\rangle\right|^2 & \\ + \left|\sum_{l,m\neq 0}\eta^*_{lm}\langle\psi_f^{(0,s)}|g_m^\dagger e_l A_0(t)|\psi_0\rangle\right|^2 & \\ + 2\Re\left\{\sum_l \eta^*_{l0}|\langle\psi_f^{(0,s)}|g_0^\dagger e_l A_1(t)|\psi_0\rangle\left(\sum_{l,m\neq 0}\eta^*_{lm}\langle\psi_f^{(0,s)}|g_m^\dagger e_l A_0(t)|\psi_0\rangle\right)^*\right\} & \end{aligned} \tag{3.16}$$

where $\Re$ denotes the real part. The first and second terms in Eq. (3.16) are respectively depicted in Fig. 3.1(b) and (c), whereas the last term corresponds to the interference between the energetically equivalent paths which are shown in that figures.

From Eqs. (3.15), (3.16) one obtains $P_{N_0+2} = \sum_s < P^s_{N_0+2} >$, and

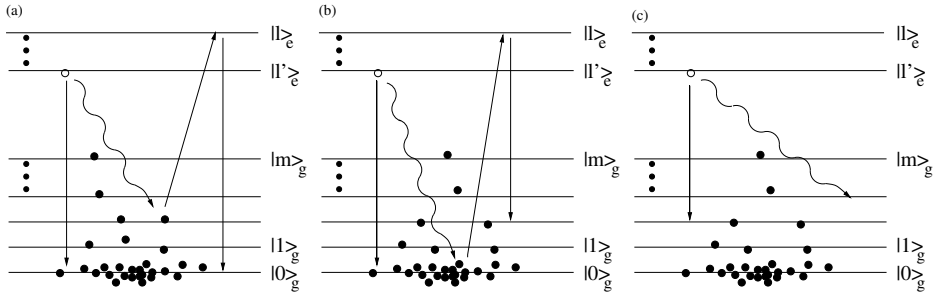

Figure 3.1: Schematic representation of the different processes appearing in Eqs. (3.15) and (3.16). Straight lines denote atomic transitions, whereas waved lines represent the photons produced in the decays. Note the possibility of reabsorption in Figs. (a) and (b).

$P_{N_0} = \sum_s < P^s_{N_0} >$, where <> denotes the average of the possible initial ground–state populations following the corresponding Bose–Einstein distribution at a given temperature T_g. We have numerically calculated the probabilities P_{N_0} and P_{N_0+2}. From Eqs. (3.15),(3.16) it becomes clear that such calculation requires to take into account all the possible paths connecting a particular initial and final state which eventually involves an arbitrary number of emission-reabsorption cycles. This fact by itself makes the calculation extremely demanding. In addition, several important technical difficulties appear. First, we must note that in order to calculate the coefficients A_0 and A_1, one has to evaluate the exponential $\exp(-i\hat{M}t)$, where

$$\hat{M} = \sum_{l,l'} \alpha_{l00l'} e_l^\dagger e_{l'} \tag{3.17}$$

is not an Hermitian matrix. The real part of the complex $\alpha_{l00l'}$ coefficient acquires the form

$$\begin{aligned}\alpha^r_{l00l'}(k_0) = \frac{1}{4\pi}\int d\Omega \eta_{l0}(k_0,\Omega)\eta_{l'0}(k_0,\Omega)^* = e^{-\eta^2}\eta^{\vec{l}+\vec{l}'} \\ \times\frac{1}{16\pi}\frac{(-1)^{(\vec{l}-\vec{l}')/2}}{\sqrt{\vec{l}!\vec{l}'!}}(1+(-1)^{l_x+l'_x})(1+(-1)^{l_y+l'_y})(1+(-1)^{l_z+l'_z}) \\ \times B[\frac{l_x+l_y+l'_x+l'_y+2}{2},\frac{l_z+l'_z+1}{2}]B[\frac{l_y+l'_y+1}{2},\frac{l_x+l'_x+1}{2}]\end{aligned} \tag{3.18}$$

where $\eta^2 = E_R/\hbar\omega_g = k_0^2 x_0^2$ is the Lamb-Dicke parameter, where $x_0^2 = \hbar/2m\omega_g$ is the oscillator length. In Eq. (3.19) $B[l, l']$ denote the Beta functions. The imaginary part of α is:

$$\begin{aligned}\alpha^i_{l00l'} &= -\frac{P}{\pi}\int_{-\infty}^{\infty} du \frac{u^3}{u-1}\int \frac{d\Omega}{4\pi}\eta_{l0}(uk_0,\Omega)\eta^*_{l'0}(uk_0,\Omega) \\ &= -\frac{P}{\pi}\int_{-\infty}^{\infty} du \frac{u^3}{u-1}\alpha^r_{l00l'}(uk_0). \end{aligned} \tag{3.19}$$

Applying the solution of the Cauchy principal part (see App. B) , we obtain

$$\begin{aligned}\alpha_{l00l'} &= \frac{1}{16\pi}\frac{(-1)^{(\vec{l}-\vec{l}')/2}}{\sqrt{\vec{l}!\vec{l}'!}} \\ &\times(1+(-1)^{l_x+l'_x})(1+(-1)^{l_y+l'_y})(1+(-1)^{l_z+l'_z}) \\ &\times B[\frac{l_x+l_y+l'_x+l'_y+2}{2}, \frac{l_z+l'_z+1}{2}] \times B[\frac{l_y+l'_y+1}{2}, \frac{l_x+l'_x+1}{2}] \\ &\times\eta^{\vec{l}+\vec{l}'}(e^{-\eta^2} - i\frac{1}{2\pi}\sum_{i=0}^{\vec{l}+\vec{l}'+2}(1+(-1)^i)\eta^{-(1+i)}\Gamma(\frac{i+1}{2}) + i\mathrm{erf}(\eta)e^{-\eta^2}),\end{aligned} \tag{3.20}$$

where $\vec{l}-\vec{l}' = l_x+l_y+l_z-(l'_x+l'_y+l'_z)$, and $\vec{l}! = l_x!l_y!l_z!$.

As previously mentioned, $\hat{M}$ is non-Hermitian. Therefore, it becomes necessary to introduce a biorthogonal set of operators in order to diagonalize $\hat{M}$:

$$f^\dagger_R(k) = \sum_l v^R_l(k)e^\dagger_l, \tag{3.21}$$

and

$$f_L(k) = \sum_l \bar{v}^L_l(k)e_l, \tag{3.22}$$

where $v^R_l(k)$ and $\bar{v}^L_l(k)$ are the right and the left (complex conjugate) eigenvectors of $\hat{M}$, i.e.

$$\sum_j M_{ij}v^R_j(k) = \lambda_k v^R_i(k) \tag{3.23}$$

$$\sum_j \bar{v}^L_j(k)M_{ji} = \lambda_k \bar{v}^L_i(k), \tag{3.24}$$

where λ_k are the corresponding eigenvalues. Using this set of biorthogonal

operators the matrix $\hat{M}$ becomes

$$\hat{M} = \sum_k \lambda_k f_R^\dagger f_L. \tag{3.25}$$

The biorthogonal operators fulfill the commutation rules:

$$\begin{aligned} [f_L(k), f_R(k')] = \left[f_L^\dagger(k), f_R^\dagger(k')\right] &= 0, & (3.26)\\ \left[f_R(k), f_L^\dagger(k')\right] = \left[f_R^\dagger(k), f_L(k)\right] &= \delta_{k,k'}, & (3.27)\\ [f_L(k), M] &= \lambda_k f_L(k). & (3.28) \end{aligned}$$

Writing the transition probabilities, A_0, and A_1 in terms of the biorthogonal operators, using $e_l^\dagger = \sum_k \bar{v}_l^\dagger(k) f_R^\dagger(k)$ and $e_l = \sum_k v_l^R(k) f_L(k)$, and applying $e^{\hat{M}\tau} f_L(k) e^{-\hat{M}\tau} = e^{\lambda_k \tau} f_L(k)$ and $e^{\hat{M}\tau} f_R^\dagger(k) e^{-\hat{M}\tau} = e^{\lambda_k \tau} f_R^\dagger(k)$, we obtain:

$$\begin{aligned} &\langle \psi_f^{(0,s)} | g_0^\dagger e_l A_1(t) | \psi_0^j \rangle = \\ &\quad -\sqrt{N_s+1} \sum_{a,a'} \alpha_{a0sa'} \sum_{k.k'} v_l^R(k) \bar{v}_{a'}^L(k') \bar{v}_j^L(k') \frac{e^{-\lambda_{k'} t} - e^{-\lambda_k t}}{\lambda_k - \lambda_{k'}} \end{aligned} \tag{3.29}$$

and

$$\langle \psi_f^{(0,s)} | g_m^\dagger e_l A_0(t) | \psi_0^j \rangle = \delta_{s,m} \sqrt{N_s+1} \sum_k v_l^R(k) \bar{v}_j^L(k) e^{-\lambda_k t}. \tag{3.30}$$

Applying this two Eqs. (3.29 and 3.30) we finally obtain for the transition probability for the final state in which the number of condensed atoms does not change:

$$\langle P_{N_0} \rangle = P_{N_0}^{(C_1)} + P_{N_0}^{(C_2)} + P_{N_0}^{(C_3)}, \tag{3.31}$$

where

$$\begin{aligned} P_{N_0}^{(C_1)} &= \frac{1}{2\pi N_0} \sum_s d_s (N_s+1) \sum_j D_j 4\pi \sum_{l\tilde{l}} \alpha_{\tilde{l}00l}^r \sum_{kk'} \sum_{\tilde{k}\tilde{k}'} D_{lkk'}^{sj} (D_{\tilde{l}\tilde{k}\tilde{k}'}^{sj})^* \\ &\quad \times \frac{\lambda_{k'} + \lambda_k + \lambda_{\tilde{k}'}^* + \lambda_{\tilde{k}}^*}{(\lambda_{k'} + \lambda_{\tilde{k}'}^*)(\lambda_{k'} + \lambda_{\tilde{k}}^*)(\lambda_k + \lambda_{\tilde{k}'}^*)(\lambda_k + \lambda_{\tilde{k}}^*)}, \end{aligned} \tag{3.32}$$

$$P_{N_0}^{(C_2)} = \frac{1}{2\pi N_0} \sum_s d_s(N_s+1) \sum_j D_j 4\pi \sum_{l\tilde{l}} \alpha^r_{\tilde{l}ssl} \sum_{k,\tilde{k}} \frac{v_l^R(k)\bar{v}_j^L(k)\bar{v}_{\tilde{l}}^R v_j^L(\tilde{k})}{\lambda_k + \lambda_{\tilde{k}}^*}, \quad (3.33)$$

and

$$P_{N_0}^{(C_3)} = \frac{1}{2\pi N_0} \sum_s d_s(N_s+1) \sum_j D_j \left(-2\Re \left\{ 4\pi \sum_{l,\tilde{l}} \sum_{k,k'} \sum_{\tilde{k}} \alpha_{\tilde{l}s0l} \frac{D^{sj}_{lkk'} \bar{v}_{\tilde{l}}^R(\tilde{k}) v_j^L(\tilde{k})}{(\lambda_{k'} + \lambda_{\tilde{k}}^*)(\lambda_k + \lambda_{\tilde{k}}^*)} \right\} \right), \quad (3.34)$$

where $d_s = [\exp[\omega_s^g / K_B T_g] - 1]$ is the Bose-Einstein distribution in the ground-state trap, D_j is the Maxwell-Boltzmann distribution in the excited-state trap at a given temperature T_e, and

$$D^{sj}_{lkk'} = \sum_{aa'} \alpha_{a0sa'} v_l^R(k) \bar{v}_a^L(k) v_{a'}^R(k') \bar{v}_j^L(k'). \quad (3.35)$$

In the same way we obtain the transition probability into a final state in which the number of condensed atoms increases to $N_0 + 2$:

$$\begin{aligned} P_{N_0+2} &= \frac{1}{2\pi N_0} \sum_s d_s N_s \sum_j D_j 4\pi \sum_{l\tilde{l}} \alpha^r_{l00l} \sum_{kk'} \sum_{\tilde{k}\tilde{k}'} \tilde{D}^{sj}_{lkk'} (\tilde{D}^{sj}_{\tilde{l}\tilde{k}\tilde{k}'})^* \\ &\times \frac{\lambda_{k'} + \lambda_k + \lambda_{\tilde{k}'}^* + \lambda_{\tilde{k}}^*}{(\lambda_{k'} + \lambda_{\tilde{k}'}^*)(\lambda_{k'} + \lambda_{\tilde{k}}^*)(\lambda_k + \lambda_{\tilde{k}'}^*)(\lambda_k + \lambda_{\tilde{k}}^*)}, \end{aligned} \quad (3.36)$$

where

$$\tilde{D}^{sj}_{lkk'} = \sum_{aa'} \alpha_{as0a'} v_l^R(k) \bar{v}_a^L(k) v_{a'}^R(k') \bar{v}_j^L(k'). \quad (3.37)$$

3.4 Numerical Results

In order to evaluate Eqs. (3.31) and (3.36), one needs to calculate the eigenvectors and eigenvalues. Additionally, we note that the α coefficients constitute a 12 dimensional tensor, and that in order to evaluate every component, it is necessary to calculate the Frank–Condon factors for each possible excited-ground transition, and to perform the non–trivial task of calculating the Cauchy principal part integral appearing in the imaginary part of the α

coefficients [13]. Such strong technical difficulties make eventually impossible to solve in a reasonable computational time, 3D systems with more than 4 excited–state shells (20 levels), and therefore we have been constrained by such limit.

We have analyzed the case of different number of energy shells of the $|e\rangle$ and $|g\rangle$ trap, for different temperatures and different number of atoms. For each case, we have calculated the probabilities (3.31),(3.36), in order to evaluate the new relative number of condensed atoms n'. For the particular case of a single level in the excited state trap, results similar to those obtained in Ref. [13] were obtained. Figure 3.2 shows for different temperatures of the excited and ground trap, the case of 4 shells (20 levels) in the $|e\rangle$ trap, 10 shells (220 levels) in the $|g\rangle$ trap, $N = 7 \times 10^4$ atoms, and a Lamb–Dicke parameter $\eta^2 = \omega_r/\omega = 2$, where ω_r is the recoil energy of the scattered photon. One can observe that for certain temperatures T_e and T_g of the $|e\rangle$ and $|g\rangle$ traps, the change in the relative number of condensed particles, $n' - n$ is maximally positive, *i.e.* at these maxima the reabsorption effects help in the most efficient way to load the condensate. Away from such maxima, $n' - n$ is positive for low temperature T_e of the excited state trap and not very low temperatures T_g of the $|g\rangle$. For very low T_g, however, the positive processes described by P_{N0+2} tend to vanish, since the number of non–condensed atoms which eventually could be repumped to the condensate becomes very small. On the top of Fig. 3.2, such regions are those enclosed by the contours. Out of these regions, $n' - n$ becomes negative, i.e. the reabsorption tends to decrease the condensation relative number. In all our calculations the BAR expansion has been proved to be valid, by checking the condition $P_{N_0}, P_{N_0+2} \ll 1$. We have in general observed that the BAR can fail not only for large T_g, as expected from Ref. [13], but eventually also, for a given total number of atoms N, for large T_e at the $n' - n$ maxima. The latter is due to the large values of the imaginary part of the α coefficients at those peaks under such conditions, which invalid the expansion performed to obtain Eqs. (3.15) and (3.16). In the presented example, the condition above is fulfilled except for the maxima in the region $k_B T_e > \omega$ and $k_B T_g > 50\omega$. As discussed in Ref. [13], the phenomenon behind the positive effects of

the reabsorption ($n' - n > 0$) cannot be explained by using (classical) rate equations, since it is given by the interference between the different paths which lead to the same final state. In particular, it becomes decisive that the interference term in Eq. (3.16) is always destructive, since the process of Fig. 3.1(b) includes an additional absorption–emission cycle (which gives a minus sign in the amplitude, like for a 2π–laser pulse). The consequence of this interference is that P_{N_0} decreases, which favors that the excited atom goes to the state $|N_0 + 1\rangle$, and therefore it contributes to an increase of the proportion of condensed atoms.

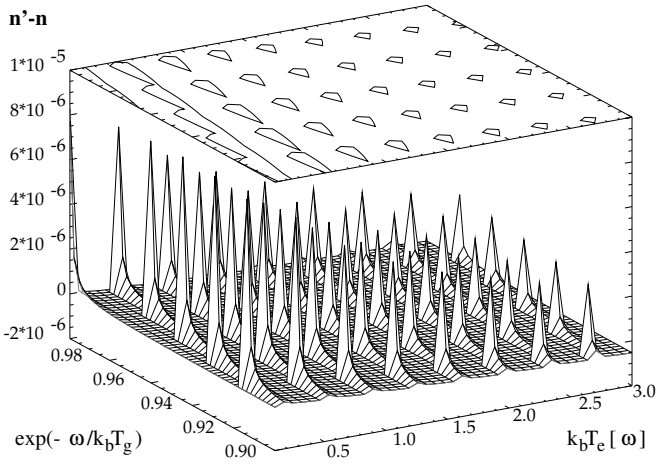

Figure 3.2: Change of the condensate fraction after a decay process as a function of the temperature T_e of the $|e\rangle$–trap and T_g of the $|g\rangle$–trap, the latter in exponential scale. The case of a total number of atoms $N = 7 \times 10^4$, 10 energy shells in the $|g\rangle$–trap, 4 energy shells in the $|e\rangle$–trap and $\eta^2 = 2$ is considered. On the top of the figure, the regions enclosed by the contours denote those temperatures for which the condensate fraction increases during the decay process

We have numerically simulated the pumping of atoms into a BEC in the $|g\rangle$ trap, under the BAR conditions. In our calculations, we have assumed that the collisions act on a shorter time scale than the spontaneous optical pumping. In that case, collisions will provide a fast thermalization mechanism of the $|g\rangle$ trap, between the two pump acts. After each pumping process we calculate the new condensate fraction, and accordingly the new T_g, which we employ to evaluate the next pumping, and so on. In Fig. 3.3

we analyze the same trap as in Fig. 3.2, for $k_B T_e = \omega$, and an initial number of trapped atoms $N = 5 \times 10^4$, for initial $N_0/N = 0.9$, 0.98 and 0.99. One can observe that the positive effects of the reabsorption in the BAR regime allow to increase the condensate fraction during the pumping process, up to almost complete condensation. However, as pointed out previously, for very low T_g the positive effects of BAR vanish. This explains the fact that the N_0/N is slightly lower than 1, as well as the fact that for initial $N_0/N = 0.99$ the condensate fraction initially decreases.

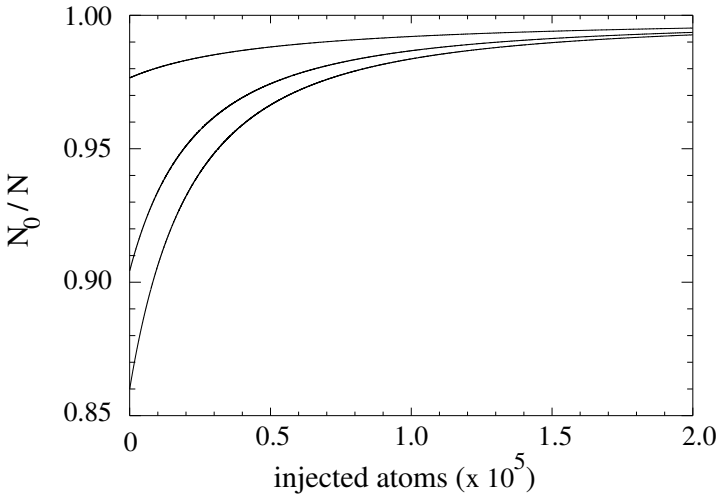

Figure 3.3: Mean condensate fraction as a function of the number of loaded atoms, for the case of 10 energy shells in the $|g\rangle$–trap, 4 energy shells in the $|e\rangle$–trap and $\eta^2 = 2$, and an initial total number of atoms $N = 5 \times 10^4$. From top to bottom, the curves represent, respectively, the case of an initial number of condensed particles $N_0 = 49632$, 48828 and 45211.

3.5 Conclusion

In this chapter we have extended the results presented in Ref. [13] for a much more general 3D situation, in which the excited state atoms can occupy more than one trapped state. We have shown that under the appropriate conditions, the BAR expansion is still valid for this more general case, and that the reabsorptions can play a positive role in the loading of the condensate.

Such effect is a consequence of the always destructive interference between the processes which tend to lower the condensate fraction. The generalized treatment shows that the BAR condition presented in [13] is not enough to guarantee the BAR expansion, since for more than one excited–trap level, the temperature of such trap is also important, and must be kept sufficiently low. Although for complexity reasons we have not analyzed the situation in which the trap levels are distorted by the mean field provided by the atom–atom collisions, we must stress that similar analysis could be applied also if the atom–atom collisions modify the levels, if instead of the bare trap levels, self–consistent levels were considered, as in Ref.[82]. Therefore, under the BAR conditions, i.e. large condensation, the reabsorption processes favor the optical pumping of atoms via spontaneous emission into a BEC. Such a quantum effect is of fundamental interest, and as discussed in the introduction of this thesis, can be important when considering the repairing of condensate losses, and the achievement of a continuously–loaded atom laser.

Chapter 4

Optical loading in the Branching-Ratio Expansion

4.1 Introduction

In this chapter, we concentrate on the continuous optical pumping into a BEC in three-level atoms. In the first part of the chapter we present a new scenario in which the reabsorption is suppressed, in much less restrictive conditions as those discussed in the introduction to this thesis for the Festina Lente regime. In this scenario, an atom possesses an accessible three level Λ scheme, in which one of the atomic transitions decays much faster than the other. By employing Master Equation (ME) techniques, we show that photon reabsorptions in the slow transition are largely suppressed because the respective coherences are destroyed due to the decay via the fast transition. Since the "bad" reabsorptions are not present, this scheme can be employed to continuously pump atoms into the lower level of the slower transition. In the second part of the paper we analyze the dynamics of such pumping in the presence of atom–atom collisions, and show that the combination of elastic collisions (evaporative cooling), and bosonic enhancement of the spontaneous emission, can create a condensate, and refill it in the presence of outcoupling or losses. Therefore, this scheme could be considered as a possible way towards a continuously loaded atom laser. As a possible exper-

imental realization we consider laser-cooled Chromium, but the ideas can be generalized to any atom that provides an asymmetric three–level system.

The structure of the chapter is as follows. In Sec. 4.2 we introduce the physical model, as well as the quantum ME that determines the loading dynamics. In Sec. 4.3 we introduce the so–called Branching Ratio Expansion (BRE), which allows us to analyze the hierarchy of processes which occur in the system. In Sec. 4.4 we analyze in detail the suppression of the reabsorption effects. Sec. 4.5 is devoted to the treatment of the atom–atom collisions. In Sec. 4.6 we present the numerical Monte Carlo results of the loading dynamics. Finally, we summarize some conclusions in Sec. 4.7.

4.2 Model

We consider a set of atoms with an accessible three level Λ system (see Fig. 4.1), formed by the levels $|r\rangle$, $|e\rangle$ and $|g\rangle$. The atoms are trapped in an isotropic harmonic trap which, depending of the internal state of the atoms, has frequencies ω_r, ω_e and ω_g, respectively. This could be, for instance, the

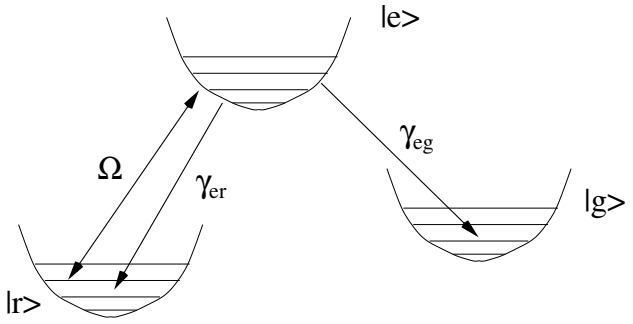

Figure 4.1: Atomic scheme considered throughout the paper.

case of Chromium ^{52}Cr, in which the electronic levels would be $^7S_3$, $^7P_4$, and $^5D_4$, respectively. The transition $|r\rangle \leftrightarrow |e\rangle$ is assumed to be driven by a laser, which has a Rabi frequency Ω. The spontaneous emission frequencies associated with the transitions $|r\rangle \leftrightarrow |e\rangle$ and $|g\rangle \leftrightarrow |e\rangle$ are, respectively, γ_{er} and γ_{eg}, such that $\gamma_{er} \gg \gamma_{eg}$. In the case of ^{52}Cr, $\gamma_{er} = 2\pi \times 5$MHz $\gg \gamma_{eg} = 2\pi \times 30$Hz. The branching ratio $\epsilon \equiv \gamma_{eg}/\gamma_{er}$ is therefore very small

($\sim 10^{-5}$ in ^{52}Cr). The fact that $\epsilon \ll 1$, will lead to the suppression of the reabsorption of scattered photons. In this section, we shall not consider the collisions between the atoms in the $|g\rangle$ state. Such collisions are introduced in our formalism in the weak-condensation regime in Sec. 4.5. For a discussion of the collisional effects in the Thomas-Fermi regime we refer to chapter 5.

In the following we consider $\hbar = c = 1$ for simplicity. Let us introduce the annihilation and creation operators of atoms in the $|r\rangle$, $|e\rangle$ and $|g\rangle$ states and in the trap levels s, l, and m which we shall call $r_s, r_s^\dagger$, $e_l, e_l^\dagger$, and $g_m, g_m^\dagger$. These operators fulfill the standard bosonic commutation relations.

The Hamiltonian which describes the coupling of the system of bosons to the laser field, as well as to the vacuum electromagnetic modes is of the form:

$$\hat{H} = \hat{H}_0 + \hat{H}_{er} + \hat{H}_{af}^{er} + \hat{H}_{af}^{eg} + \hat{H}_f. \tag{4.1}$$

This Hamiltonian presents the following terms:

- Free atomic Hamiltonian (describing internal and center–of–mass degrees of freedom):

$$\hat{H}_0 = \sum_s \omega_s^r r_s^\dagger r_s + \sum_l (\omega_l^e + \omega_0) e_l^\dagger e_l + \sum_s \omega_m^g g_m^\dagger g_m, \tag{4.2}$$

  with ω_s^r, ω_l^e and ω_m^g, denoting the energies of the level s of the $|r\rangle$ trap, the level l of the $|e\rangle$ trap, and the level m of the $|g\rangle$ trap, respectively. ω_0 is the transition frequency between $|r\rangle$ and $|e\rangle$.

- Interactions of the laser quasi resonant with the transition $|r\rangle \leftrightarrow |e\rangle$:

$$H_{er} = \frac{\Omega}{2} \sum_{l,s} \eta_{l,s} e^{-i\omega_L t} e_l^\dagger r_s + h.c., \tag{4.3}$$

  where $\eta_{l,s}$ is the Frank–Condon factor which describes the transition between a level s of the $|r\rangle$ trap, and a level l of the $|e\rangle$ trap, and ω_L is the frequency of the applied laser.

- Spontaneous emission processes $|e\rangle \rightarrow |r\rangle$:

$$\hat{H}_{af}^{er} = -i \sum_{l,s} \sum_{\mu} \int d^3\vec{k} \sqrt{\frac{k}{2\epsilon_0 (2\pi)^3}} (\vec{d}_{er} \cdot \vec{\epsilon}_{\vec{k}\mu}) \times \eta_{ls}(\vec{k}) e_l^\dagger r_s a_{\vec{k}\mu} + h.c., \quad (4.4)$$

  where where $a_{\vec{k}\mu}$, $a_{\vec{k}\mu}^\dagger$ are the annihilation and the creation operators of a vacuum photon characterized by a wavevector $\vec{k}$ and a polarization μ, with polarization vector $\vec{\epsilon}_{\vec{k}\mu}$; $\vec{d}_{er}$ is the dipole vector of the transition $|r\rangle \leftrightarrow |e\rangle$.

- Spontaneous emission $|e\rangle \rightarrow |g\rangle$:

$$\hat{H}_{af}^{eg} = -i \sum_{l,m} \sum_{\mu} \int d^3\vec{k} \sqrt{\frac{k}{2\epsilon_0 (2\pi)^3}} (\vec{d}_{eg} \cdot \vec{\epsilon}_{\vec{k}\mu}) \times \eta_{lm}(\vec{k}) e_l^\dagger g_m a_{\vec{k}\mu} + h.c., \quad (4.5)$$

  where d_{eg} is the dipole vector of the transition $|g\rangle \leftrightarrow |e\rangle$.

- Free Hamiltonian of the electromagnetic (EM) field

$$\hat{H}_f = \sum_{\mu} \int d^3\vec{k} k a_{\vec{k}\mu}. \quad (4.6)$$

Starting from the Hamiltonian (4.1), one can trace the full density matrix of the system over the vacuum modes of the EM field. Using standard methods of quantum stochastic processes [83, 84, 85], one can derive then the Quantum ME in Born–Markov approximation [86] (see App. A). In principle such ME fully describes all the processes which happen in the system, including eventual reabsorptions in the fast transition $|e\rangle \rightarrow |r\rangle$. However, for simplicity of the analysis we shall consider the case in which we can neglect the reabsorption phenomena for the reservoir atoms ($|e\rangle$ and $|r\rangle$). Although what follows is true also in presence of those reabsorptions, the approximation will allow us to concentrate on the much simpler problem of the pumping of a single atom from the reservoir $\{|e\rangle, |r\rangle\}$ into the $|g\rangle$ trap, where of course, collective phenomena are important, and therefore taken into account. In

this case, the ME takes the form

$$\dot{\rho} = -iH_{eff}\rho + i\rho H_{eff} + \mathcal{J}\rho, \tag{4.7}$$

where ρ is the density matrix, $H_{eff} = H_{eff}^{(0)} + H_{eff}^{(1)}$ and $\mathcal{J} = \mathcal{J}^{(0)} + \mathcal{J}^{(1)}$, with

$$\begin{aligned}
H_{eff}^{(0)} &= \sum_s \omega_s^r r_s^\dagger r_s + \sum_l (\omega_l^e - \delta - i\gamma_{er}) e_l^\dagger e_l + \sum_s \omega_m^g g_m^\dagger g_m + H_{er}, & (4.8)\\
H_{eff}^{(1)} &= -i\gamma_{eg} \sum_{l,m} \sum_{l',m'} \alpha_{lmm'l'} e_l^\dagger g_m g_{m'}^\dagger e_{l'}, & (4.9)\\
\mathcal{J}^{(0)}\rho &= 2\gamma_{er} \sum_{l,s} \sum_{l',s'} \beta^R_{lss'l'} r_{s'}^\dagger e_{l'} \rho e_l^\dagger r_s, & (4.10)\\
\mathcal{J}^{(1)}\rho &= 2\gamma_{eg} \sum_{l,m} \sum_{l',m'} \alpha^R_{lmm'l'} g_{m'}^\dagger e_{l'} \rho e_l^\dagger g_m. & (4.11)
\end{aligned}$$

Here $\delta = \omega_L - \omega_0$ is the detuning,

$$H_{er} = \frac{\Omega}{2} \sum_{l,s} \eta_{l,s} e_l^\dagger r_s + H.c., \tag{4.12}$$

whereas $\alpha_{lss'l'} = \alpha^R_{lss'l'} + i\alpha^I_{lss'l'}$, and $\beta_{lmm'l'} = \beta^R_{lmm'l'} + i\beta^I_{lmm'l'}$, with

$$\begin{aligned}
\alpha^R_{lmm'l'}(k_0^{eg}) &= \int d\hat{k} \mathcal{W}(\hat{k}) \eta_{ls}(k_0^{eg}\hat{k}) \eta^*_{l'm'}(k_0^{eg}\hat{k}), & (4.13)\\
\alpha^I_{lmm'l'}(k_0^{eg}) &= -\frac{1}{\pi} P \int_{-\infty}^{\infty} d\xi \frac{\xi^3}{\xi - 1} \alpha^R_{lmm'l'}(\xi k_0^{eg}). & (4.14)
\end{aligned}$$

In the previous equations $\hat{k}$ indicates the solid angle coordinates, $\mathcal{W}(\hat{k})$ represents the dipole pattern of the spontaneous emission, k_0^{eg} is the wave number associated with the transition $|g\rangle \leftrightarrow |e\rangle$, and P denotes the Cauchy Principal part. Finally, $\beta^R_{lss'l'}$ has an identical form as $\alpha^R_{lmm'l'}$, but for the transition $|r\rangle \leftrightarrow |e\rangle$.

4.3 Branching Ratio Expansion

In this section we shall show that if $\epsilon \ll 1$, the reabsorption effects on the slow transition can be safely neglected, because they occur with a probability $1/\epsilon$ times smaller than the spontaneous emission processes $|e\rangle \to |g\rangle$ without any reabsorption. In order to demonstrate that, we shall perform the analysis of the different processes that could happen in the system.

We shall consider the situation in which some atoms are already accumulated in the level $|g\rangle$ at the time t_0 at which a single atom is being pumped from the level $|r\rangle$ to the level $|e\rangle$. This atom undergoes then spontaneous emission, having two different possibilities. First, it may undergo a transition $|e\rangle \to |r\rangle$, and the emitted photon will then leave the system (we assume no reabsorptions at $|e\rangle \leftrightarrow |r\rangle$ line due to the low density of $|r\rangle$ atoms). Second, the excited atom may undergo a transition $|e\rangle \to |g\rangle$. We allow for the possibility that the emitted photon in this process may be reabsorbed several times, until it leaves the system or until the emission $|e\rangle \to |r\rangle$ will take place. We shall analyze the hierarchy of possible processes which can be produced on the time scale of the above described processes. We shall assume that no other atom is pumped from the level $|r\rangle$ to $|e\rangle$ within this time scale. Technically, this approximation means that we exclude the possibility of multiple quantum jumps from $|e\rangle$ to $|r\rangle$, i.e. we assume that the whole process consists of the sequence of processes, each involving an atom being pumped from $|r\rangle$ to $|e\rangle$, which then undergoes spontaneous emission processes (including reabsorptions) until it either lands on the level $|r\rangle$ or $|g\rangle$, after which another atom is being pumped from $|r\rangle$ to $|e\rangle$, and so on.

This approximation is performed here just for reasons of technical simplicity, but we want to stress that:

- The approximation describes well the experimental situation with ^{52}Cr atoms in which the Rabi frequency $\Omega < \gamma_{er}$. The pumping process has thus indeed an incoherent character, consisting in a sequence of jumps $|e\rangle \to |r\rangle$ followed by spontaneous emission events. Of course, it may happen that several atoms are being excited simultaneously to $|e\rangle$. Each of them, however, behaves independently of the others, so

that the analysis pertaining to just one excited atom is valid.

- The result obtained below is indeed more general, because at any time scale the hierarchy of probabilities is maintained. The latter statement means that our results hold also for $\Omega > \gamma_{er}$. This can be at best understood using a dressed–state picture with respect to the $|e\rangle \leftrightarrow |r\rangle$ transition. In the limit $\Omega \gg \gamma_{er}$ the dynamics reduces to a situation in which a single atom is being pumped to one of the dressed states $|+\rangle$ ($|-\rangle$), and undergoes spontaneous emission consisting in arbitrary number of incoherent $|+\rangle \rightarrow |+\rangle$ ($|-\rangle \rightarrow |-\rangle$) transitions, ending either in $|g\rangle$, or in $|-\rangle$ ($|+\rangle$). This process is followed by an arrival of another atom in the state $|+\rangle$ ($|-\rangle$), followed by successful spontaneous emission, etc. Each one of these steps can be understood with the model presented below.

The formal solution of the ME (4.7) after a photon escapes from the system is given by:

$$\rho_\infty = \int_0^\infty dt \mathcal{J}\{e^{-i\mathcal{L}_{eff}t}\rho\}. \tag{4.15}$$

We have used in the expression (4.15) the shortened notation

$$\mathcal{L}_{eff}\rho = -iH_{eff}\rho + i\rho H_{eff}^\dagger. \tag{4.16}$$

In the following we shall denote $\mathcal{L}_{eff}^{(0)}\rho = -iH_{eff}^{(0)}\rho + i\rho H_{eff}^{(0)}$, $\mathcal{L}_{eff}^{(1)}\rho = -iH_{eff}^{(1)}\rho + i\rho H_{eff}^{(1)}$. Since $\gamma_{eg} \ll \gamma_{er}, \Omega$, we are going to perform an expansion in the branching ratio ϵ. We consider an initial state of the system given by $|\psi_0\rangle = |\psi_0^g\rangle \otimes |\psi_0^{e,r}\rangle$, with $|\psi_0^g\rangle = |N_0, N_1, \ldots, N_m, \ldots\rangle$, with N_m denoting the initial population of the m-th state of the $|g\rangle$ trap. $|\psi_0^{e,r}\rangle$ denotes the initial state of the $|r\rangle$ and $|e\rangle$ traps. We are interested in the probability to obtain a final state $|\psi_f\rangle = |\psi_f^g\rangle \otimes |\psi_f^{e,r}\rangle$.

The branching ratio expansion must take into account the bosonic enhancement effects. Due to the bosonic enhancement, and the fact that we consider that the ground state of the $|g\rangle$ can be macroscopically populated, the expansion must be done in the parameter ϵN_0, and not only in ϵ. Nevertheless, we expect that the expansion and the conclusions that we draw from

it will remain valid until $\epsilon N_0 \simeq 1/2$. To use this expansion in the considered experimental situation we have to limit ourselves to the case of $N_0 \leq 10^5/2$. That means, however, that the expansion can nevertheless be safely used during the onset of the condensation, and the dangerous reabsorptions can be neglected in that regime. The situation in which $\epsilon N_0 \ll 1$ requires the treatment of higher order terms in the expansion, but does not mean that in such a case the reabsorptions will cause troubles. In the case when very many atoms are already condensed, the dynamics is dominated by bosonic statistical effects. The use of similar ideas and techniques as those employed in the previous chapter for the BAR [13] should be then possible.

Employing standard methods of time–dependent perturbation theory in the small parameter ϵN_0 we obtain:

$$\langle \psi_f | \rho_\infty | \psi_f \rangle = A_0 + A_1 + A_2 + \mathcal{O}((\epsilon N_0)^3), \tag{4.17}$$

where A_j is the term of order $\mathcal{O}((\epsilon N_0)^j)$. Let us now analyze step by step each of the terms of the branching ratio expansion (BRE):

4.3.1 Zeroth Order

The zeroth order term is of the form:

$$A_0 = \langle \psi_f | \int_0^\infty dt \mathcal{J}^{(0)} \{ e^{\mathcal{L}^{(0)}_{eff} t} \rho_0 \} | \psi_f \rangle, \tag{4.18}$$

This process is by far the most probable one, and implies an spontaneous emission into the $|r\rangle$ state These processes (and the subsequent repumping by the laser) induce a thermal distribution of the $|e\rangle$ and $|r\rangle$ traps, and do not affect directly the populations of the $|g\rangle$ trap.

4.3.2 First Order

The first order term of the BRE is of the form $A_1 = A_{1a} + A_{1b}$, where

$$A_{1a} \;=\; \langle \psi_f | \int_0^\infty dt \mathcal{J}^{(1)} \{ e^{\mathcal{L}^{(0)}_{eff} t} \rho_0 \} | \psi_f \rangle, \tag{4.19}$$

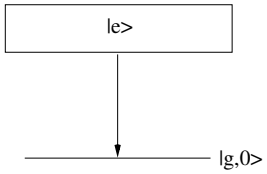

Figure 4.2: Scheme of the process of first BRE order A_{1a}, whereas the dashed line represents the photon which is spontaneously emitted and further reabsorbed.

$$A_{1b} = \langle\psi_f| \int_0^\infty dt \mathcal{J}^{(0)} \left\{ \int_0^t dt' e^{\mathcal{L}_{eff}^{(0)}(t-t')} \left\{ \mathcal{L}_{eff}^{(1)} \left\{ e^{\mathcal{L}_{eff}^{(0)} t'} \rho_0 \right\} \right\} \right\} |\psi_f\rangle. \quad (4.20)$$

A_{1a} corresponds to the case in which an atom in the state $|e\rangle$ decays (without any further reabsorption) into a state of the $|g\rangle$ trap (see Fig. 4.2). A_{1b} is given by the interference of two different process: a process like the one considered in the zeroth order, and a process in which (i) a decay is produced into some state of the $|g\rangle$ trap, (ii) a subsequent reabsorption is produced from the same state of the $|g\rangle$ trap, and finally a process as that of the zeroth order is produced. The processes described by A_{1b}, although containing reabsorptions, do not change the population distribution of the $|g\rangle$ trap, and can be considered as small quantitative corrections to the zeroth order term.

4.3.3 Second Order

The second order term of the BRE is of the form $A_2 = A_{2a} + A_{2b}$, with

$$A_{2a} = \langle\psi_f| \int_0^\infty dt \mathcal{J}^{(0)} \int_0^t dt' e^{\mathcal{L}_{eff}^{(0)}(t-t')} \left\{ \mathcal{L}_{eff}^{(1)} \left\{ \int_0^{t'} dt'' e^{\mathcal{L}_{eff}^{(0)}(t'-t'')} \left\{ \mathcal{L}_{eff}^{(1)} \left\{ e^{\mathcal{L}_{eff}^{(0)} t'} \rho_0 \right\} \right\} \right\} \right\} |\psi_f\rangle \quad (4.21)$$

$$A_{2b} = \langle\psi_f| \int_0^\infty dt \mathcal{J}^{(1)} \left\{ \int_0^t dt' e^{\mathcal{L}_{eff}^{(0)}(t-t')} \left\{ \mathcal{L}_{eff}^{(1)} \left\{ e^{\mathcal{L}_{eff}^{(0)} t'} \rho_0 \right\} \right\} \right\} |\psi_f\rangle. \quad (4.22)$$

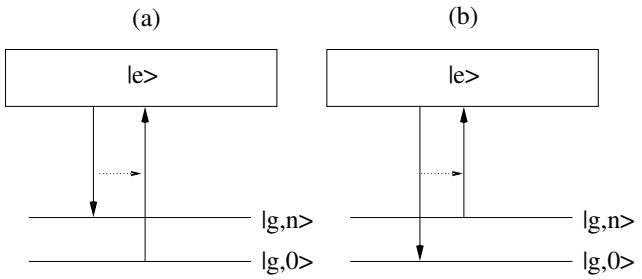

Figure 4.3: (a) and (b) represent respectively the negative and positive reabsorption effects which appear in the second BRE order processes A_{2a}, whereas the dashed line represents the photon which is spontaneously emitted and further reabsorbed.

Let us consider the term A_{2a}. This term involves processes in which an atom originally in some state of the $|e\rangle$ trap, decays into some state m of the $|g\rangle$ trap, producing an spontaneously emitted photon, which is reabsorbed by other atom in some other state $n \neq m$ of the $|g\rangle$ trap. These processes are of order ϵ^2, except the case in which $n = 0$ or $m = 0$ (Figs.4.3(a) and (b)); in such a case, if the system is already condensed, the probability associated with these processes is of order $\epsilon^2 N_0$. We must note that the process of Fig. 4.3(a) introduces a negative effect of the photon reabsorption in our system, because produces a non–condensed atom, while destroys an already condensed one (of course the opposite process of Fig. 4.3(b) corresponds to positive effects, and is of the same order). The term A_{2b} is due to the interference effects between the process considered in A_{1a} and the processes of Figs.4.4(a) and (b). These process do not cause any negative or positive effects of the reabsorption, and simply introduce small quantitative corrections to A_{1a}.

As observed, the "bad" reabsorption processes which change the $|g\rangle$ trap population distribution (i.e. may lead to undesired heating) are of order $\epsilon^2 N_0$, and therefore are $1/\epsilon$ times less probable than the single spontaneous emission into the $|g\rangle$ trap without any reabsorption. Hence, the reabsorption effects can be safely neglected, i.e. the atoms in the $|g\rangle$ trap can be considered as transparent for the spontaneously emitted photons on the $|e\rangle \rightarrow |g\rangle$ transition. We shall show in Sec. 4.6 that this effect can be used to optically

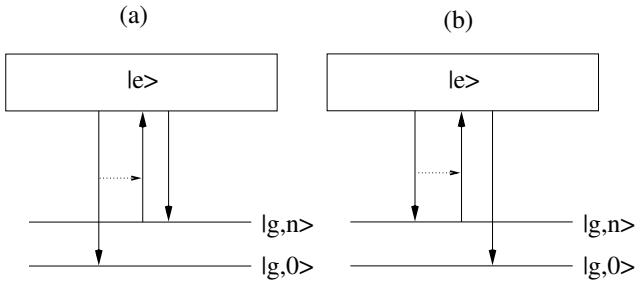

Figure 4.4: The interference between the processes of Fig. 4.2, and (a,b) constitutes the term A_{2b} of the second order of the BRE.

pump atoms from the reservoir $\{|r\rangle, |e\rangle\}$ into the $|g\rangle$ trap, and eventually into a condensate created in it.

4.4 Suppression of the reabsorption effects

In this section we analyze in detail the physical effect behind the decreasing of the reabsorption probability in the considered system. The physical picture can be understood by taking a closer look to the expression (4.21) which, after eliminating the terms which do not change the populations of the $|g\rangle$ trap, takes the form

$$\int_0^\infty dt \int_0^t dt' \int_0^{t'} dt'' \langle\psi_f|\mathcal{J}^{(0)} = \\ \{|\psi(t;t')\rangle\langle\psi(t;t'')| + |\psi(t;t'')\rangle\langle\psi(t;t')|)\}\,|\psi_f\rangle, \tag{4.23}$$

where

$$|\psi(t;t')\rangle = e^{-iH_{eff}^{(0)}(t-t')} H_{eff}^{(1)} e^{-iH_{eff}^{(0)}t'} |\psi_0\rangle. \tag{4.24}$$

Therefore, the process can be divided into three parts: (i) From time 0 to some t', the system evolves following the effective Hamiltonian $H_{eff}^{(0)}$; (ii) At t' a spontaneous emission occurs from $|e\rangle$ to $|g\rangle$, followed by a reabsorption; (iii) The system undergoes after t' the same dynamics as in the part (i), until time t where a jump $\mathcal{J}^{(0)}$ is produced into the $|r\rangle$ state.

As observed in the expression (4.23), the term A_{2a} depends on the correlation of the amplitudes of probability of two processes (i–iii) in which (ii)

is produced at two different times, t' and $t'' < t'$. In the interval t'' to t' a jump into $|r\rangle$ is produced with large probability, and therefore the probability amplitude is reduced, roughly speaking, by a factor $\exp(-\gamma_{er}(t'-t''))$. Therefore, the correlation decays very rapidly (in comparison with γ_{eg}^{-1}) with the time difference $t'-t''$. This leads to the strong reduction of the reabsorption probability.

A very intuitive picture of the underlying physics in 3-level atoms can be obtained in the following way: The reabsorption on the $|g\rangle$ to $|e\rangle$ transition has an oscillator strength γ_{eg}. However the excited state coherence is rapidly destroyed due to the decay of state $|e\rangle$ to $|r\rangle$, with a rate γ_{er}. Therefore the absorption line width on the $|g\rangle$ to $|e\rangle$ transition is dominated by γ_{er}. Similar to other broadening mechanisms the effective reabsorption cross section is reduced by a factor $\epsilon = \gamma_{er}/\gamma_{eg}$. The atomic sample can be ϵ-fold more dense than in the normal two level case before it becomes optically thick and reabsorption becomes a relevant process.

It is perhaps interesting to mention here the differences and similarities with the Festina Lente regime [32], which, as discussed in the introduction to this Thesis, constitutes a known way to avoid the reabsorption problem. As pointed out previously, the reabsorption probability is determined (as already shown in [32]) by the correlation at different times of the amplitude of reabsorption probability. In the case considered in [32], the correlation decays with the same frequency Γ as the spontaneous emission frequency of the system, and therefore the probability of decay plus reabsorption is that of the decay without further reabsorption (multiplied by some geometrical factor, specially important in the so–called free–space limit [32]). In the case of the Festina Lente regime ($\Gamma \ll \omega$) [32] the reabsorptions which do not preserve the energy are suppressed due to a different reason than that considered in the present paper. In the Festina Lente conditions the interference terms in the amplitude of probability of "bad" reabsorptions at different times have a phase which rapidly oscillates in time; therefore, the time integration leads to a strong reduction of the reabsorption probability (by the small factor Γ/ω). In this sense, therefore, the Festina Lente Regime can be understood in terms of an expansion similar to the BRE. The case considered in this

paper is, however, different. The spontaneous emission rate γ_{eg} is now a factor ϵ smaller than the rate of decay of the correlation, given by γ_{er}. This explains why the reabsorption is a factor ϵ less probable than a decay without reabsorption.

As a final remark, let us point out that the BRE does not necessarily imply small spontaneous emission rates ($\gamma_{eg} < \omega$), as it was the case of Festina Lente, but just the relative condition $\gamma_{eg} \ll \gamma_{er}$. In particular, γ_{eg} could be larger (or even much larger) than the trap frequency. Therefore, in principle, the atoms could be pumped into the $|g\rangle$ trap much faster than in the Festina Lente limit. This is of special interest when considering a sufficiently fast continuous loading of a condensate.

4.5 Collisions

In this section we introduce the collisions between atoms in the $|g\rangle$ trap. In particular, no collision is considered between the atoms in the $|g\rangle$ trap, and those in the $|e\rangle$ and $|r\rangle$ trap. Such approximation is valid assuming the situation in which the reservoir atoms are at much larger temperature and lower densities than those atoms in the $|g\rangle$ trap. Since we shall consider a $|g\rangle$ trap of a finite depth, the eventual collisions with the relatively much hotter reservoir atoms would lead to losses in the $|g\rangle$ trap, and eventually to a depopulation of the condensate created in it. Since we consider a loss mechanism from the condensate anyway (Sec. 4.6) such collisional losses could be easily taken into account phenomenologically in our simulations as an effective outcoupling rate.

The effects of the elastic collisions within the $|g\rangle$ trap are accounted by a new term in the Hamiltonian (4.1):

$$\hat{H}_{coll} = \sum_{m_1,m_2,m_3,m_4} \frac{1}{2} U_{m_1,m_2,m_3,m_4} g^\dagger_{m_4} g^\dagger_{m_3} g_{m_2} g_{m_1}. \tag{4.25}$$

In the regime we want to study, only the s–wave scattering is important, and

then:

$$U_{m_1,m_2,m_3,m_4} = \frac{4\pi\hbar^2 a}{m} \int_{R^3} d^3x \; \psi^*_{m_4}\psi^*_{m_3}\psi_{m_2}\psi_{m_1}, \tag{4.26}$$

where ψ_{m_j} denotes the harmonic oscillator wavefunctions and a denotes the scattering length.

In the following we are going to work in the so-called *weak-condensation regime*, where no mean–field effects are considered. This means that we consider that the mean–field energy provided by the collisions is smaller than the oscillator energy. Therefore the model is only valid to describe either the onset of the condensation, or the full condensation but with the constraint that the condensate cannot contain more than, say 500-1000 particles. A realistic calculation of the dynamics beyond the weak-condensation regime requires the self-consistent calculation of the atomic states, which due to mean-field effects change during the dynamics, and it will be the subject of chapter 5. In this chapter we concentrate in the weak-condensation regime, where one can apply the formalism of Quantum–Boltzmann Master Equation (QBME) [87, 52] to treat the collisional effects. By using similar arguments as those employed in the context of collective laser cooling in the presence of atomic collisions in the weak–condensation regime [80], one can show that the ME which describes in this regime the loading dynamics from the reservoir $\{|e\rangle, |r\rangle\}$ to the $|g\rangle$ can be divided into two independent parts:

$$\dot{\rho}(t) = \mathcal{L}_{coll}\rho(t) + \mathcal{L}_{load}\rho(t) \tag{4.27}$$

where $\mathcal{L}_{load}\rho(t)$ is the rhs of Eq. (4.7), and $\mathcal{L}_{coll}$ describes the collisions, and has the form of a QBME as that described in Refs. [87, 52].

Summarizing, the dynamics of the system splits into two parts, (i) collisional part, described by a QBME, and (ii) loading part, described by the same ME (4.7) as without collisions. The independence of both dynamics, constitutes the main technical advantage of considering the weak–condensation regime, and allows for an easy simulation of the loading process in the presence of $|g\rangle$-$|g\rangle$ collisions. In particular, we simulate both dynamics using Monte Carlo methods, combining the numerical method of Ref.[52], with simulations similar as those already presented in Refs. [86].

The numerical simulation of the collisional dynamics for a three–dimensional harmonic trap is demanding, due to both the degeneracy of the levels, and the difficulties to obtain reliable values for the integrals $U(n_1, n_2, n_3, n_4)$. Therefore, we shall limit ourselves to the use of the ergodic approximation [88, 52], i.e. we shall assume that states with the same energy are equally populated. The populations of the degenerate energy levels equalize on a time scale much faster than the collisions between levels of different energies, and than the loading typical time. Following Ref. [88] the probability of a collision of two atoms in energy shells m_1 and m_2, to give two atoms in shells m_3 and m_4 (where this collision is assumed to change the energy distribution function), is of the form:

$$P(m_1, m_2 \to m_3, m_4) = \Delta(m_j + 1)(m_j + 2)\times \frac{N_{m_1}(N_{m_2} - \delta_{m_2,m_1})(N_{m_3} + g_{m_3})(N_{m_4} + g_{m_4} + \delta_{m_3,m_4})}{g_{m_1} g_{m_2} g_{m_3} g_{m_4}}, \tag{4.28}$$

where $g_{m_k} = (m_k + 1)(m_k + 2)/2$ is the degeneracy of the energy shell m_k, $m_j = \min\{m_1, m_2, m_3, m_4\}$, and $\Delta = (4a^2\omega_g^2 m)/(\pi\hbar)$. In the following we shall use for the calculations the mass of ^{52}Cr. We shall adopt a scattering length $a = 6$ nm (similar to that of Rubidium). We shall consider a trap frequency $\omega_g = 2\pi \times 1$kHz.

4.6 Numerical Results

In this section we consider two different physical problems. First, we shall show that under appropriate conditions it is possible to load an initially empty trap for atoms in the state $|g\rangle$ via spontaneous emission from a thermal reservoir of particles $|e\rangle$. This allows to achieve the condensation in the trap $|g\rangle$ in a finite time, which depends on the physical parameters. Secondly, we shall show that in presence of an outcoupling (or, as discussed in Sec. 4.5, in presence of trap losses) it is possible to maintain the condensate population by refilling the condensate via the spontaneous emission from the thermal cloud.

The zero order term of the BRE corresponds to the fastest transition, but does not affect directly the loading process. Here we shall concentrate on the process provided by A_{1a}, i.e. the spontaneous emission $|e\rangle \rightarrow |g\rangle$. The loading rate of a state $|g,n\rangle$ from a state $|e,l\rangle$ is therefore given by

$$\Gamma(l,n) = 2\gamma_{eg} \int d\hat{k}\mathcal{W}(\hat{k})|\langle n|e^{i\vec{k}\vec{r}}|l\rangle|^2(N_n+1). \tag{4.29}$$

Let us assume that N_{ex} atoms are in the level $|e\rangle$ with a thermal distribution of temperature T. The total loading rate into the state $|g,n\rangle$ is provided by:

$$\Gamma(n) = \sum_l p(l)\Gamma(l,n), \tag{4.30}$$

where $p(l) = N_{ex}\exp\{-\hbar\omega_e\tilde{l}/k_BT\}/\mathcal{Z}$ is the thermal distribution, with $\tilde{l} = l_x + l_y + l_z$ and $\mathcal{Z} = (1-\exp\{-\hbar\omega_e/k_BT\})^{-3}$ is the canonical partition function. Thus, the loading rate can be rewritten as:

$$\begin{aligned}\Gamma(n) = 2\gamma_{eg} &\int d\hat{k}\mathcal{W}(\hat{k}) \\ &\langle n|e^{i\vec{k}\vec{r}}\left[\sum_l N_{ex}\frac{e^{-\hbar\omega_e\tilde{l}/k_BT}}{\mathcal{Z}}|l\rangle\langle l|\right]e^{-i\vec{k}\vec{r}}|n\rangle(N_n+1)\end{aligned} \tag{4.31}$$

Let us consider now the following conditions which greatly simplify the numerical calculation of the loading process. We are going to assume that $\omega_e < \omega_g + 2\omega_{rec}/3$, so that there is always at least a state of the excited–state trap in an interval $\pm\omega_{rec}$ (with ω_{rec} being the recoil frequency) around any considered state of the ground–state trap. The ground state trap has a finite depth, i.e. it possesses a maximal energy shell at $\hbar\omega_g m_{max}$ [1]. Therefore, only those $|e\rangle$ atoms with energies $E < \hbar\omega_g m_{max} + \hbar\omega_{rec} \equiv E_{max}$ can effectively load the trap. Let us consider that the reservoir has a temperature T such that $k_BT \gg E_{max}$. Under the previous conditions, the expression between

[1] The large–temperature approximation is assumed since it simplifies the numerical simulation. Although this approximation has certain physical consequences, we want to stress that similar effects as the ones discussed in this paper are not only possible for the case of lower temperatures, but should in principle allow for faster loading. In such a case, the Frank–Condon factors of the different transitions should be properly calculated [72, 86]

the brackets in (4.31) can be safely substituted by $1/\mathcal{Z}$. Since the previous conditions also imply $\hbar\omega_e \ll k_B T$, the loading rate can be rewritten as:

$$\Gamma(n) = \gamma_{eff}(N_n + 1) \tag{4.32}$$

with $\gamma_{eff} = 2\gamma_{eg} N_{ex}(\hbar\omega_e/k_B T)^3$. In other words, if the previous conditions are satisfied, all the levels of the ground state trap are equally loaded.

In our numerical simulations we consider a $|g\rangle$ trap which is cut at an energy shell $m_{max} = 10$–60 (which for $\omega_g = 2\pi \times 1$kHz, implies a trap depth of 0.5–3.0μK). In the simulations we have used a "virtual" trap of $m_{max} + 10$ energy shells in order to take into account the atoms which do not decay into the trap, and also to calculate the evaporative cooling dynamics. We have checked that such chosen "virtual" trap does not affect the physics of the problem. The levels $m > m_{max}$ are continuously emptied in the simulations, and those atoms are considered as lost. We have numerically simulated the loading dynamics of an initially empty $|g\rangle$ trap for different values of the parameter γ_{eff}, m_{max} and the scattering length. It is worthy to note that γ_{eff} is related to the phase space density of the thermal cloud by the relation $\gamma_{eff} = 2\gamma_{eg} \times 5.2 n_{ex}\lambda(T)^3$, being $\lambda(T) = (2\pi\hbar^2/M k_B T)^{1/2}$ the thermal de Broglie wavelength, and n_{ex} the density in the $|e\rangle$ trap. Since the $|e\rangle$ atoms are considered at a temperature far above the critical temperature of the onset of the condensation, then $n_{ex}\lambda(T)^3$ is necessarily much smaller than 1, restricting the possible range of values that γ_{eff} can take. We study below the dependence of the loading dynamics on γ_{eff}. It is also interesting to point out the limits of the large–temperature approximation, in which all the levels are equally loaded. If such approximation is valid, for a fixed phase space density ϕ, a constraint to the density of the reservoir is introduced by $n_{ex} \gg \phi(M\omega\tilde{m}_{max}/2\pi\hbar)^{3/2}$, with $\tilde{m}_{max} = m_{max} + \omega_{rec}/\omega_g$. For the case of ^{52}Cr and $\omega_g = 2\pi \times 1$kHz, this constraint implies $n \gg 7.45\phi m_{max}^{3/2} \times 10^{11}\mathrm{cm}^{-3}$.

As an example of loading dynamics we show in Fig. 4.5 the case of $\gamma_{eff} = 0.01\omega_g$, $m_{max} = 50$, and $\omega_g = 2\pi \times 1$kHz. For the case of ^{52}Cr, $2\gamma_{eg} = 200 s^{-1}$, this would imply a phase space density $\phi = 10^{-5}$, and a constraint $n_{ex} \gg 10^8 cm^{-3}$ in order to satisfy the large–temperature approximation.

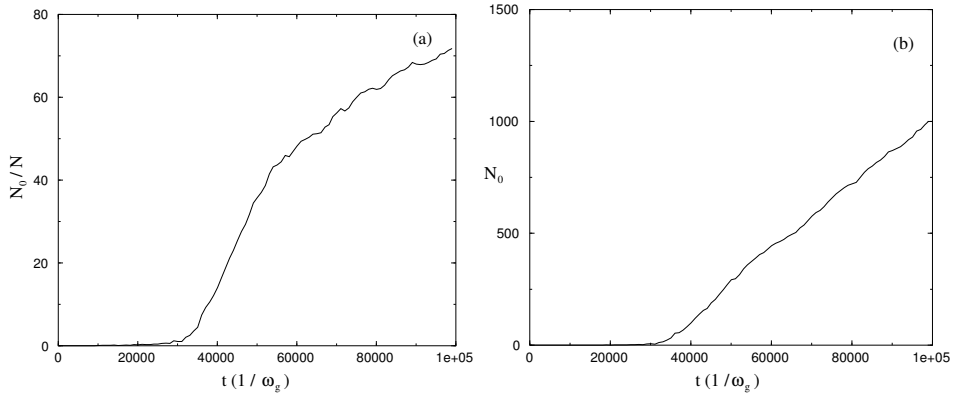

Figure 4.5: (a) Condensate fraction (N_0/N) as a function of time, in units of the ω_g^{-1}, for the case of $\gamma_{eff} = 0.01\omega_g$, $a = 6$nm and $m_{max} = 50$; (b) Dynamics of N_0 for the same situation.

Due to the random character of the process, we have averaged over several Monte Carlo realizations, in order to obtain smoother curves. Typically the loading process is characterized by a time scale of the onset of condensation, after which, as observed in Fig. 4.5, the condensation in the ground–state of the trap appears. In the case of Fig. 4.5 the onset of the condensation appears at approximately $3\times10^4\omega_g^{-1}$, which for $\omega_g = 2\pi\times1$kHz would require $t = 4.8$s. After a time $10^5\omega_g$ (16s) more than 1000 atoms are condensed with a condensate fraction of 70%.

Let us discuss the physics behind the presented numerical results. Since the trap is initially empty, and all the loading rates are equal, the higher shells of the trap are initially loaded with larger probability, due to their larger degeneracy. Once a sufficient number of particles is loaded inside the trap, the collisions produce the evaporation of part of the particles, whereas part of them are transported via collisions to lower levels of the trap. During this process the energy per particle is continuously decreased in the trap (see Fig. 4.6). Finally, the condensation is produced in the ground state. Once this happens, a new mechanism which reduces the energy per particle in the trap appears, namely the bosonic enhancement of the spontaneous emission into the condensate. In effect, the condensate loading becomes faster. When the number of condensed particles becomes large the QBME equation is

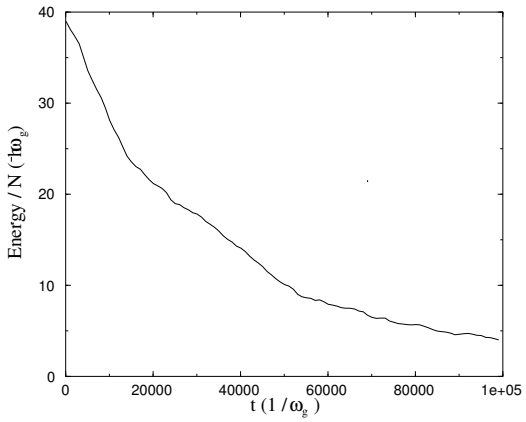

Figure 4.6: Evolution of the energy per particle for the same conditions, for the case of $\gamma_{eff} = 0.01\omega_g$, $a = 6$nm and $m_{max} = 50$.

no more valid, as discussed in Sec. 4.5. The mean field effects appearing beyond the weak condensation should not, however, distort the qualitative effect of speeding up of the loading rate[82]. It is also worthy to note that for condensate densities larger than 10^{15} atoms/cm^3 inelastic processes (as three–body recombination) are expected. Such processes would lead to losses of condensed atoms, which can be repaired by the continuous loading in a similar way as described below for the case of atom laser outcoupling. Let us also note that, eventually, if the number of condensed particles were much larger than the number of levels in the trap, the system would enter into the Bosonic Accumulation Regime discussed in the previous chapter, where the vast majority of the decays were produced into the condensed state.

With this physical picture in mind, it is possible to understand the dependences on the different physical parameters. From the previous discussion it becomes clear the crucial role played by the collisions in the process. Therefore the larger the collisional probability, the faster the condensation is achieved. This can be obtained in a two–fold way, (i) by increasing the scattering length a and/or (ii) by increasing the number of trapped atoms. Point (i) have been studied in Fig. 4.7 , where we have analyzed the case of $m_{max} = 50$, $\gamma_{eff} = 0.01\omega_g$ for values of the scattering length ranging from $a = 1.25$nm to $a = 24$nm. As pointed out previously, larger values of the scattering length produce faster condensation onset. Note, however, that the

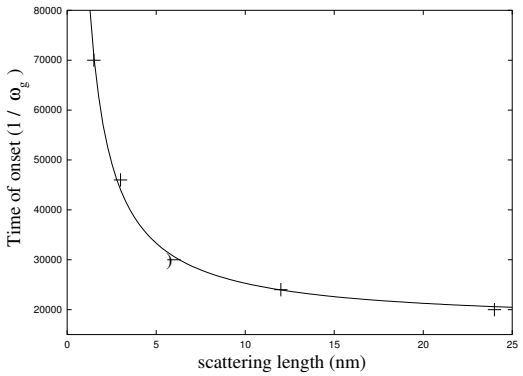

Figure 4.7: Time of onset of the condensation for $\gamma_{eff} = 0.01\omega_g$, $m_{max} = 50$, as a function of the scattering length.

time of onset of the condensation reaches a constant value for large scattering length; this is simply because there is, as pointed above, a time in which the initially empty trap is being loaded, and in this initial time the collisions play no significant role. Such initial time depends basically on m_{max} and γ_{eff}, as pointed out below.

A faster increase of the number of particles in the trap can be achieved in two different ways:

- Increasing γ_{eff}. In Fig. 4.8 we show the example of $m_{max} = 50$, and

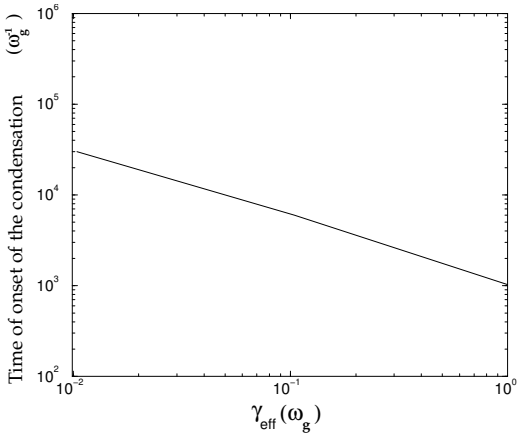

Figure 4.8: Time of onset of the condensation for $a = 6$nm, $m_{max} = 50$, as a function of γ_{eff}.

a scattering length $a = 6$nm, for γ_{eff}/ω_g ranging between 1 and 0.01.

As one could expect the onset of the condensation appears faster for faster loading. In order to achieve a larger γ_{eff}, it is necessary either to increase the phase space density of the thermal cloud, or perhaps more interestingly to consider experimental situations with bigger γ_{eg}. Note that an increase of γ_{eg} by a factor 100 in the case consider above, still very well satisfies the requirements of the BRE. We should stress once more at this point that one of the main advantages of the BRE is the fact that contrary to Festina Lente it is possible to pump with a frequency larger than that of the loaded trap, without having problems with the photon reabsorption. Therefore, it could be in principle possible to consider faster natural transitions, or even controllable quenched ones. In such cases, a fast onset of the condensation could be possible for low phase space densities of the reservoir.

- Increasing m_{max}. In this way the total number of atoms in the trap becomes larger at any given time. As an example, we have considered in Fig. 4.9 the case of $\gamma_{eff} = 0.01\omega_g$, for $m_{max} = 30$ and 60. The

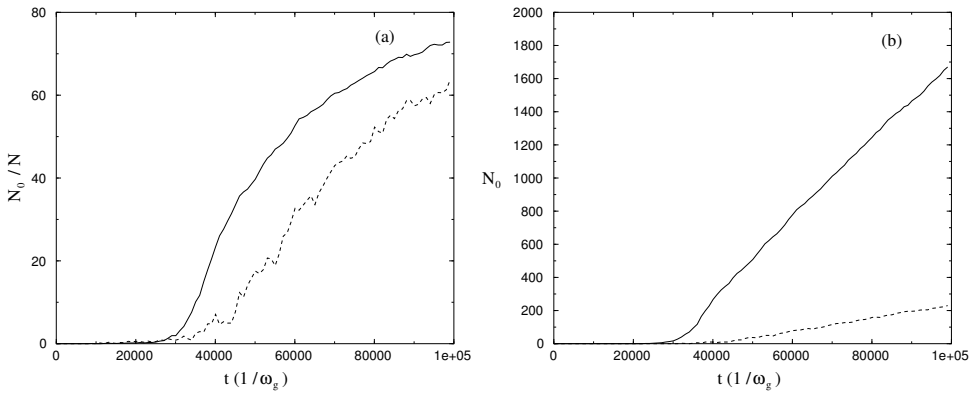

Figure 4.9: (a) Condensate fraction (N_0/N) as a function of time, in units of ω_g^{-1}, for the case of $\gamma_{eff} = 0.01\omega_g$, and $a = 6$nm, and $m_{max} = 60$ (solid) and 30 (dashed); (b) Dynamics of N_0 for the same situation.

increase of the condensate fraction becomes faster for larger m_{max}, although the onset time remains approximately the same (Fig. 4.9(a)). The absolute number of condensed atoms is larger for larger values of m_{max} (Fig. 4.9(b)), because the total number of atoms is also larger.

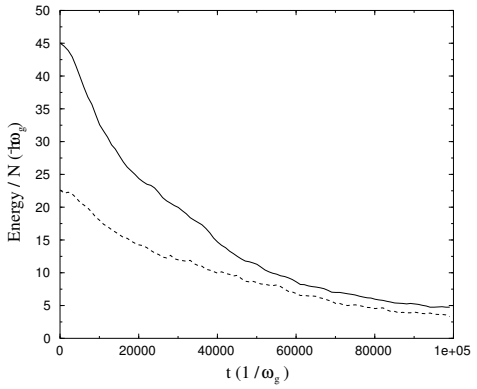

Figure 4.10: (c) Evolution of the energy per particle , for the case of $\gamma_{eff} = 0.01\omega_g$, and $a = 6$nm, and $m_{max} = 60$ (solid) and 30 (dashed).

> Therefore for practical purposes (e.g. detection) it would be recommendable to use larger m_{max}. However, we must stress at this point that a larger m_{max} needs a larger reservoir density n_{ex} if one wants to remain within the limits of the large–temperature approximation.

We have also analyzed the case in which an already formed condensate is emptied via outcoupling, and continuously pumped via spontaneous emission from the thermal reservoir. In our simulations we just consider outcoupling from the condensate, although similar methods could be employed to simulate losses affecting the whole trap. We simulate without outcoupling the creation of a condensate as described above, for the case of $\gamma_{eff} = 6.28\omega_g$, and $m_{max} = 10$. For the case of ^{52}Cr, and $2\gamma_{eg} = 200\text{s}^{-1}$. This represents a quite large phase space density 6×10^{-3}; however, we must again stress that the BRE allows to work with much larger γ_{eg}, and therefore with much lower phase space densities of the reservoir. At $t = 350$ms (when $N_0 \simeq 950$), we begin the outcoupling. We have analyzed different outcoupling rates γ_{out} (Fig. 4.11) , and monitored the population N_0 after 16s. This allows us to find a critical threshold ξ_0 (for this case 1.14) for the ratio $\xi = \gamma_{out}/\gamma_{eff}$. For $\xi > \xi_0$ the loading ("gain") is faster than the outcoupling ("loss"), and the number of condensate atoms increases with time. For $\xi < \xi_0$, the number of particles decreases and stabilizes for a lower N_0. For $\xi \ll \xi_0$ no condensate can be kept.

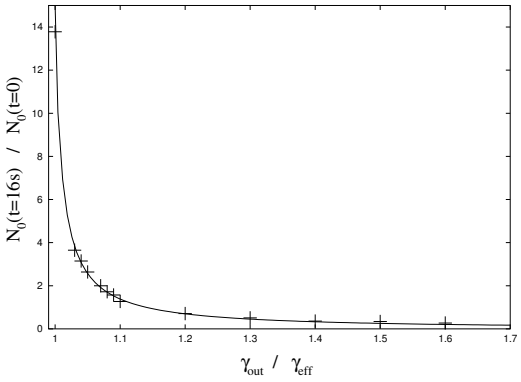

Figure 4.11: Number of condensed particles after 16s (after initially loading an empty $|g\rangle$ trap during 350ms) for the case of $\omega = 2\pi \times 1$kHz, $m_{max} = 10$, $\gamma_{eff} = 6.28\omega_g$, and different outcoupling rates γ_{out}.

It turns out to be important to maintain the population as constant as possible, for the reasons that we clarify below, and therefore to work in the regime of $\xi = \xi_0$. It is however not an easy task, due to the stochastic nature of both, the collisions and the pumping mechanism. In order to stabilize the noise optimally, i.e. to preserve the population of the condensate as constant as possible it is useful to introduce a random temporal variation of the outcoupling rate. Fig. 4.12shows the averaged distribution of population of the condensate during 40 s of continuous outcoupling, for the case of an outcoupling rate $\gamma_{out} = (1.17 - f(t))\gamma_{eff}$, with $0 < f(t) < 0.05$ chosen randomly from an uniform distribution, and the same conditions as in Fig. 4.11. The population of the condensate is maintained quasi constant with an average value of $\langle N_0 \rangle = 940$, and a variance $(\langle N_0^2 \rangle - \langle N_0 \rangle^2)^{1/2} = 80$. During these 40s, 3×10^5 atoms are extracted from the condensate, with a rate of 7500 atoms/s.

Let us briefly comment about the importance of keeping the population of the condensate as constant as possible. The mean–field interaction translates the variations of the condensate population into variations of the energy of the outcoupled atoms, being the variance of the energy related to the variance of the condensate density: $\sigma(E) = 4\pi\hbar^2 a\sigma(n_0)/m$. Therefore, the narrower the population distribution of the condensate, the more "monochromatic" will be the atom–laser source, and consequently the larger the coherence time

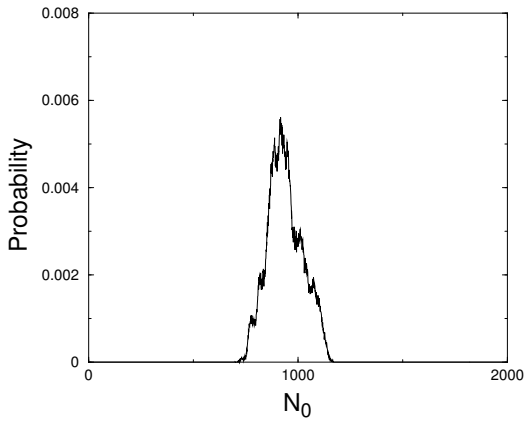

Figure 4.12: Condensate population, averaged during 40s for the case of $m_{max} = 10$, $\gamma_{eff} = 6.28\omega_g$, $\omega_g = 2\pi \times 1$kHz, $\gamma_{out} = (1.17 - f(t))\gamma_{eff}$, with $0 < f(t) < 0.05$ chosen randomly from an uniform distribution.

will be [89]. Let us point out finally, that an additional way to control the fluctuations of the condensate population could be provided by monitoring the energy of the outcoupled atoms, which would inform about the variations of the condensate density. Such information could be used in a feedback loop to dynamically adapt the outcoupling rate to reduce the energy variance of the outcoupled atoms, and therefore increase their temporal coherence.

4.7 Conclusions

In this paper we have analyzed a possible mechanism which could allow the creation and continuous loading of a condensate from a thermal reservoir, by optical pumping. In order to achieve such loading mechanism, it is necessary to guarantee that the reabsorptions of the spontaneously emitted photons do not lead to undesired heating of the atoms in the trap. We have analyzed a particular scheme which allows to satisfy such condition. In this scheme an atom forms a three level Λ system, in which one of the transitions decays much faster than the other one. By using quantum Master Equation techniques we have shown that the very small branching ratio between both transitions induces very large reduction of probability of the reabsorption processes which change the population in the lowest state of the slower tran-

sition. We have explained such effect by identifying the photon reabsorption as a process whose probability depends on the correlation between the reabsorption amplitudes at different times. Such correlation is rapidly destroyed by the fast decay into the other possible channel. The destruction of this correlation causes the desired effect, i.e. the reduction of the "bad" reabsorption processes, responsible for possible heating.

Once we have shown that the reabsorption has no significant effect on the system, we have analyzed the loading dynamics from a thermal reservoir, using Monte Carlo simulations, including the atom–atom collisions in the QBME formalism. We have analyzed the loading of an initially empty trap, demonstrating that the onset of the condensation appears after a finite time, which depends on the physical parameters of the system. The condensation appears due to the joint combination of thermalization via collisions, evaporative cooling due to the finite depth of the considered trap, and bosonic enhancement of the pumping process. We have also analyzed the continuous refilling of the condensate, once it has been formed, taking at the same time into account continuously outcoupling. We have shown that the refilling mechanism allows the compensation of the losses introduced by the outcoupling, and we have analyzed the best strategies to keep the condensate population quasi constant, which is important in order to achieve a "monochromatic" atom laser output. In the paper we have only analyzed the outcoupling mechanism, but the same reasonings applies to possible condensate losses, produced by inelastic processes, such as three–body recombination, or collisions with the thermal atoms in the reservoir.

All our simulations and estimates have been done for Chromium atoms, and for the parameters of the experiment currently performed at the University of Stuttgart. It is however interesting to stress that the same scheme is general, and in particular can be applied for other atomic systems, such as Magnesium. The latter possibility is considered by the W. Ertmer/E. Rasel group at the University of Hannover. As a final remark, we would like to stress that the mechanism of avoiding the "bad" reabsorption processes, considered in this paper (i.e. regime of BRE) allows for faster pumping than other reabsorption remedies (such as Festina Lente, for instance), and there-

fore allows for more effective compensation of the condensate losses. It offers a novel and interesting perspective towards a continuously loaded atom laser.

Chapter 5

Loading of a BEC in the Thomas-Fermi regime

5.1 Introduction

In this chapter, we extend the analysis of the previous chapter to the Thomas-Fermi regime, in which the mean interaction energy is much larger than the separation between the trap levels. In that case, the condensate wavefunction and the excitations depend on the number of particles in the trap, and as consequence the wavefunction vary dynamically during the pumping process, complicating the analysis of the problem. In this chapter we develop the necessary theory, and present the procedure which allows us to analyze the problem. In particular, we analyze the modification of the condensate temperature during the pumping process, identifying the regimes of parameters for which the system is cooled or heated. We show that there is a threshold temperature achievable for a given number of trapped particles, and show that this effect could be employed to control the condensate temperature.

The structure of the chapter is as follows. In Sec. 5.2 we discuss the physical model under consideration, and the basic equations. Sec. 5.3 is devoted to the re-thermalization process after every optical pumping. In Sec. 5.4 we discuss our numerical results.

5.2 Model

In the following we consider a sample of ultracold atoms of mass m with an accessible electronic two-level system, formed by the ground state $|g\rangle$ and an excited state $|e\rangle$. Both $|g\rangle$ and $|e\rangle$ atoms are confined in a harmonic trap, which for simplicity is considered as isotropic, with frequencies ω_g and ω_e, respectively. The $|g\rangle$ atoms are assumed as being Bose condensed, i.e. with a temperature $T \ll T_c$, where T_c is the critical temperature for onset of the condensation. The formation of the condensate using spontaneous emission has been already discussed in the previous chapter. The $|e\rangle$ atoms, which eventually decay spontaneously into the $|g\rangle$ state, are considered as thermally distributed.

The atoms in the $|g\rangle$ trap are described by the corresponding field operator $\hat{\Psi}_g(\vec{r})$. For sufficiently low T, when the number of condensed atoms in the $|g\rangle$ trap, N_0, is comparable to the total number of atoms, N, one can employ the Bogoliubov approximation and substitute $\hat{\Psi}_g$ by a c-number, ψ_0, the BEC wave function, whose stationary value is provided by the time-independent Gross-Pitaevskii equation (GPE)

$$\mathcal{H}_{GP}\psi_0(\vec{r}) = \left(-\frac{\hbar^2}{2m}\nabla^2 + \frac{m}{2}\omega_g^2 r^2 + U_{gg}N|\psi_0|^2 - \mu\right)\psi_0(\vec{r}) = 0, \qquad (5.1)$$

where μ is the chemical potential, and $U_{gg} = 4\pi\hbar^2 a_{gg}/m$ is the coupling constant for the collisions between $|g\rangle$ atoms, with a_{gg} the scattering length. In Eq. (5.1) we have neglected the $e-g$ collisions, since the number of atoms in the $|e\rangle$ state is assumed very small

The excitation spectrum is obtained after linearizing $\hat{\Psi}_g$ around the ground-state solution, $\hat{\Psi}_g(\vec{r}) = \psi_0(\vec{r}) + \delta\hat{\psi}(\vec{r})$. The perturbation $\delta\hat{\psi}$ is then expanded in the standard form [90]

$$\delta\hat{\psi}(\vec{r}) = u^*_{\vec{n}}(\vec{r})\tilde{g}_{\vec{n}} - v_{\vec{n}}(\vec{r})\tilde{g}^\dagger_{\vec{n}}, \qquad (5.2)$$

where $\tilde{g}_{\vec{n}}$ and $\tilde{g}^\dagger_{\vec{n}}$ are the annihilation and creation operators for the quasiparticles with spherical quantum numbers $\vec{n} = n, l, m$. The wave functions $u_{\vec{n}}(\vec{r})$

and $v_{\vec{n}}(\vec{r})$ obey the standard orthogonalization rules [90]. Linearizing in the $u_{\vec{n}}(\vec{r})$ and $v_{\vec{n}}(\vec{r})$ wavefunctions, one obtains the corresponding Bogoliubov equations

$$\begin{aligned}(\mathcal{H}_{GP} + U_{gg}N_0Q\psi_0^2Q)u_{\vec{n}} + U_{gg}N_0Q\psi_0^2Q^*v_{\vec{n}} &= \hbar\tilde{\omega}^g_{\vec{n}}u_{\vec{n}} \quad (5.3)\\ -U_{gg}N_0Q^*\psi_0(\vec{r})^2Qu_{\vec{n}} - (\mathcal{H}_{GP} + U_{gg}N_0Q\psi_0^2Q)^*v_{\vec{n}} &= \hbar\tilde{\omega}^g_{\vec{n}}v_{\vec{n}} \quad (5.4)\end{aligned}$$

where we have used the projection operators $Q = 1 - |\psi_0\rangle\langle\psi_0|$ (Q^*) orthogonally to ψ_0 and (ψ_0^*) [87], and $\tilde{\omega}^g_{\vec{n}}$ denotes the quasiparticle excitation spectrum.

The physics of the atoms in the $|e\rangle$ state is described by the Schrödinger equation:

$$\mathcal{H}_e\psi^e_{\vec{m}}(\vec{r}) = \left(-\frac{\hbar^2}{2m}\nabla^2 + \frac{m}{2}\omega_e^2r^2 + 2U_{ge}N_0|\psi_0|^2\right)\psi^e_{\vec{m}}(\vec{r}) = \hbar\tilde{\omega}^e_{\vec{m}}\psi^e_{\vec{m}}(\vec{r}), \quad (5.5)$$

where we have taken into account that the $|e\rangle$ atoms are affected by the mean-field potential induced by the collisions with the $|g\rangle$ atoms, which are characterized by a coupling constant $U_{ge} = 4\pi\hbar^2a_{ge}/m$, with a_{ge} the corresponding scattering length. Due to the low density in the $|e\rangle$ trap, we have neglected in Eq. (5.5) the $e-e$ collisions. In the following, $\tilde{e}^\dagger_{\vec{m}}$ and $\tilde{e}_{\vec{m}}$ denote the creation and annihilation operators in the eigenstate $\psi^e_{\vec{m}}$, with eigenfrequency $\tilde{\omega}^e_{\vec{m}}$.

The interaction of the atoms with the vacuum electromagnetic field is given by

$$\begin{aligned}\mathcal{H}_{af} = i\sum_{\vec{m}}\sum_{v}\int d^3k\rho(\vec{k})(\vec{d}\vec{\epsilon}_{kv})\\ \left(\eta^c_{0\vec{m}}\tilde{g}^\dagger_0e_{\vec{m}} + \sum_{\vec{n}}\eta^u_{\vec{n}\vec{m}}\tilde{g}^\dagger_{\vec{n}}e_{\vec{m}} - \sum_{\vec{n}}\eta^v_{\vec{n}\vec{m}}\tilde{g}_{\vec{n}}e_{\vec{m}}\right)a^\dagger_{\vec{k}v} + \text{h.c.}, \quad (5.6)\end{aligned}$$

where $a^\dagger_{\vec{k}\nu}$ and $a_{\vec{k}\nu}$ are annihilation and creation operators of photons of wavenumber $\vec{k}$, polarization ν, and frequency $\omega_\nu(\vec{k})$. In Eq. (5.6), $\vec{d}$ is the atomic dipole, $\vec{\epsilon}_{kv}$ is the polarization vector, and $\rho(\vec{k})$ the density of states. The Frank-Condon (FC) factors $\eta^c_{0\vec{m}} = \int d\vec{r}\psi^e_{\vec{m}}(\vec{r})\exp(i\vec{k}\vec{r})\psi_0(\vec{r})$ characterize

the transitions into the condensate, whereas $\eta^u_{\vec{n}\vec{m}} = \int d\vec{r}\psi^e_{\vec{m}}(\vec{r})\exp(i\vec{k}\vec{r})u_{\vec{n}}(\vec{r})$ determine the transition into the u quasiparticle wavefunctions. In the same way, the coefficients $\eta^v_{\vec{n}}$ characterize the transition into the v wavefunctions. Finally, the vacuum energy is provided by the Hamiltonian:

$$\mathcal{H}_f = \sum_\nu \int \vec{dk}\,\omega_\nu(\vec{k})\,a^\dagger_{\vec{k}\nu}a_{\vec{k}\nu}. \tag{5.7}$$

The physics of the system is therefore described by the Hamiltonian

$$\mathcal{H} = \mathcal{H}_a + \mathcal{H}_{af} + \mathcal{H}_f, \tag{5.8}$$

where the atomic Hamiltonian can be written in the form (extracting the condensate energy)

$$\mathcal{H}_a = \sum_{\vec{n}} \tilde{\omega}_{\vec{n}}\tilde{g}^\dagger_{\vec{n}}\tilde{g}_{\vec{n}} + \sum_{\vec{m}}(\omega_0 + \tilde{\omega}^e_{\vec{m}})\tilde{e}^\dagger_{\vec{m}}\tilde{e}_{\vec{m}}, \tag{5.9}$$

where ω_0 is the transition frequency between $|g\rangle$ and $|e\rangle$.

From the previous Hamiltonian, and employing standard techniques of quantum stochastic processes [83], we can obtain in Born-Markov approximation the corresponding quantum Master equation (ME) for the density matrix ρ (see App. A):

$$\dot{\rho}(t) = -iH_{eff}\rho + i\rho H^\dagger_{eff} + \mathcal{J}\rho, \tag{5.10}$$

where

$$\begin{aligned} H_{eff} = -i\Gamma\Bigg\{ &\sum_{\vec{m}} \alpha^c_{\vec{m}00\vec{m}}\tilde{g}_0\tilde{e}^\dagger_{\vec{m}}\tilde{g}^\dagger_0\tilde{e}_{\vec{m}} \\ &+ \sum_{\vec{m},\vec{n}} \alpha^u_{\vec{m}\vec{n}\vec{n}\vec{m}}\tilde{g}_{\vec{n}}\tilde{e}^\dagger_{\vec{m}}\tilde{g}^\dagger_{\vec{n}}\tilde{e}_{\vec{m}} + \sum_{\vec{m},\vec{n}} \alpha^v_{\vec{m}\vec{n}\vec{n}\vec{m}}\tilde{g}^\dagger_{\vec{n}}\tilde{e}^\dagger_{\vec{m}}\tilde{g}_{\vec{n}}\tilde{e}_{\vec{m}}\Bigg\}, \end{aligned} \tag{5.11}$$

is the effective (non Hermitian) Hamiltonian, and

$$\mathcal{J}\rho = 2\Gamma\Bigg\{\sum_{\vec{m}} \Re^c_{\vec{m}00\vec{m}}\tilde{g}^\dagger_0\tilde{e}_{\vec{m}}\rho\tilde{g}_0\tilde{e}^\dagger_{\vec{m}}$$

$$+\sum_{\vec{m},\vec{n}} \Re^{u}_{\vec{m}\vec{n}\vec{n}\vec{m}} \tilde{g}^{\dagger}_{\vec{n}} \tilde{e}_{\vec{m}} \rho \tilde{g}_{\vec{n}} \tilde{e}^{\dagger}_{\vec{m}} + \sum_{\vec{m},\vec{n}} \Re^{v}_{\vec{m}\vec{n}\vec{n}\vec{m}} \tilde{g}_{\vec{n}} \tilde{e}_{\vec{m}} \rho \tilde{g}^{\dagger}_{\vec{n}} \tilde{e}^{\dagger}_{\vec{m}} \Bigg\}, \tag{5.12}$$

is the jump super operator. The spontaneous emission rate is $\gamma = 2\Gamma$, and $\alpha^{a}_{\vec{m}\vec{n}\vec{n}'\vec{m}'} = \Re^{a}_{\vec{m}\vec{n}\vec{n}'\vec{m}'} + i\Im^{a}_{\vec{m}\vec{n}\vec{n}'\vec{m}'}$ (a=c, u, v), where

$$\Re^{a}_{\vec{m}\vec{n}\vec{n}'\vec{m}'}(\omega_0) = \int d\Omega \mathcal{W}(\Omega_k) \eta^{a}_{\vec{m}\vec{n}}(\omega_0, \Omega_k) \eta^{a}_{\vec{m}'\vec{n}'}(\omega_0, \Omega_k)^{*}, \tag{5.13}$$

with $\mathcal{W}(\Omega_k)$ the emission pattern, and

$$\Im^{a}_{\vec{m}\vec{n}\vec{n}'\vec{m}'} = -\frac{P}{\pi} \int du \frac{u^3}{u-1} \Re^{a}_{\vec{m}\vec{n}\vec{n}'\vec{m}'}(u\omega_0),$$

where P denotes the Cauchy principal part.

As discussed in the previous chapters, the effective Hamiltonian H_{eff} is related with photon reabsorption processes, whereas the jump superoperator describes an spontaneous emission without any further reabsorption. In this chapter, we consider the reabsorption processes as negligible (either because we work in the Festina Lente regime [70] or because we consider the situation discussed in the previous chapter), and constrain ourselves to the analysis of the jump processes from $|e\rangle$ to $|g\rangle$. From Eq. (5.12) the amplitude for a jump from a state $\vec{n}_e$ of the $|e\rangle$ trap to a state $\vec{n}^{(a)}_g$ ($a = u, v, c$) of the $|g\rangle$ one is given by

$$\Gamma_{\vec{n}^{(a)}_g, \vec{n}_e} = \int d\Omega_k \mathcal{W}(\Omega_k) |\langle \vec{n}^{(a)}_g | e^{i\vec{k}\vec{r}} | \vec{n}_e \rangle|^2, \tag{5.14}$$

with $\langle \vec{r} | \vec{n}_e \rangle = R_{l_e n_e}(r) Y_{l_e m_e}(\Omega_r)$, and $\langle \vec{r} | \vec{n}^{(a)}_g \rangle = R^{(a)}_{l_g n_g}(r) Y_{l_g m_g}(\Omega_r)$. The FC factors are of the form

$$\langle \vec{n}^{(a)}_g | e^{i\vec{k}\vec{r}} | \vec{n}_e \rangle = 4\pi \sum_{l''=0}^{\infty} \sum_{m=-l''}^{l''} (i)^{l''} Y^{*}_{l''m}(\Omega_k) A^{l''(a)}_{n_g l_g n_e l_e} B^{l''}_{l_g m_g l_e m_e}, \tag{5.15}$$

where $A^{l''(a)}_{n_g l_g n_e l_e} = \int dr r^2 \; R^{(a)}_{l_g n_g}(r) \; j_{l''}(kr) R_{l_e n_e}(r)$ is the radial integral, and the coefficients $B^{l''}_{l_g m_g, l_e m_e}$ are related with the angular part of the integral, and are solvable in terms of the corresponding 3-j Wigner symbols:

$$B^{l''}_{l_g m_g, l_e m_e} = \int d\Omega_r Y^{*}_{l_g m_g}(\Omega_r) Y_{l''m}(\Omega_r) Y_{l_e m_e}(\Omega_r) = \tag{5.16}$$

$$(-1)^{m_g}\begin{pmatrix} l_g & l_e & l'' \\ -m_g & m_e & m \end{pmatrix}\begin{pmatrix} l_g & l_e & l'' \\ 0 & 0 & 0 \end{pmatrix}\sqrt{\frac{(2l_g+1)(2l_e+1)(2l''+1)}{4\pi}}.$$

Due to the properties of these symbols, $B^{l''}_{l_g m_g l_e m_e}$ is independent of m since $-m_g + m_e + m = 0$, $l_g + l_e + l'' = 2p$ (where p is an integer), and $|l_g - l'_e| \leq l'' \leq l_g + l_e$. Substituting (5.15) into (5.14) we find the transition amplitudes.

$$\begin{aligned}\Gamma_{\vec{n}_g^{(a)},\vec{n}_e} = \; & 16\pi^2 \sum_{l'',L'=|l_g-l_e|}^{l_g+l_e} (i)^{l''}(-i)^{L''}\int d\Omega_k W(\Omega_k) Y^*_{l'',m_g-m_e}(\Omega_k) Y_{L',m_g-m_e}(\Omega_k) \\ & \times A^{l''(a)}_{n_g l_g n_e l_e} \times A^{L''(a)}_{n_g l_g n_e l_e} \times B^{l''}_{l_g m_g l_e m_e} \times B^{L''}_{l_g m_g l_e m_e}. \end{aligned} \tag{5.17}$$

From the transition amplitudes (5.17) and the populations of the corresponding levels, we obtain the transition probabilities describing the creation of a quasiparticle $n = (n_g l_g)$

$$P^u_n = (\langle N_n(T)\rangle + 1) \sum_{n_e,l_e} \langle N_{\vec{n}_e}(T_e)\rangle \sum_{m_g,m_e} \Gamma_{\vec{n}_g^{(u)},\vec{n}_e}. \tag{5.18}$$

Similarly, we obtain the transition probabilities

$$P^v_n = \langle N_n(T)\rangle \sum_{n_e,l_e} \langle N_{\vec{n}_e}(T_e)\rangle \sum_{m_g,m_e} \Gamma_{\vec{n}_g^{(v)},\vec{n}_e} \tag{5.19}$$

describing the destruction of a quasiparticle $n = (n_g l_g)$ associated with a transfer of an atom into the condensate after the subsequent thermalization. Finally, the direct decay process into the condensate is described by

$$P^c = (\langle N_0(T)\rangle + 1) \sum_{n_e,l_e} \langle N_{\vec{n}_e}(T_e)\rangle \sum_{m_e} \Gamma_{\vec{n}_g^{(c)}\vec{n}_e}. \tag{5.20}$$

In the previous expressions, $\langle N_n(T)\rangle = (\exp[E_n/K_B T] - 1)^{-1}$ is the Bose-Einstein distribution in the $|g\rangle$ trap, and $\langle N_{\vec{n}_e}(T_e)\rangle = \hat{N}\exp[-E_{\vec{n}_e}/K_B T_e]$ is the Boltzmann distribution (normalized to 1) in the $|e\rangle$ trap. The sums in

Eqs. (5.18), (5.19) and (5.20) can be easily evaluated, e.g.

$$\sum_{m_g,m_e} \Gamma_{\vec{n}_g^{(u)},\vec{n}_e} = 16\pi^2 \sum_{l'',L'=|l_g-l_e|}^{l_g+l_e(*)} (-1)^{\frac{3L''+l''}{2}} A^{l''(u)}_{n_g l_g n_e l_e} \times A^{L''(u)}_{n_g l_g n_e l_e} \times C^{l'',L''}_{l_g,l_e}, \quad (5.21)$$

where $\sum^{(*)}$ denotes that the sum is just over numbers with the same parity, and

$$C^{l'',L''}_{l_g,l_e} = \sum_{m_g=-l_g}^{l_g} \sum_{m_e=-l_e}^{l_e} B^{l''}_{l_g m_g l_e m_e} \times B^{L''}_{l_g m_g l_e m_e} \times \int d\Omega \mathcal{W}(\Omega_k) Y^*_{l'',m_g-m_e}(\Omega_k) Y_{L'',m_g-m_e}(\Omega_k), \quad (5.22)$$

where the final integral over Ω_k can be easily solved by considering $\mathcal{W}(\Omega_k)$ as a dipole pattern in the z direction,

$$\mathcal{W}(\Omega_k) = \frac{3}{4\pi}\cos(\theta)^2 = \frac{1}{\sqrt{4\pi}} Y_{00}(\Omega_k) + \frac{1}{\sqrt{5\pi}} Y_{20}(\Omega_k), \quad (5.23)$$

and employing once more the 3-j Wigner symbols.

5.3 Re-thermalization

From Eqs. (5.18), (5.19), and (5.20), we can simulate the effects of a spontaneous emission process. We assume that the time scale of thermalization in the $|g\rangle$ trap is much faster than the time interval between different pump events, i.e. the collisional rate in the ground-state trap is much larger than γ. In this way, after every pump, the system re-thermalizes, redistributing the energy gained or lost during the pump process. We analyze in the following the variation of the condensate temperature after the pumping.

After an spontaneous emission occurs, the number of $|g\rangle$ atoms increases to $N' = N + 1$, and the new energy becomes:

$$\langle E' \rangle = E + \mu P^c + \sum_n (\epsilon_n + \mu C_n)(P^u_n - P^v_n). \quad (5.24)$$

where E is the energy before the pumping, and $C_n = |u_n|^2 + |v_n|^2$. Therefore

the increase of the total energy is:

$$\delta E = \langle E' \rangle - E = \mu P^c + \sum_n (\epsilon_n + \mu C_n)(P_n^u - P_n^v). \tag{5.25}$$

After the re-thermalization, the system acquires a new temperature T' which can be evaluated numerically from the expressions:

$$E' = E_0(N_0(T')) + \sum_n N_n(T')(\epsilon_n + \mu C_n) - \sum_n (\epsilon_n - \mu)|v_n|^2 \tag{5.26}$$

$$N_0(T') = N + 1 - \sum_n N_n(T') C_n + |v_n|^2, \tag{5.27}$$

where $N_n(T) = (\exp[\epsilon_n / K_B T] - 1)^{-1}$ denotes the Bose-Einstein distribution of the populations in the excited states of the $|g\rangle$ trap, and

$$E_0(N_0) = \langle \psi_0 | \mathcal{H}_{GP} - \frac{U_{gg}}{2} |\psi_0|^2 |\psi_0\rangle. \tag{5.28}$$

In Eqs. (5.26) and (5.27), we assume the excitation spectrum as that calculated for N particles, i.e. before the pumping. This approximation is valid as long as the number of excited particles $N - N_0 \gg 1$.

Assuming $T' = T + \delta T$ with $\delta T \ll T$, we can perform a Taylor expansion up to first order in $\delta T / T$. For the Bose-Einstein distribution we obtain:

$$N_n(T + \delta T) = N_n(T) + \delta T \frac{\epsilon_n}{K_B T^2} \frac{\exp[\epsilon_n / K_B T]}{(\exp[\epsilon_n / K_B T] - 1)^2}. \tag{5.29}$$

Substituting Eqs. (5.29) and $N_0(T') = N_0 + \delta N_0$ into Eqs. (5.26) and (5.27) we obtain for:

$$\begin{aligned} \delta E = E(T + \delta T) - E(T) = \mu(N_0)\delta N_0 + \\ \frac{\delta T}{T} \sum_n \frac{\epsilon_n}{K_B T} (\epsilon_n + \mu(|u_n|^2 + |v_n|^2) \frac{\exp[\epsilon_n / K_B T]}{(\exp[\epsilon_n / K_B T] - 1)^2} \end{aligned} \tag{5.30}$$

and

$$\delta N_0 = 1 - \frac{\delta T}{T} \sum_n \frac{\epsilon_n}{K_B T} (|u_n|^2 + |v_n|^2) \frac{\exp[\epsilon_n / K_B T]}{(\exp[\epsilon_n / K_B T] - 1)^2}. \tag{5.31}$$

Substituting Eqs. (5.31) into Eqs. 5.30 we obtain:

$$\delta E = \mu(N_0) + \frac{\delta T}{T}\sum_n \frac{\epsilon_n^2}{K_B T}\frac{\exp[\epsilon_n/K_B T]}{(\exp[\epsilon_n/K_B T]-1)^2}. \tag{5.32}$$

With Eqs. 5.32 we have found an expression for $\delta E \equiv \delta E(T, N_0, \delta T)$ Equating Eqs. (5.32) and (5.25) we obtain:

$$\frac{\delta T}{T} = -\frac{\tilde{\mu}(N_0)(1-P^c) - \sum_n(\tilde{\epsilon}_n + \tilde{\mu}C_n)(P_n^u - P_n^v)}{\sum_n \tilde{\epsilon}_n^2 \frac{\exp[\tilde{\epsilon}_n]}{(\exp[\tilde{\epsilon}_n]-1)^2}}, \tag{5.33}$$

where $\tilde{\mu} = \mu/K_B T$, $\tilde{\epsilon} = \epsilon_n/K_B T$. Additionally,

$$\begin{aligned}\delta N_0 &= 1 + \left\{\frac{\tilde{\mu}(N_0)(1-P^c) - \sum_n(\tilde{\epsilon}_n + \tilde{\mu}C_n)(P_n^u - P_n^v)}{\sum_n \tilde{\epsilon}_n^2 \frac{\exp[\tilde{\epsilon}_n]}{(\exp[\tilde{\epsilon}_n]-1)^2}}\right\} \\ &\times \sum_n \tilde{\epsilon}_n C_n \frac{\exp[\tilde{\epsilon}_n]}{(\exp[\tilde{\epsilon}_n]-1)^2}.\end{aligned} \tag{5.34}$$

From Eq. (5.34) we can obtain the expression for $\xi = (N_0/N' - N_0/N)/(N_0/N)$. If $\xi > 0$, the pumping increases the relative population in the condensate, and therefore the temperature of the sample is reduced. On the contrary, if $\xi < 0$ the system is heated by the pumping. Expanding $n' = N_0'/(N+1)$ in the small parameter $1/N$ one obtains

$$\frac{N_0 + \delta N_0}{N+1} = \frac{N_0}{N}\left(\frac{1 + \frac{\delta N_0}{N_0}}{1 + \frac{1}{N}}\right) \tag{5.35}$$

$$= \frac{N_0}{N}\left(1 + \frac{\delta N_0}{N_0}\right)\left(1 - \frac{1}{N} + \frac{2}{N^2} + O(N^{-3})\right). \tag{5.36}$$

Additionally,

$$\begin{aligned}\xi &= \frac{\frac{N_0(T+\delta T)}{N+1} - \frac{N_0(T)}{N}}{N_0/N} \\ &= \frac{1}{N_0}\{\delta N_0 - 1\} + \frac{1}{N_0^2}\{\delta N + 1 - \delta N_0\} + \mathcal{O}(\delta N_0/N_0^3).\end{aligned} \tag{5.37}$$

It is therefore easy to see that up to terms of order $\delta N/N_0^2$, where $\delta N =$

$N - N_0$, the system is cooled ($\xi > 0$) when the condition

$$\begin{aligned} \delta N &< (N_0 - 1)\frac{\tilde{\mu}(N_0)(1-P^c) - \sum_n(\tilde{\epsilon}_n + \tilde{\mu}C_n)(P_n^u - P_n^v)}{\sum_n \tilde{\epsilon}_n^2 \frac{\exp[\tilde{\epsilon}_n]}{(\exp[\tilde{\epsilon}_n]-1)^2}} \\ &\times \sum_n \tilde{\epsilon}_n C_n \frac{\exp[\tilde{\epsilon}_n]}{(\exp[\tilde{\epsilon}_n]-1)^2} \end{aligned} \tag{5.38}$$

is fulfilled. For large temperatures, δN can increase enough to violate (5.38). On the other hand for very low temperatures the transition probability into the condensate $P^c \to 1$, and also in this case the condensate is heated. Hence, there is a transition from heating to cooling at some finite threshold temperature, T_{th}, which depends on four different system parameters: the total number of atoms N, the temperature, T_e, of the excited state trap, the coupling constant U_{eg} for the collisions between $|e\rangle$ and $|g\rangle$ atoms, and the ratio ω_e/ω_g between the frequencies of the $|g\rangle$ and $|e\rangle$ traps. When N increases, so does $\tilde{\mu}$ and it s easy to see that T_{th} decreases. If T_e increases the transition to higher lying excited states are more favorable, and as one could expect T_{th} increases. The parameters U_{eg} and ω_e/ω_g influence the spectrum of the excited state trap. For $U_{eg} = 0$ the harmonic oscillator spectrum is recovered. However, when U_{eg} grows, the mean-field repulsion leads to an expulsion of the $|e\rangle$ atoms from the trap center, increasing the probability for a transition into excited states of the $|g\rangle$ trap. On the other hand, if $\omega_e \gg \omega_g$, and T_e is sufficiently small, the mean-field shift just provides an overall homogeneous shift of the levels of the $|e\rangle$ trap, and the threshold temperature becomes comparable to that for $U_{eg} = 0$.

5.4 Numerical results

We have analyzed δT after a spontaneous emission pumping using the following procedure. For a given total number of atoms, N, and a given initial temperature, T, we first calculate the number of atoms in the condensate N_0, and then evaluate ψ_0 by evolving the GPE (5.1) in imaginary time. Once obtained ψ_0, we diagonalize equations (5.3) and (5.4) employing a

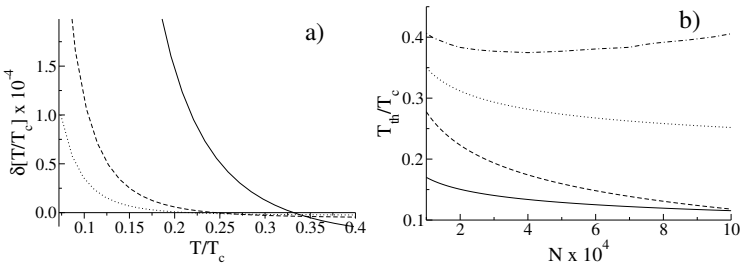

Figure 5.1: a) variation of T/T_c after a spontaneous emission as a function of the initial T/T_c for $\omega = 20 \times 2\pi$ Hz, $\omega_e = 10\omega_g$, $T_e = 21\hbar\omega_g$, and $N = 10^4$, 5×10^4 and 10^5; b) dependence of T_{th} on N for $\omega_e = \omega_g$ and $U_{eg}/U_{gg} =$ 1(dotted–dashed curve), 0.5 (dotted curve), and 0 (dashed curve); the solid curve shows the case $\omega_e = 10\omega_g$ and $U_{eg}/U_{gg} = 1$

harmonic oscillator basis, to find the $\{u, v\}$ eigenfunctions, and the corresponding eigenenergies. As a next step, we calculate $\Gamma_{\vec{n}_g^{(a)},\vec{n}_e}$ $(a = c, u, v)$ using Eq. (5.14). For a given temperature T_e of the $|e\rangle$ trap, we evaluate from Eqs. (5.18), (5.19) and (5.20) the decay probabilities into the different states of the $|g\rangle$ trap. From Eq. (5.24) we obtain the new average energy after the pumping. Finally, from Eqs. (5.26) and (5.27) we obtain the new temperature after the rethermalization.

Fig. 5.1a shows the variation of T/T_c after a spontaneous emission as a function of the initial T/T_c for $\omega = 20 \times 2\pi$ Hz, $\omega_e = 10\omega_g$, $T_e = 21\hbar\omega_g$, and $N = 10^4$, 5×10^4 and 10^5. In the calculation of the FC factors (5.15), we have considered a Lamb-Dicke parameter $\eta^2 \equiv E_{rec}/\hbar\omega_g = 1$, where E_{rec} is the energy associated with the recoil of a single photon. The choice of η and T_e is motivated by our numerical limitations, but we expect qualitatively similar results for other values of these parameters. As previously discussed, the system is cooled for temperatures T larger than a threshold one, which is progressively lower for larger number of atoms. In the figure, due to the low value of T_e chosen, it is not possible to observe the heating region for large temperatures, which for this case is located at T close to T_c. For other ranges of parameters the qualitative picture does not change significantly, i.e. always a threshold temperature separating heating and cooling regions exists. We have analyzed the dependence of T_{th} on different physical param-

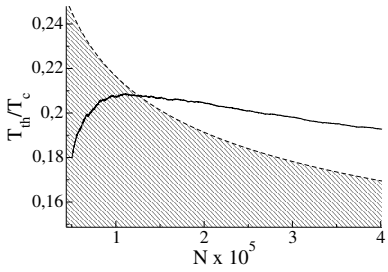

Figure 5.2: Solid line indicates Monte Carlo and dashed line T_{th} for $\omega_e = 10\omega_g$, $T_e = 21\hbar\omega_g$

eters. Fig. 5.1b shows the dependence of T_{th} on N for $\omega_e = \omega_g$ and different values of U_{eg}. For $U_{eg} \to 0$ the temperature T_{th} decays monotonically with N. However, when U_{eg} increases, and due to the repulsive mean-field induced by the eg collisions, the eigenfunctions of the $|e\rangle$ trap possess a local minimum at the trap center, and the pumping into the condensate becomes less effective. Consequently, T_{th} increases for large N, as clearly observed for the case of $U_{eg} = g$. This effect is less pronounced, for larger values of ω_e keeping fixed T_e, since then the lower levels of the $|e\rangle$ trap have an extension smaller than the condensate wavefunction, and hence the mean-field just produces a global energy shift of the lowest $|e\rangle$ levels, without any consequence for the pumping process (see Fig. 5.1b). Finally, we have simulated under different conditions the continuous optical pumping of atoms into the condensate. To this aim, we have employed Monte Carlo methods to evaluate the corresponding rate equations, with the probabilities provided by Eqs. (5.18), (5.19) and (5.20). In principle, after every pumping all the previously described steps of our algorithm should be repeated. In practice, it is enough to do so after a number of steps $N_{steps} \ll \delta N$, which is dynamically adjusted in our calculations. Fig. 5.2 shows our Monte Carlo results for $\omega_e = 10\omega_g$, $T_e = 21\hbar\omega_g$. The dashed curve in Fig. 5.2 indicates T_{th}. The simulation is started with $N = 4.8 \times 10^4$, and $T/T_c = 0.18$. For this initial value, the pair $(N, T/T_c)$ is below the T_{th} curve, and consequently within the heating region. As expected, the temperature of the system increases with the pumping. However, once $(N, T/T_c)$ crosses the T_{th} curve, the temperature begins to decrease when pumping. Therefore, interestingly, the temperature of the

system should asymptotically approach the curve T_{th}.

5.5 Conclusions

In this chapter, we have analyzed the continuous optical loading of a BEC in the Thomas-Fermi regime. Contrary to the weak condensation case, the condensate and excited-state wavefunctions vary dynamically during the loading. This fact has been taken into account in our procedure. By means of GPE and Bogoliubov equations, we determine before every pumping the proper wavefunctions, and transition probabilities. Assuming a rapid thermalization, we have monitored the variation of the temperature during the loading. We have observed that for a given number of trapped atoms, there is always a threshold temperature, T_{th}, below which the condensate is heated. We have analyzed the dependence of T_{th} on different experimental parameters, in particular the total number of atoms, N, the trap geometries, and the interparticle interactions. A lower T_{th} is obtained for smaller interactions between excited-state and ground-state atoms, since repulsive interactions tend to displace the excited-state atoms away from the trap center, preventing the effective pumping into the condensate. Our analysis shows that, not only the number of atoms in the trap, but also the temperature of the system, can be maintained by means of optical loading. To this aim, the condensate should be created with a temperature and a number of atoms, lying close to the curve $T_{th}(N)$. In that case, in the presence of outcoupling or other loss sources, if the loss mechanism leads to heating, the temperature will be over $T_{th}(N)$, and the system will be cooled by the pumping, whereas the opposite will be true if the loss mechanism cools. Interestingly, this could allow for the sustained analysis of condensates at a quasi-fixed constant temperature.

Several physical scenarios could be devised to employ our analysis for the continuous loading of a BEC. For example, an optical lattice could be employed to move atoms in an internal state $|r\rangle$ from a relatively hot reservoir into the condensate region. In the center of the condensate region a Raman pulse could be employed to transfer the $|r\rangle$ atoms into an state $|e\rangle$, which

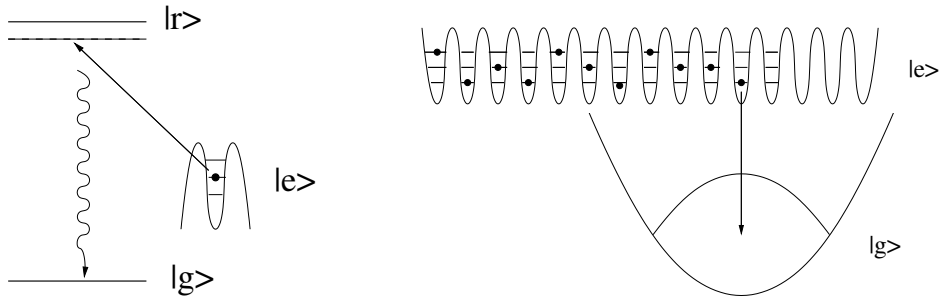

Figure 5.3: The right figure depicts a possible physical scenario for the continuous optical loading of a BEC from excited state atoms in a lattice. In the region of the condensate the atoms may undergo a laser-induced spontaneous Raman transition into the $|g\rangle$, as shown in the left figure.
.

decays into the ground-state $|g\rangle$. In this way, it could be achieved that only those lattice sites near the condensate center actually decay into the $|g\rangle$ trap (see Fig. 5.3). For a sufficiently strong optical lattice each one of the lattice wells will behave as a single trap with few occupied levels, as that discussed in our chapter. Interestingly, in this scenario, due to the small size of the $|e\rangle$ trap, T_{th} should monotonically decay with N, since the mean-field effects should just shift globally the states of the $|e\rangle$ trap. Therefore, in this system the pumping could be employed to post-cool an already formed condensate down to $T = 0$, and maintain the condensate temperature very low against possible loss sources.

Chapter 6

Conclusions

In this thesis we have analyzed different physical scenarios in which a BEC could be continuously pumped using optical means. In all the explored methods an atom in an excited electronic state decays via spontaneous emission into the condensate, which is formed in the ground electronic state. We have identified the reabsorption of the spontaneously emitted photons as the main source of heating, which should be avoided in order to realize optical loading. Chapters 3 and 4 were devoted to the detailed analysis of two different ways to avoid the heating effects induced by reabsorption:

In chapter 3, we considered the BAR regime, extending the previous analysis of Ref. [13] to a general 3D situation, in which the excited-state atoms can occupy more than one trapped state. We have shown that under appropriate conditions, the BAR expansion is still valid for this more general case, and that the reabsorptions can play a positive role in the loading of the condensate. Such effect has a quantum character, and results from the destructive interference between the processes which tend to lower the condensate fraction. We have analyzed in detail the conditions for the validity of the BAR expansion, showing that in general the BAR condition presented in Ref. [13] is not enough to guarantee the BAR expansion, since for more than one excited–trap level, the temperature of such trap is also important, and must be kept sufficiently low. We have simulated the loading in the BAR regime and shown that under proper conditions the positive effects of the

reabsorption lead to cooling during the loading process.

In chapter 4, we analyzed the case of an atom with an accessible three level Λ system, in which one of the transitions decays much faster than the other one. By using quantum Master Equation techniques we have shown that the very small branching ratio between both transitions induces a very large reduction of the probability of the reabsorption processes which lead to heating. We have explained such effect by identifying the photon reabsorption as a process whose probability depends on the correlation between the reabsorption amplitudes at different times. Such correlation is rapidly destroyed by the fast decay into the other possible decay channel, explaining the suppression of the reabsorption.

Once we have shown that, under proper conditions, the reabsorption has no significant effects on the system, we have analyzed the process of creation and loading of a BEC via spontaneous emission for different interaction strengths: weak-condensation (chapter 4) and Thomas-Fermi regime (chapter 5):

In chapter 4, we considered the weak-condensation case in which the mean-field energy induced by collisions can be considered smaller than the energy separation between trap levels. In that case, we have analyzed the loading dynamics from a thermal reservoir, using Monte Carlo simulations, including the atom–atom collisions, which in the weak-condensation regime can be treated in the QBME formalism. We have analyzed the loading of an initially empty trap, demonstrating that the onset of the condensation appears after a finite time, which depends on the physical parameters of the system. The condensation appears due to the joint combination of thermalization via collisions, evaporative cooling due to the finite depth of the considered trap, and bosonic enhancement of the pumping process. We have also analyzed the continuous refilling of the condensate, once it has been formed, taking at the same time into account continuously outcoupling. We have shown that the refilling mechanism allows for the compensation of the losses introduced by the outcoupling, or eventually by any other source of losses, such as three–body recombination, or collisions with the thermal atoms in the reservoir.

Finally, in chapter 5 we have analyzed the continuous optical loading of a BEC in the Thomas-Fermi regime. Contrary to the weak condensation case analyzed in chapter 4, the condensate and excited-state wavefunctions vary dynamically during the loading. By means of GPE and Bogoliubov equations, we determine before every pumping the proper wavefunctions, and transition probabilities. Assuming a rapid thermalization, we have monitored the variation of the temperature during the loading. We have observed that for a given number of trapped atoms, there is always a threshold temperature, T_{th}, below which the condensate is heated. We have analyzed the dependence of T_{th} on different experimental parameters, in particular the total number of atoms, N, the trap geometries, and the interparticle interactions. Our analysis shows that, not only the number of atoms in the trap, but also the temperature of the system, can be maintained by means of optical loading.

The results of this Thesis show that under appropriate (but realistic) conditions, optical pumping can be employed to continuously populate a BEC in the presence of losses, either due to outcoupling in an atom laser, or due to inelastic processes. The continuous loading of a BEC offers exciting possibilities:

- The continuous repairing of a BEC against losses could be employed to enlarge (in principle indefinitely) the life time of the current experiments, which are largely limited by the loss rate induced either by background collisions, or two- and three-body losses. In this sense a completely new generation of experiments could be possible.

- The loading of a BEC in a continuous way, opens the fascinating perspective to accomplish a cw atom laser, which could be eventually employed in future applications, as e.g. atom lithography and atom clocks.

In this sense, we expect that the results of this Thesis could stimulate future works in these directions.

Appendix A

Quantum Master Equation

This Appendix is devoted to the presentation of the formalism of quantum master equation (QME), which is extensively employed all throughout this thesis. For more details, see e.g. [83, 84, 85]. In the following we shall derive in detail the QME from the corresponding Hamiltonian, which in our case, as discussed in different chapters of this thesis, is of the form:

$$\mathcal{H} = \mathcal{H}_a + \mathcal{H}_f + \mathcal{H}_{af}. \tag{A.1}$$

where $\mathcal{H}_a$ is the atomic Hamiltonian describing the physics of the atoms without any atom-light interaction, $\mathcal{H}_f$ is the Hamiltonian of the reservoir in which the considered system is immersed (in our case the vacuum of the electromagnetic field), and $\mathcal{H}_{af}$ describes the atom-light interaction. The von Neumann equation for the density matrix describing both the system and the reservoir is

$$\dot{\rho} = -\frac{i}{\hbar}[\mathcal{H}, \rho_{tot}] = -\frac{i}{\hbar}[\mathcal{H}_a + \mathcal{H}_f + \mathcal{H}_{af}., \rho_{tot}]. \tag{A.2}$$

We are interested in the physics of the atomic system considered, and not in the details of the dynamics of the reservoir. Therefore, we shall study the dynamics of the reduced density matrix:

$$\rho_s(t) = Tr_B\{\rho(t)\}, \tag{A.3}$$

where Tr_B indicates the trace over the degrees of freedom of the reservoir.

Transforming into interaction picture

$$\rho_{int}(t) = e^{\frac{i}{\hbar}(\mathcal{H}_a+\mathcal{H}_f)t}\rho(t)e^{-\frac{i}{\hbar}(\mathcal{H}_a+\mathcal{H}_f)t}, \tag{A.4}$$

we can re-write Eq. (A.2) in the form

$$\dot{\rho}_{int}(t) = -\frac{i}{\hbar}[\mathcal{H}_{af}(t), \rho_{int}(t)]. \tag{A.5}$$

Note that ρ_s and ρ_{int} are related by

$$\rho_s(t) = e^{-\frac{i}{\hbar}H_{sys}t}Tr_B\{\rho_{int}(t)\}e^{\frac{i}{\hbar}H_{sys}t}. \tag{A.6}$$

Integrating Eq. (A.5) from 0 to t we obtain

$$\rho_{int}(t) = \rho_{int}(0) - \frac{i}{\hbar}\int_0^t dt'[\mathcal{H}_{af}(t'), \rho_{int}(t')]. \tag{A.7}$$

Inserting into Eq. (A.5):

$$\dot{\rho}_{int}(t) = -\frac{i}{\hbar}[\mathcal{H}_{af}(t), \rho_{int}(0)] - \frac{1}{\hbar^2}\int_0^t dt'[\mathcal{H}_{af}(t), \mathcal{H}_{af}(t'), \rho_{int}(t')]]. \tag{A.8}$$

Up to this point, no assumption was used and the equation of motion is basically exact. Tracing over the reservoir we obtain

$$Tr_B\{\dot{\rho}_{int}(t)\} = -\frac{1}{\hbar^2}\int_0^t dt' Tr_B\{[\mathcal{H}_{af}(t), \mathcal{H}_{af}(t'), \rho_{int}(t')]]\}, \tag{A.9}$$

where we have employed that $Tr_B\{\mathcal{H}_{af}\rho_{int}(0)\} = 0$, since, assuming that the bath and the system are initially independent, i.e. $\rho_{int}(0) = \rho(0) = \rho_s(0) \otimes \rho_B$, $\mathcal{H}_{af}$ has no diagonal elements in the reservoir variables. Assuming that at any time the reservoir remains practically unaffected by the interaction with the system, we can extend the initial factorization to any later time t, i.e. $\rho_{int}(t) \approx \rho_s(t) \otimes \rho_B$. This is the so-called Born approximation. After

employing this approximation we obtain

$$\dot{\rho}_s(t) = -\frac{1}{\hbar^2}\int_0^t dt' Tr_B\{[\mathcal{H}_{af}(t), \mathcal{H}_{af}(t'), \rho_s(t') \otimes \rho_B]]\}. \tag{A.10}$$

Finally we perform the so-called Markov approximation, i.e. we assume that the reservoir correlation function decays much faster than any typical time scale of the system dynamics. Therefore, we can substitute in Eq. (A.10) $\rho_s(t') \to \rho_s(t)$. Additionally, for t much larger then any reservoir correlation time, one can substitute $\int_0^t \to \int_{-\infty}^t$. These approximations lead to the final form of the QME

$$\dot{\rho}(t) = -\frac{1}{\hbar^2}\int_0^\infty d\tau Tr_B\{[\mathcal{H}_{af}(t), \mathcal{H}_{af}(t-\tau), \rho(t) \otimes \rho_B]]\}. \tag{A.11}$$

Performing the commutators, and tracing over the degrees of freedom of the vacuum of the electromagnetic field, we obtain a first order differential equation in time for the density operator, which acquires the so-called Lindblad Form

$$\frac{d}{dt}\rho(t) = \mathcal{L}\rho = -iH_{eff}(t)\rho(t) + i\rho(t)H_{eff}(t) + \mathcal{J}(t)\rho(t), \tag{A.12}$$

where H_{eff} and $\mathcal{J}$ are, respectively, the so-called effective Hamiltonian and the jump superoperator.

Appendix B

Solution of the integral (2.11)

In this Appendix we shall discuss the solution of Eq. (3.19). This equation presents an integral of the form:

$$P\int d\lambda \frac{\lambda^n}{\lambda-1}e^{-C\lambda^2} \tag{B.1}$$

where P is the Cauchy principle part of the integral and C is a constant. Re-expressing

$$\frac{\lambda^n}{\lambda-1} = \sum_{i=0}^{n-1}\lambda^i + \frac{1}{\lambda-1}, \tag{B.2}$$

we can rewrite:

$$\begin{aligned} & P\int d\lambda \frac{\lambda^n}{\lambda-1}e^{-C*\lambda^2} \\ &= \sum_{i=0}^{n-1}\int d\lambda\lambda^i e^{-C\lambda^2} + P\int d\lambda\frac{1}{\lambda-1}e^{-C*\lambda^2} \\ &= \sum_{i=0}^{n-1}\frac{(1+(-1)^i)}{2}C^{-\frac{1+i}{2}}\Gamma(\frac{1+i}{2}) + P\int d\lambda\frac{1}{\lambda-1}e^{-C\lambda^2}. \end{aligned} \tag{B.3}$$

Employing the relation

$$e^{-C\lambda^2} = \sqrt{\frac{C}{\pi}}\int dy e^{-C(y+i\lambda)^2-C\lambda^2} = \sqrt{\frac{C}{\pi}}\int_{-\infty}^{\infty} dy e^{-Cy^2-2iCy\lambda}, \tag{B.4}$$

we can re-express the integral in the form:

$$\begin{aligned}
&P\int d\lambda \frac{1}{\lambda-1}e^{-C\lambda^2} \\
&= \sqrt{\frac{C}{\pi}}\int dy e^{-Cy^2} P\int d\lambda \frac{1}{\lambda-1}e^{-2iCy\lambda} \\
&= \sqrt{\frac{C}{\pi}}(\int_{-\infty}^{0} dy e^{-Cy^2} + \int_{0}^{\infty} dy e^{-Cy^2}) P\int d\lambda \frac{1}{\lambda-1}e^{-2iCy\lambda} \\
&= \sqrt{\frac{C}{\pi}}\int_{0}^{\infty} dy e^{-Cy^2} P\int d\lambda \frac{1}{\lambda-1}(e^{-2iCy\lambda} + e^{+2iCy\lambda}) \\
&= 2\sqrt{\frac{C}{\pi}}\int_{0}^{\infty} dy e^{-Cy^2} P\int d\lambda \frac{1}{\lambda-1}\cos[2Cy\lambda] \\
&= 2\sqrt{\frac{C}{\pi}}\Re\left\{\int_{0}^{\infty} dy e^{-Cy^2} P\int d\lambda \frac{1}{\lambda-1}e^{2iCy\lambda}\right\}. \qquad \text{(B.5)}
\end{aligned}$$

The last Cauchy integral can be calculated using the residues theorem [91], $P\int d\lambda/(\lambda-1)e^{2iCy\lambda} = \pi i \exp[2iCy]$. Finally, after integrating over y one obtains

$$\begin{aligned}
P\int d\lambda \frac{1}{\lambda-1}e^{-C\lambda^2} &= -2\sqrt{\frac{C}{\pi}}\int_{0}^{\infty} dy e^{-Cy^2}\sin[2Cy] \\
&= -\pi \text{erfi}[\sqrt{C}]e^{-C}, \qquad \text{(B.6)}
\end{aligned}$$

and consequently

$$P\int d\lambda \frac{\lambda^n}{\lambda-1}e^{-C\lambda^2} = \sum_{i=0}^{n-1}\frac{(1+(-1)^i)}{2}C^{-\frac{1+i}{2}}\Gamma(\frac{1+i}{2}) - \pi\text{erfi}[\sqrt{C}]e^{-C} \qquad \text{(B.7)}$$

Bibliography

[1] S. Chu, C. Cohen-Tannoudji, and W. D. Phillips, Rev. o. Mod. Phys. **70**, 685 (1998).

[2] M. H. Anderson *et al.*, Science **269**, 198 (1995).

[3] K. Davis *et al.*, Phys. Rev. Lett. **75**, 3969 (1995).

[4] C. C. Bradley, C. A. Sackett, and R. G. Hulet, Phys. Rev. Lett. **78**, 985 (1997).

[5] *Proceedings of the International School of Physics "Enrico Fermi"*, edited by M. Inguscio, S. Stringari, and C. Wieman (IOS Press, Amsterdam, 1996).

[6] M.-O. Mewes *et al.*, Phys. Rev. Lett. **78**, 582 (1997).

[7] M. R. Andrews *et al.*, Science **275**, 627 (1997).

[8] I. Bloch, T. W. Hänsch, and T. Esslinger, Nature **403**, 166 (2000).

[9] S. Burger, K. Bongs, K. Sengstock, and W. Ertmer, *Proc. Int. Scholl of Quant. Elec., 27th Course* (Academic, Amsterdam, 2000).

[10] E. W. Hagley *et al.*, Science **283**, 1706 (1999).

[11] A. Chikkatur *et al.*, Science **296**, 2193 (2002).

[12] P. Cren *et al.*, Eur. Phys. J. D **20**, 107 (2002).

[13] J. I. Cirac and M. Lewenstein, Phys. Rev. A **35**, 647 (1996).

[14] L. de Broglie, La physique nouvelle et les Quanta, Flammarion, 1937.

[15] K. Huang, *Statistical Mechanics* (John Wiley & Sons, Second Edition, New York, 1992).

[16] L. Marton, J. A. Simpson, and J. A. Suddeth, Phys. Rev. **90**, 490 (1953).

[17] D. M. Greenberger and A. W. Overhauser, Rev. Mod. Phys. **51**, 43 (1979).

[18] T. Hänsch and A. Schawlow, Opt. Commun. **13**, 68 (1975).

[19] S. Chu *et al.*, Phys. Rev. Lett. **55**, 48 (1985).

[20] C. Cohen-Tannoudji, in *Fundamental Systems in Quantum Optics*, edited by J. Dalibard, J. M. Raimond, and J. Zinn-Justin (North-Holland, Amsterdam, 1992).

[21] G. Morigi, J. Eschner, and C. H. Keitel, Phys. Rev. Lett. **85**, 4458 (2000).

[22] M. Kasevich and S. Chu, Phys. Rev. Lett. **69**, 1741 (1992).

[23] A.Aspect *et al.*, Phys. Rev. Lett. **61**, 826 (1988).

[24] A.Aspect *et al.*, J. Opt. Soc. Am. **B6**, 2112 (1989).

[25] G. Alzeta, A. Gozzini, L. Moi, and G. Orriols, Nuovo Cimento **36B**, 5 (1976).

[26] E. Arimondo and G. Orriols, Nuovo Cimento **17**, 333 (1976).

[27] K. Moler, D. Weiss, M. Kasevich, and S. Chu, Phys. Rev. A **45**, 342 (1992).

[28] A. L. Migdall *et al.*, Phys. Rev. Lett. **54**, 2596 (1985).

[29] S. Chu, J. E. Bjorkholm, A. Ashkin, and A. Cable, Phys. Rev. Lett. **57**, 314 (1986).

[30] E. Raab *et al.*, Phys. Rev. Lett. **59**, 2631 (1987).

[31] I. Marzioli, J. I. Cirac, R. Blatt, and P. Zoller, Phys. Rev. A **49**, 2771 (1994).

[32] J. I. Cirac, M. Lewenstein, and P. Zoller, Europhys. Lett. **35**, 647 (1996).

[33] G. Morigi, J. I. Cirac, M. Lewenstein, and P. Zoller, Europhys. Lett. **39**, 13 (1997).

[34] L. Santos and M. Lewenstein, Phys. Rev. A **59**, 613 (1999).

[35] L. Santos and M. Lewenstein, Phys. Rev. A **60**, 3951 (1999).

[36] Z. Idziaszek, L. Santos, and M. Lewenstein, Phys. Rev. A **64**, 051402 (2001).

[37] T. Busch, J. R. Anglin, J. I. Cirac, and P. Zoller, Europhys. Lett. **44**, 1 (1998).

[38] L. Santos, Z. Idziaszek, M. Baranov, and M. Lewenstein, Preprint : cond-mat / 0212538 .

[39] L. Santos, Z. Idziaszek, M. Baranov, and M. Lewenstein, Preprint : cond-mat / 0211060 .

[40] P. G. de Gennes, *Superconductivity in metals and alloys* (W. A. Benjamin, New York, 1966).

[41] N. Masuhara *et al.*, Phys. Rev. Lett. **61**, 935 (1988).

[42] H. Hess *et al.*, Phys. Rev. Lett. **59**, 672 (1987).

[43] R. van Roijen, J. J. Berkhout, S. Jaakkola, and J. T. M. Walraven, Phys. Rev. Lett. **61**, 931 (1988).

[44] C. Sackett, C. Bradley, and R. Hulet, Phys. Rev. A **55**, 3797 (1997).

[45] W. Ketterle and N. van Druten, Adv. At. Mol. Opt. Phys. **37**, 181 (1996).

[46] K. Davis, M.-O. Mewes, and W. Ketterle, Appl. Phys. B **60**, 155 (1995).

[47] O. Luiten, M. Reynolds, and J. T. M. Walraven, Phys. Rev. A **53**, 381 (1996).

[48] H. Wu, E. Arimondo, and C. J. Foot, Phys. Rev. A **56**, 560 (1997).

[49] E. Arimondo, E. Cerboneschi, and H. Wu, in *Proceedings of the International School of Physics - Enrico Fermi*, edited by M. Inguscio, S. Stringari, and C. Wieman (IOS Press, Amsterdam, 1999), p. 573.

[50] F. Dalfovo, S. Giorgini, L. P. Pitaevskii, and S. Stringari, Rev. Mod. Phys. **71**, 463 (1999).

[51] M. Baranov *et al.*, Phys. Scripta T **102**, 74 (2002).

[52] D. Jaksch, C. W. Gardiner, and P. Zoller, Phys. Rev. A **56**, 575 (1997).

[53] Y. C. R. Dum, Phys. Rev. A **10**, 3008 (1998).

[54] O. M. Moragò *et al.*, Phys. Rev. Lett. **84**, 2056 (2000).

[55] C. Raman *et al.*, Phys. Rev. Lett. **83**, 2502 (1999).

[56] M. R. Matthews *et al.*, Phys. Rev. Lett. **83**, 2498 (1999).

[57] K. W. Madison, F. Chevy, W. Wohlleben, and J. Dalibard, Phys. Rev. Lett. **84**, 806 (2000).

[58] C. Adams, M. Sigel, and J. Mlynek, Phys. Rep. **240**, 145 (1994).

[59] S. Inouye *et al.*, Nature **402**, 641 (1999).

[60] M. Kozuma *et al.*, Science **286**, 2309 (1999).

[61] K. Bongs *et al.*, Phys. Rev. Lett. **83**, 3577 (1999).

[62] L. Deng *et al.*, Nature **398**, 218 (1999).

[63] J. Denschlag *et al.*, Science **287**, 97 (2000).

[64] S. Burger *et al.*, Phys. Rev. Lett. **83**, 5198 (1999).

[65] L. Khaykovich *et al.*, Science **296**, 1290 (2002).

[66] K. E. Strecker, G. B. Partridge, A. G. Truscott, and R. G. Hulet, Nature **417**, 150 (2002).

[67] A. Donley *et al.*, Nature **412**, 295 (2001).

[68] P. Meystre, *Atom Optics* (Springer Verlag, Berlin Heidelberg New York, 2001).

[69] P. Milonni and J. Eberly, *Lasers* (John Wiley & Sons, New York, 1988).

[70] E. Mandonnet *et al.*, Eur. Phys. J. D **10**, 9 (1999).

[71] C. Roos, P. Cren, Guere-Odelin, and J. Dalibard, Europhys. Lett. **61**, 187 (2003).

[72] R. J. C. Spreeuw, T. Pfau, U. Janicke, and M. Wilkens, Europhys. Lett. **32**, 469 (1995).

[73] M. Olshan'ii, Y. Castin, and J. Dalibard, in *Proc. 12*$^{\text{th}}$ *Int. Conf. on Laser Spectroscopy*, edited by M. Inguscio, M. Allegrini, and A. Lasso (World Scientific, Singapour, 1996).

[74] T. Pfau and J. Mlynek, OSA Trends in Optics and Photonics Series **7**, 33 (1997).

[75] Y. Castin, J. I. Cirac, and M. Lewenstein, Phys. Rev. Lett. **7**, 33 (1998).

[76] U. Janicke and M. Wilkens, Europhys. Lett. **35**, 561 (1996).

[77] L. Santos, F. Floegel, T. Pfau, and M. Lewenstein, Phys. Rev. A **63**, 063408 (2001).

[78] J. Stenger *et al.*, Phys. Rev. Lett. **82**, 2422 (1999).

[79] S. L. Cornish *et al.*, Phys. Rev. Lett. **85**, 1795 (2000).

[80] L. Santos and M. Lewenstein, Appl. Phys. B **69**, 363 (1999).

[81] J. L. Roberts, N. R. Claussen, S. L. Cornish, and C. E. Wieman, Phys. Rev. Lett. **85**, 728 (2000).

[82] L. Santos, Z. Idziaszek, J. I. Cirac, and M. Lewenstein, J. Phys. B **33**, 4131 (2000).

[83] C. W. Gardiner and P. Zoller, *Quantum Noise* (Springer-Verlag, Berlin Heidelberg New York, 1999).

[84] C. Gardiner, *Handbook of Stochastic Methods* (Springer-Verlag, Berlin Heidelberg New York, 1985).

[85] H. Carmichael, *An Open Systems Approach to Quantum Optics* (Springer-Verlag, Berlin Heidelberg New York, 1993).

[86] L. Santos and M. Lewenstein, Phys. Rev. A **60**, 3851 (1999).

[87] C. Gardiner and P. Zoller, Phys. Rev. A **55**, 2902 (1997).

[88] M. Holland, J. Williams, and J. Cooper, Phys. Rev. A **55**, 1997 (1997).

[89] M. Holland *et al.*, Phys. Rev. A **54**, R1757 (1996).

[90] F. Dalfovo, S. Giorgini, L. P. Pitaevskii, and S. Stringari, Rev. o. Mod. Phys. **71**, 463 (1999).

[91] K. Jänich, *Analysis für Physiker und Ingenieure* (Springer Verlag, Berlin Heidelberg New York, 1995).

Danksagung

Zuallererst möchte ich mich bei Herrn Prof. Dr. M. Lewenstein bedanken, der er es mir ermöglicht hat, in so einer tollen Gruppe phantastische Physik zu machen. Es war mir eine Ehre ihn als Doktorvater gehabt zu haben. Ich möchte ihm auch dafür danken, dass er es für mich möglich gemacht hat, für 4 Monate nach Warschau gehen zu können, um mit seinem Doktorvater Prof. Dr. K. Rzazewski zusammenarbeiten zu können.

Ich bedanke mich bei Herrn Juniorprof. Dr. J. Arlt für die Übernahme des Koreferats und für die gute Zusammenarbeit während der letzten Jahre.

Einen besonderen Dank an Herrn Dr. L. Santos, der seit Anbeginn mir immer nicht nur in der Physik sondern auch als Freund mit Rat und Tat in der Gruppe Lewenstein zur Seite stand. Die Diskussionen mit ihm waren immer von besonderer Qualität. Es war schon ziemlich außergewöhnlich mit ihm zusammengearbeitet zu haben.

Ich möchte mich auch noch mal bei Herrn Prof. Dr. W. Ertmer bedanken, ohne den diese Arbeit wohl sonst nie zustande gekommen wäre, wenn er nicht damals für eine Diplomarbeit mit Herrn Prof. Dr. M. Lewenstein vermittelt hätte.

Meinen Physiker-Kollegen aus der Gruppe Lewenstein aber auch aus der Gruppe Ertmer einen grossen Dank für die vielen anregenden Diskussionen. Herrn Dr. P. Öhberg möchte ich speziell dafür danken, dass er mich bei meinen ersten Schritten, Bogoliubov-Spektren numerisch zu berechnen, unterstützt hat.

Für die Unterstützung in Organisation und dem Verwaltungstechnischen danke ich Frau Franko und dem SFB-Team (Frau Faber, Frau Pfennig). Ich möchte mich auch bei Herrn Dr. R. Gaul für die gute Zusammenarbeit bedanken, wenn es sich um das Regeln von Institutsproblemen und sonstigen nicht einzuordnenden Problemen handelte.

Herrn Prof. Dr. K. Rzazewski, Dr. M. Gajda und Dr. K. Góral danke ich für die spannende Zeit in Warschau, in der ich Wirbel in BECs bei endlicher Temperatur habe "sterben" lassen können. Ich habe dort unglaublich viel gelernt, und großen Spaß hat es auch gemacht.

Meinen ganzen Freunden möchte ich natürlich auch danken. Sie haben mich immer wieder auf unterschiedlichste Weise unterstützt und waren immer interessiert an dem was ich mache. Insbesonder Christian und Serdal danke ich, dass sie immer mal wieder bei mir vorbeikamen und mir die nötigen Denkpausen zu verordnen, um dann wieder motiviert weiter arbeiten zu können.

Zu guter Letzt kommen meine Eltern (Brita & Dietmar) an die Reihe. Das bedeutet aber nicht, dass sie weniger wichtig waren. Nein, sie haben mir den nötigen Rückhalt gegeben. Aber nicht nur das. Wenn es hart auf hart ging, konnte ich mich auf sie verlassen.

Lebenslauf

Geburtsdatum/-ort

15. 07. 1973 in Hamburg

Schulausbildung

07/1979–06/1983	Grundschule am Lindener Markt
08/1979–06/1992	Integrierte Gesamtschule Hannover Linden
05/1992	Abschluß mit Abitur

Wehrdienst

10/1992–09/1999	Ersatzdienst beim THW Hannover

Hochschulstudium

10/1992–02/1999	Studium der Physik an der Universität Hannover
04/1995	Diplomvorprüfung
03/1998–02/1999	Diplomarbeit am Institut für Theoretische Physik der Universität Hannover bei Prof. Dr. M. Lewenstein Thema:"Reabsorption von Photonen in einem Optischen Gitter"
04/1995	Abschluß mit Diplom
seit 03/1999	Wissenschaftlicher Mitarbeiter am Institut für Theoretische Physik der Universität Hannover

Veröffentlichungen

F. Floegel, L. Santos and M. Lewenstein, "Continuous Optical loading of a Bose-Einstein Condensate in the Thoms-Fermi regime", submitted to *Euro. Phys. Lett.*, cond-mat/0303358.

H. Schmidt, K. Goral, F. Floegel, M. Gajda, K. Rzazewski, "Probing the classical field approximation – thermodynamics and decaying vortices", *J. Optics* B, accepted.

L. Santos F. Floegel, T. Pfau and M. Lewenstein, "Continuous optical loading of a Bose–Einstein Condensate", *Phys. Rev.* A **23**, 33 (2000).

F. Floegel, L. Santos and M. Lewenstein, "Loading of a Bose-Einstein condensate in the boson–accumulation regime", *Euro. Phys. Lett.* **23**, 33 (2000).